

USARTL-TR-78-17

LEVEL

12



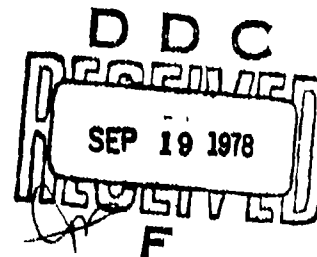
**STRUCTURAL CONCEPTS AND AERODYNAMIC ANALYSIS FOR
LOW RADAR CROSS SECTION (LRCS) FUSELAGE CONFIGURATIONS**

DDC FILE COPY, AD A058906

David W. Lowry, Melvin J. Rich, Saul Rivera, Thomas W. Sheehy
Sikorsky Aircraft Division
United Technologies Corporation
Stratford, Conn. 06603

July 1978

Final Report



Approved for public release;
distribution unlimited.

Prepared for

APPLIED TECHNOLOGY LABORATORY

U. S. ARMY RESEARCH AND TECHNOLOGY LABORATORIES (AVRADCOM)

Fort Eustis, Va. 23604

10 10 001

APPLIED TECHNOLOGY LABORATORY POSITION STATEMENT

This report provides a study of fuselage concepts for three low radar cross section aircraft configurations. An assessment of these concepts in terms of cost, weight, safety, advanced materials, risk, maintainability and aerodynamic performance was made, including comparisons with the UH-60A helicopter.

The three LRCS configurations were developed by the Applied Technology Laboratory. The study was conducted by Sikorsky Aircraft Division of United Technologies Corporation under Contract DAAJ02-76-C-0062.

Mr. Bill W. Scruggs, Jr., of the Military Operations Technology Division served as project engineer for this effort.

DISCLAIMERS

The findings in this report are not to be construed as an official Department of the Army position unless so designated by other authorized documents.

When Government drawings, specifications, or other data are used for any purpose other than in connection with a definitely related Government procurement operation, the United States Government thereby incurs no responsibility nor any obligation whatsoever; and the fact that the Government may have formulated, furnished, or in any way supplied the said drawings, specifications, or other data is not to be regarded by implication or otherwise as in any manner licensing the holder or any other person or corporation, or conveying any rights or permission, to manufacture, use, or sell any patented invention that may in any way be related thereto.

Trade names cited in this report do not constitute an official endorsement or approval of the use of such commercial hardware or software.

DISPOSITION INSTRUCTIONS

Destroy this report when no longer needed. Do not return it to the originator.

Unclassified

SECURITY CLASSIFICATION OF THIS PAGE (When Data Entered)

17 REPORT DOCUMENTATION PAGE		READ INSTRUCTIONS BEFORE COMPLETING FORM
1. REPORT NUMBER (18) USARTL TR-78-17	2. GOVT ACCESSION NO.	3. RECIPIENT'S CATALOG NUMBER
4. TITLE (and Subtitle) (6) STRUCTURAL CONCEPTS AND AERODYNAMIC ANALYSIS FOR LOW RADAR CROSS SECTION (LRCS) FUSELAGE CONFIGURATIONS	5. TYPE OF REPORT & PERIOD COVERED (7) Final Report	
6. AUTHOR(S) (10) David W./Lowry, Melvin J./Rich, Saul/Riversa and Thomas W./Sheehy	7. PERFORMING ORG. REPORT NUMBER (14) SER-50987	
	8. CONTRACT OR GRANT NUMBER(s) (15) DAAJ92-76-C-0862	
9. PERFORMING ORGANIZATION NAME AND ADDRESS Sikorsky Aircraft Division United Technologies Corporation Stratford, Connecticut 06603	10. PROGRAM ELEMENT, PROJECT, TASK AREA & WORK UNIT NUMBERS 62209A/1F262209AH7600 170 EK (16) 37994	
11. CONTROLLING OFFICE NAME AND ADDRESS Applied Technology Laboratory, U.S. Army Research & Technology Laboratories (AVRADCOM) Fort Eustis, Virginia 23604	12. REPORT DATE (17) July 1978	
14. MONITORING AGENCY NAME & ADDRESS (if different from Controlling Office)	13. NUMBER OF PAGES 139 (12) 144 p.	
	15. SECURITY CLASS. (of this report) Unclassified	
	15a. DECLASSIFICATION/DOWNGRADING SCHEDULE	
16. DISTRIBUTION STATEMENT (of this Report) Approved for public release; distribution unlimited.		
17. DISTRIBUTION STATEMENT (of the abstract entered in Block 20, if different from Report)		
18. SUPPLEMENTARY NOTES		
19. KEY WORDS (Continue on reverse side if necessary and identify by block number) Preliminary design concepts Helicopter Fail-safety, safety and maintainability Advanced materials application Costs Aerodynamic performance		
20. ABSTRACT (Continue on reverse side if necessary and identify by block number) (14) The objectives of this study were: (1) to develop structural concepts for three low radar cross section (LRCS) fuselage configurations constructed of con- ventional materials; (2) to determine the effects of these concepts on the weight, cost, fail-safety, and maintainability of the three configurations; (3) to compare these findings with those of a baseline UH-60A helicopter, and thus select the structural concept that is the lowest in weight and cost and the easiest to maintain; (4) to assess the application of advanced materials for each		

DD FORM 1 JAN 73 1473

EDITION OF 1 NOV 65 IS OBSOLETE
B/N 0102-014-6601

Unclassified

SECURITY CLASSIFICATION OF THIS PAGE (When Data Entered)

Unclassified

SECURITY CLASSIFICATION OF THIS PAGE(When Data Entered)

configuration; (5) to identify high technical risk areas; (6) to develop overall design trending data for helicopters, using the three fuselage configurations of conventional and advanced materials; (7) to conduct an analytical investigation of the aerodynamic loads, vertical drag and mission performance of the three low radar cross section (LRCS) configurations; and (8) to compare these findings with those of the baseline UH-60 helicopter.

Structural concepts developed for the three LRCS configurations showed that extensive reshaping, as exemplified by Configuration 2, would increase fuselage weight from that of the baseline UH-60A fuselage by 223 pounds and cost by 3.65 percent. When advanced materials were used, Configuration 2 decreased from the baseline fuselage weight and cost by 118 pounds and 3.98 percent respectively. Total aircraft performance capability was degraded primarily by drag effects. The aerodynamic analysis indicated that Configuration 2 would have a vertical climb rate at 15 percent of the baseline. Since drag is a function of area and shape, the weight savings of advanced materials had negligible effects on performance. Weight, cost, and performance penalties were less in Configurations 3 and 1 respectively.

Unclassified

SECURITY CLASSIFICATION OF THIS PAGE(When Data Entered)

PREFACE

This study of structural concepts for low radar cross section (LRCS) fuselages was conducted under Contract DAAJ02-76-C-0062 with the Applied Technology Laboratory, U. S. Army Research and Technology Laboratories (AVRADCOM), Fort Eustis, Virginia.

The work was performed under the general direction of Mr. Bill Scruggs, Jr., of the Military Operations Technology Division. Sikorsky Aircraft principal participants were Melvin Rich, Project Manager; David Lowry, Structural Concepts; George Howard, Helicopter Design; Anthony DiPierro, Weights Engineering; Neville Kefford, Helicopter Design Modeling; Brian Carnell, Survivability; and Calvin Holbert, Reliability and Maintainability.

An analytical investigation of the aerodynamic loads, drag and mission performance of low radar cross section configurations was performed by Mr. Saul Rivera, Aerodynamicist, under the direction of Mr. Thomas W. Sheehy, Aerodynamicist, both of Sikorsky Aircraft.

ACCESSION for	
NTIS	White Section <input checked="" type="checkbox"/>
DDC	Buff Section <input type="checkbox"/>
UNANNOUNCED	<input type="checkbox"/>
JUSTIFICATION	
BY	
DISTRIBUTION/AVAILABILITY CODES	
Dist.	SPECIAL
A	

TABLE OF CONTENTS

	<u>PAGE</u>
PREFACE	3
LIST OF ILLUSTRATIONS	7
LIST OF TABLES.	11
INTRODUCTION.	13
BASELINE UTTAS FUSELAGE CONFIGURATION	15
Description.	15
Baseline Fuselage Weight and Cost.	16
LOW RADAR CROSS SECTION CONFIGURATIONS.	21
Configuration 1.	21
Configuration 2.	21
Configuration 3.	22
PRELIMINARY DESIGN CONCEPTS (CONVENTIONAL MATERIALS).	29
Weight Analysis.	29
Cost Analysis.	35
APPLICATION OF DESIGN CONCEPTS TO LOW RADAR CROSS SECTION FUSELAGES	39
Configuration 1.	39
Configurations 2 and 3	39
DESCRIPTION OF EVALUATION FOR FAIL-SAFETY, SAFETY AND MAINTAIN- ABILITY	43
Fail-Safety.	43
Crash Safety/Safety.	43
Maintainability.	43
MODIFICATION OF CONFIGURATION 2	47
SELECTED CONCEPTS	48

TABLE OF CONTENTS (Cont.)

	<u>PAGE</u>
ADVANCED MATERIAL APPLICATION	49
Frames	49
Beams and Intercostals	55
Skins	55
Stringers	55
ADVANCED MATERIAL APPLICATION COSTS	56
HELICOPTER DESIGN MODEL	63
Introduction	63
HDM Results	63
TECHNICAL RISKS	68
CONCLUSIONS	69
REFERENCES	70
APPENDIX A, AERODYNAMICS ANALYSIS OF LOW RADAR CROSS SECTION CONFIGURATIONS.	71
LIST OF SYMBOLS	138

LIST OF ILLUSTRATIONS

<u>FIGURE</u>		<u>PAGE</u>
1	PROGRAM STUDY FLOW CHART	14
2	GENERAL ARRANGEMENT OF UH60A	17
3	GENERAL ARRANGEMENT OF LRCS CONFIGURATION 1.	23
4	GENERAL ARRANGEMENT OF LRCS CONFIGURATION 2.	25
5	GENERAL ARRANGEMENT OF LRCS CONFIGURATION 3.	27
6	STRUCTURAL CONCEPTS A, B AND C	30
7	BODY GROUP WEIGHT VERSUS BODY GROUP WEIGHT PARAMETERS.	32
8	ADVANCED MATERIALS APPLICATION FOR CONFIGURATION 2	51
9	ADVANCED MATERIALS APPLICATION FOR CONFIGURATION 3	53
10	PAYLOAD AND RANGE FOR LOW RADAR CROSS SECTION HELICOPTERS.	67
A-1	GEOMETRICAL REPRESENTATION OF THE UH60A FUSELAGE(BASELINE)	82
A-2	GEOMETRICAL REPRESENTATION OF THE UH60A WITH MAIN ROTOR PYLON (BASELINE)	83
A-3	GEOMETRICAL REPRESENTATION OF THE LRCS1 FUSELAGE	84
A-4	GEOMETRICAL REPRESENTATION OF THE LRCS1 FUSELAGE WITH BASELINE MAIN ROTOR PYLON.	85
A-5	GEOMETRICAL REPRESENTATION OF THE LRCS2 FUSELAGE	86
A-6	GEOMETRICAL REPRESENTATION OF THE LRCS2 FUSELAGE WITH BASELINE MAIN ROTOR PYLON.	87
A-7	GEOMETRICAL REPRESENTATION OF THE LRCS3 FUSELAGE	88
A-8	GEOMETRICAL REPRESENTATION OF THE LRCS3 FUSELAGE WITH BASELINE MAIN ROTOR PYLON.	89
A-9	COMPARISON OF THE UH60A AND LRCS1 CALCULATED SURFACE PRESSURES, TOP CENTERLINE, $\alpha = 0^\circ$, $\psi = 0^\circ$	90
A-10	COMPARISON OF THE UH60A AND LRCS1 CALCULATED SURFACE PRESSURES, BOTTOM CENTERLINE, $\alpha = 0^\circ$, $\psi = 0^\circ$	91

LIST OF ILLUSTRATIONS (cont.)

<u>FIGURE</u>		<u>PAGE</u>
A-11	COMPARISON OF THE UH60A AND LRCS1 CALCULATED SURFACE PRESSURES, LATERAL CENTERLINE, $\alpha = 0^\circ$, $\psi = 0^\circ$	92
A-12	COMPARISON OF THE UH60A AND LRCS1 CALCULATED SURFACE PRESSURES, TOP CENTERLINE, $\alpha = 4^\circ$, $\psi = 0^\circ$	93
A-13	COMPARISON OF THE UH60A AND LRCS1 CALCULATED SURFACE PRESSURES, BOTTOM CENTERLINE, $\alpha = 4^\circ$, $\psi = 0^\circ$	94
A-14	COMPARISON OF THE UH60A AND LRCS1 CALCULATED SURFACE PRESSURES, LATERAL CENTERLINE, $\alpha = 4^\circ$, $\psi = 0^\circ$	95
A-15	COMPARISON OF THE UH60A AND LRCS1 CALCULATED SURFACE PRESSURES, TOP CENTERLINE, $\alpha = 8^\circ$, $\psi = 0^\circ$	96
A-16	COMPARISON OF THE UH60A AND LRCS1 CALCULATED SURFACE PRESSURES, BOTTOM CENTERLINE, $\alpha = 8^\circ$, $\psi = 0^\circ$	97
A-17	COMPARISON OF THE UH60A AND LRCS1 CALCULATED SURFACE PRESSURES, LATERAL CENTERLINE, $\alpha = 8^\circ$, $\psi = 0^\circ$	98
A-18	COMPARISON OF THE UH60A AND LRCS1 CALCULATED SURFACE PRESSURES, TOP CENTERLINE, $\alpha = -4^\circ$, $\psi = 0^\circ$	99
A-19	COMPARISON OF THE UH60A AND LRCS1 CALCULATED SURFACE PRESSURES, BOTTOM CENTERLINE, $\alpha = -4^\circ$, $\psi = 0^\circ$	100
A-20	COMPARISON OF THE UH60A AND LRCS1 CALCULATED SURFACE PRESSURES, LATERAL CENTERLINE, $\alpha = -4^\circ$, $\psi = 0^\circ$	101
A-21	COMPARISON OF THE UH60A AND LRCS1 CALCULATED SURFACE PRESSURES, TOP CENTERLINE, $\alpha = -8^\circ$, $\psi = 0^\circ$	102
A-22	COMPARISON OF THE UH60A AND LRCS1 CALCULATED SURFACE PRESSURES, BOTTOM CENTERLINE, $\alpha = -8^\circ$, $\psi = 0^\circ$	103
A-23	COMPARISON OF THE UH60A AND LRCS1 CALCULATED SURFACE PRESSURES, LATERAL CENTERLINE, $\alpha = -8^\circ$, $\psi = 0^\circ$	104
A-24	COMPARISON OF THE UH60A AND LRCS2 CALCULATED SURFACE PRESSURES, TOP CENTERLINE, $\alpha = 0^\circ$, $\psi = 0^\circ$	105
A-25	COMPARISON OF THE UH60A AND LRCS2 CALCULATED SURFACE PRESSURES, BOTTOM CENTERLINE, $\alpha = 0^\circ$, $\psi = 0^\circ$	106
A-26	COMPARISON OF THE UH60A AND LRCS2 CALCULATED SURFACE PRESSURES, LATERAL CENTERLINE, $\alpha = 0^\circ$, $\psi = 0^\circ$	107

LIST OF ILLUSTRATIONS (cont.)

<u>FIGURE</u>		<u>PAGE</u>
A-27	COMPARISON OF THE UH60A AND LRCS2 CALCULATED SURFACE PRESSURES, TOP CENTERLINE, $\alpha = 4^\circ$, $\psi = 0^\circ$	108
A-28	COMPARISON OF THE UH60A AND LRCS2 CALCULATED SURFACE PRESSURES, BOTTOM CENTERLINE, $\alpha = 4^\circ$, $\psi = 0^\circ$	109
A-29	COMPARISON OF THE UH60A AND LRCS2 CALCULATED SURFACE PRESSURES, LATERAL CENTERLINE, $\alpha = 4^\circ$, $\psi = 0^\circ$	110
A-30	COMPARISON OF THE UH60A AND LRCS2 CALCULATED SURFACE PRESSURES, TOP CENTERLINE, $\alpha = 8^\circ$, $\psi = 0^\circ$	111
A-31	COMPARISON OF THE UH60A AND LRCS2 CALCULATED SURFACE PRESSURES, BOTTOM CENTERLINE, $\alpha = 8^\circ$, $\psi = 0^\circ$	112
A-32	COMPARISON OF THE UH60A AND LRCS2 CALCULATED SURFACE PRESSURES, LATERAL CENTERLINE, $\alpha = 8^\circ$, $\psi = 0^\circ$	113
A-33	COMPARISON OF THE UH60A AND LRCS2 CALCULATED SURFACE PRESSURES, TOP CENTERLINE, $\alpha = -4^\circ$, $\psi = 0^\circ$	114
A-34	COMPARISON OF THE UH60A AND LRCS2 CALCULATED SURFACE PRESSURES, BOTTOM CENTERLINE, $\alpha = -4^\circ$, $\psi = 0^\circ$	115
A-35	COMPARISON OF THE UH60A AND LRCS2 CALCULATED SURFACE PRESSURES, LATERAL CENTERLINE, $\alpha = -4^\circ$, $\psi = 0^\circ$	116
A-36	COMPARISON OF THE UH60A AND LRCS2 CALCULATED SURFACE PRESSURES, TOP CENTERLINE, $\alpha = -8^\circ$, $\psi = 0^\circ$	117
A-37	COMPARISON OF THE UH60A AND LRCS2 CALCULATED SURFACE PRESSURES, BOTTOM CENTERLINE, $\alpha = -8^\circ$, $\psi = 0^\circ$	118
A-38	COMPARISON OF THE UH60A AND LRCS2 CALCULATED SURFACE PRESSURES, LATERAL CENTERLINE, $\alpha = -8^\circ$, $\psi = 0^\circ$	119
A-39	COMPARISON OF THE UH60A AND LRCS3 CALCULATED SURFACE PRESSURES, TOP CENTERLINE, $\alpha = 0^\circ$, $\psi = 0^\circ$	120
A-40	COMPARISON OF THE UH60A AND LRCS3 CALCULATED SURFACE PRESSURES, BOTTOM CENTERLINE, $\alpha = 0^\circ$, $\psi = 0^\circ$	121
A-41	COMPARISON OF THE UH60A AND LRCS3 CALCULATED SURFACE PRESSURES, LATERAL CENTERLINE, $\alpha = 0^\circ$, $\psi = 0^\circ$	122
A-42	COMPARISON OF THE UH60A AND LRCS3 CALCULATED SURFACE PRESSURES, TOP CENTERLINE, $\alpha = 4^\circ$, $\psi = 0^\circ$	123

LIST OF ILLUSTRATIONS (cont.)

<u>FIGURE</u>		<u>PAGE</u>
A-43	COMPARISON OF THE UH60A AND LRCS3 CALCULATED SURFACE PRESSURES, BOTTOM CENTERLINE, $\alpha = 4^\circ$, $\psi = 0^\circ$	124
A-44	COMPARISON OF THE UH60A AND LRCS3 CALCULATED SURFACE PRESSURES, LATERAL CENTERLINE, $\alpha = 4^\circ$, $\psi = 0^\circ$	125
A-45	COMPARISON OF THE UH60A AND LRCS3 CALCULATED SURFACE PRESSURES, TOP CENTERLINE, $\alpha = 8^\circ$, $\psi = 0^\circ$	126
A-46	COMPARISON OF THE UH60A AND LRCS3 CALCULATED SURFACE PRESSURES, BOTTOM CENTERLINE, $\alpha = 8^\circ$, $\psi = 0^\circ$	127
A-47	COMPARISON OF THE UH60A AND LRCS3 CALCULATED SURFACE PRESSURES, LATERAL CENTERLINE, $\alpha = 8^\circ$, $\psi = 0^\circ$	128
A-48	COMPARISON OF THE UH60A AND LRCS3 CALCULATED SURFACE PRESSURES, TOP CENTERLINE, $\alpha = -4^\circ$, $\psi = 0^\circ$	129
A-49	COMPARISON OF THE UH60A AND LRCS3 CALCULATED SURFACE PRESSURES, BOTTOM CENTERLINE, $\alpha = -4^\circ$, $\psi = 0^\circ$	130
A-50	COMPARISON OF THE UH60A AND LRCS3 CALCULATED SURFACE PRESSURES, LATERAL CENTERLINE, $\alpha = -4^\circ$, $\psi = 0^\circ$	131
A-51	COMPARISON OF THE UH60A AND LRCS3 CALCULATED SURFACE PRESSURES, TOP CENTERLINE, $\alpha = -8^\circ$, $\psi = 0^\circ$	132
A-52	COMPARISON OF THE UH60A AND LRCS3 CALCULATED SURFACE PRESSURES, BOTTOM CENTERLINE, $\alpha = -8^\circ$, $\psi = 0^\circ$	133
A-53	COMPARISON OF THE UH60A AND LRCS3 CALCULATED SURFACE PRESSURES, LATERAL CENTERLINE, $\alpha = -8^\circ$, $\psi = 0^\circ$	134
A-54	VARIATION OF LIFT WITH ANGLE OF ATTACK FOR THE UH60A, LRCS1, LRCS2, LRCS3 CONFIGURATIONS	135
A-55	VARIATION OF DRAG WITH ANGLE OF ATTACK FOR THE UH60A, LRCS1, LRCS2, LRCS3 CONFIGURATIONS	136
A-56	VARIATION OF PITCHING MOMENT WITH ANGLE OF ATTACK FOR THE UH60A, LRCS1, LRCS2 AND LRCS3 CONFIGURATIONS	137

LIST OF TABLES

<u>TABLE</u>		<u>PAGE</u>
1	BASELINE UH60A FUSELAGE WEIGHT AND COST DATA	20
2	BASELINE FUSELAGE SKIN/STRINGER WEIGHT FROM WEIGHT AND BALANCE REPORT	34
3	CONFIGURATION 2A AND 2B SKIN/STRINGER WEIGHT	34
4	CONFIGURATION 3A AND 3B SKIN/STRINGER WEIGHT	35
5	CONFIGURATION 2C HONEYCOMB PANEL SKIN WEIGHT	37
6	CONFIGURATION 3C HONEYCOMB PANEL SKIN WEIGHT	37
7	CONFIGURATION 1 FUSELAGE WEIGHT AND COST DATA	39
8	CONFIGURATION 2A FUSELAGE WEIGHT AND COST DATA.	40
9	CONFIGURATION 2B FUSELAGE WEIGHT AND COST DATA.	40
10	CONFIGURATION 2C FUSELAGE WEIGHT AND COST DATA.	41
11	CONFIGURATION 3A FUSELAGE WEIGHT AND COST DATA.	41
12	CONFIGURATION 3B FUSELAGE WEIGHT AND COST DATA.	42
13	CONFIGURATION 3C FUSELAGE WEIGHT AND COST DATA.	42
14	SAFETY AND CRASH-SAFETY RANKING.	45
15	SUMMARY OF FUSELAGE WEIGHT AND COST DATA OF CONVENTIONAL CONSTRUCTION.	46
16	FLOOR WEIGHT COMPARISON FOR CONFIGURATION 2	47
17	COCKPIT STRUCTURAL WEIGHT	57
18	COCKPIT STRUCTURAL WEIGHT OF CONFIGURATION 1A OF CONVEN- TIONAL MATERIALS AND ADVANCED MATERIALS	58
19	COCKPIT STRUCTURAL WEIGHT OF CONFIGURATION 2A OF CONVEN- TIONAL MATERIALS AND ADVANCED MATERIALS	59
20	COCKPIT STRUCTURAL WEIGHT OF CONFIGURATION 3A OF CONVEN- TIONAL MATERIALS AND ADVANCED MATERIALS	60
21	CONFIGURATION 1 ADVANCED MATERIALS FUSELAGE WEIGHT AND COST DATA	61

LIST OF TABLES (cont.)

<u>TABLE</u>		<u>PAGE</u>
22	CONFIGURATION 2 ADVANCED MATERIALS FUSELAGE WEIGHT AND COST DATA	61
23	CONFIGURATION 3 ADVANCED MATERIALS FUSELAGE WEIGHT AND COST DATA	62
24	SUMMARY OF WEIGHT AND COST DATA FOR CONCEPT A AND ADVANCED MATERIALS	62
25	PRELIMINARY DRAG ESTIMATE	64
26	HELICOPTER DESIGN MODEL CONSTANT GROSS WEIGHT RESULTS. .	65
27	HELICOPTER DESIGN MODEL TRENDING RESULTS	66
A-1	UH-60A VERTICAL DRAG CALCULATION	76
A-2	LRCS 1 VERTICAL DRAG CALCULATION	77
A-3	LRCS 2 VERTICAL DRAG CALCULATION	78
A-4	LRCS 3 VERTICAL DRAG CALCULATION	79
A-5	SUMMARY OF PARASITE AND VERTICAL DRAG	80
A-6	PRIMARY MISSION PERFORMANCE SUMMARY	81

INTRODUCTION

The objectives of this study were: (a) to develop structural concepts and determine their effects on weight, cost, fail-safety and maintainability for three low radar cross section fuselages constructed of conventional materials, and to compare these to a baseline Sikorsky Utility Tactical Transport Aircraft System (UH60A) helicopter; (b) based upon the results of the study to select the structural concept for the three configurations that is the lowest in weight and cost, and is the easiest to maintain; (c) to assess the application of advanced materials for each configuration; (d) to develop design trending data for helicopters, using the three configurations of conventional and advanced materials; and (e) to identify high technical risk areas.

Three fuselage configurations for low radar cross sections were developed by the Applied Technology Laboratory. Mold line drawings of each configuration were provided by the Army for this study. The main rotor pylon fairings and tail surfaces aft of a tail fold hinge for each configuration were the same as those for the baseline UH60A.

In the initial portion of this study, the weight and costs (percent of total) were developed for sections of the baseline UH60A fuselage. General arrangement drawings of each configuration were developed from the mold line drawings. Structural concepts were developed which could be applied to each configuration using conventional materials. An assessment of safety, fail-safety, and maintainability for each configuration was performed. The change in structural weight and the percentage change in cost for each configuration using the concepts developed were compared to those of the baseline. One concept was selected and applied to the three configurations.

Having selected the structural concept with the lowest weight change and percentage cost change for the three fuselage configurations, the effect on weight and costs using advanced materials was developed and applied to the three configurations.

To evaluate the impact of the results of the fuselage study, design attributes of six helicopters were developed using a Helicopter Design Model (HDM) computer program.

The six helicopters (three of conventional materials and three of advanced materials) were compared to the baseline UH60A. Technical risks were assessed.

The approach to this study is illustrated on the flow chart of Figure 1.

A detailed analytical aerodynamic investigation of the fuselage configurations was undertaken at the conclusion of the above study. The results of this additional work are reported in Appendix A.

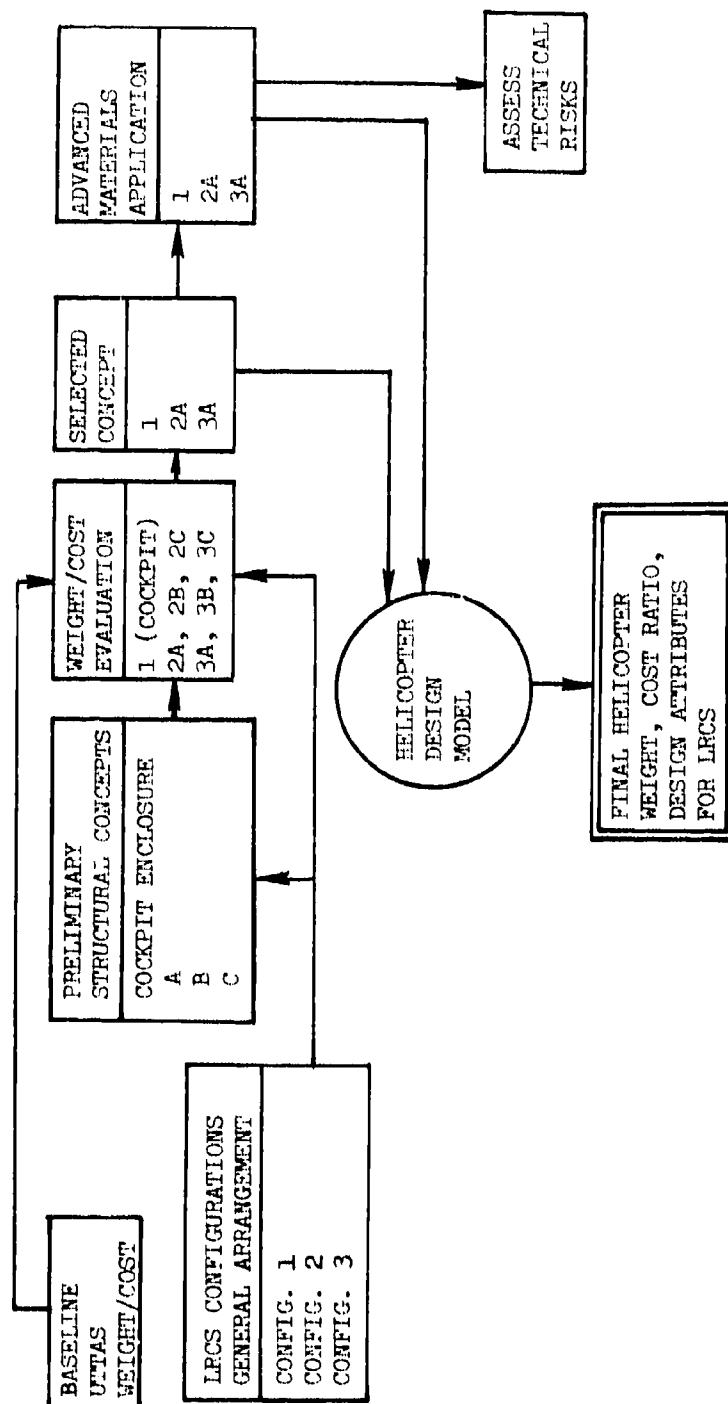


FIGURE 1. PROGRAM STUDY FLOW CHART

BASELINE UH60A FUSELAGE CONFIGURATION

DESCRIPTION

The baseline fuselage of this study, shown in Figure 2, is that of the Sikorsky UH-60A. The fuselage is made up of six major sections:

1. Cockpit (or nose)
2. Mid-cabin
3. Aft-cabin (or transition)
4. Tail cone
5. Pylon
6. Stabilizer

The cockpit section is a molded fiberglass/epoxy framework above the floor. The framework supports the windshields, doors, and overhead controls. Structure below the floor is of built-up aluminum beams and frames. The structure supports the pilot and copilot seats, flight controls and electronic equipment.

The cockpit section is of double contour with many cutouts and supports for a variety of equipment.

The mid-cabin section is of forged and built-up aluminum frames and beams. The mid-cabin consists of an upper section, two side sections, a tub section and a combination walking cargo floor. The entire section supports the engines, transmission, flight controls, troop seats, litters, cargo and the main landing gears.

The aft-cabin section, double contoured, is of honeycomb sandwich bulkheads, aluminum intercostals, stringers and skins. This section supports two fuel cells and a small cargo deck.

The tail cone is constructed of bent-up aluminum frames which support rolled formed stringers and aluminum sheet skins. The tail cone is a single-wrapped contour where the skin/stringer combination is riveted to floating frames. Floating frames do not have a direct shear tie to the skins. The tail cone supports the tail rotor drive shaft, tail landing gear and the tail pylon fold hinges.

The pylon and the stabilizers are airfoil shaped structures of built-up spars, formed ribs and formed stiffeners covered with aluminum sheet skins. The pylon supports the tail rotor and gearbox. The stabilizers provide pitch control for the helicopter.

BASELINE FUSELAGE WEIGHT AND COST

The structural weights of the six sections of the baseline fuselage were obtained from the actual weight and balance report for the UH-60A (Reference 1).

The costs of the six sections of the baseline fuselage were obtained from a cost/weight relationship study conducted by Sikorsky Aircraft after the detail design of the UH60A aircraft had been completed.

The costs were determined for materials and labor for each section of the baseline fuselage, based on the production of 276 fuselages. The costs reflect 1977 pricing.

Material costs included purchased items such as formed stringers, rolled sheet stock, extruded shapes, forgings and windshields. The total material costs required to produce each section of the baseline fuselage were given in terms of dollars per pound of structural weight of the section. The material costs ranged from a low of approximately \$2.00 per pound to a high of approximately \$10.00 per pound.

Labor hours required to fabricate each section were determined as follows:

1. Fabrication of individual structural elements that make up frames, beams, bulkheads, fittings, stringers, intercostals, longerons, and floors.
2. Assembly of the structural elements to produce frames, beams, etc.
3. Installation of frames, etc., to produce a structural section of the fuselage.

Labor costs were based on \$22.50 per hour.

No tooling, engineering, or development costs were considered. It should be noted that tooling costs are relatively small for production helicopters (less than 3 percent; Reference 2).

-
1. UH-60A VOLUME 3, PART 1-III WEIGHT AND BALANCE dated September 27, 1976.
 2. Rich, M. J., INVESTIGATION OF ADVANCED HELICOPTER STRUCTURAL DESIGNS, VOLUME 1 - ADVANCED STRUCTURAL COMPONENT DESIGN CONCEPTS STUDY, Sikorsky Aircraft Div., USAAMRD-L-TR-75-59A, U.S. Army Air Mobility Research and Development Laboratory, Fort Eustis, Va. 23604, May 1976, AD A026246.

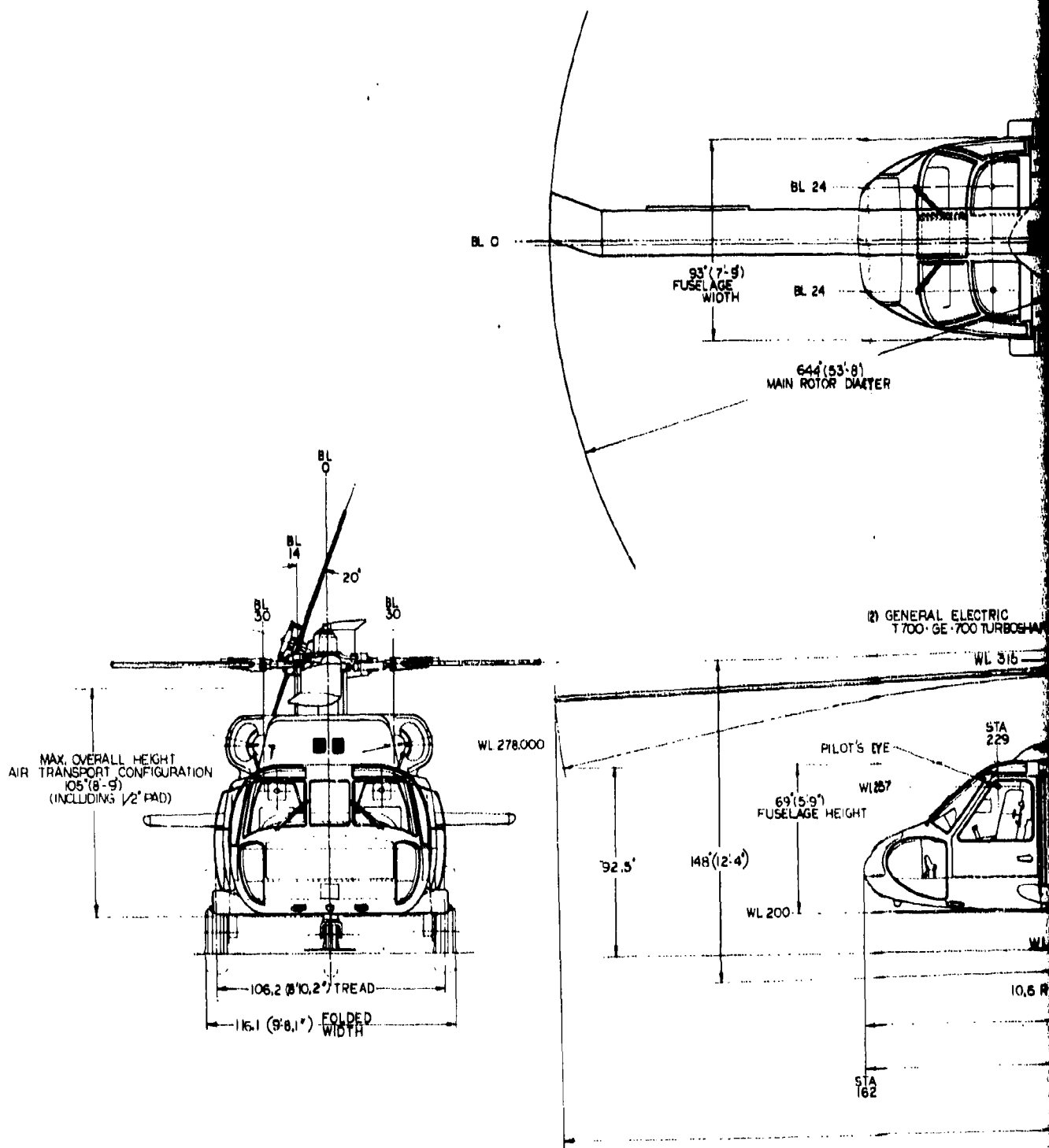
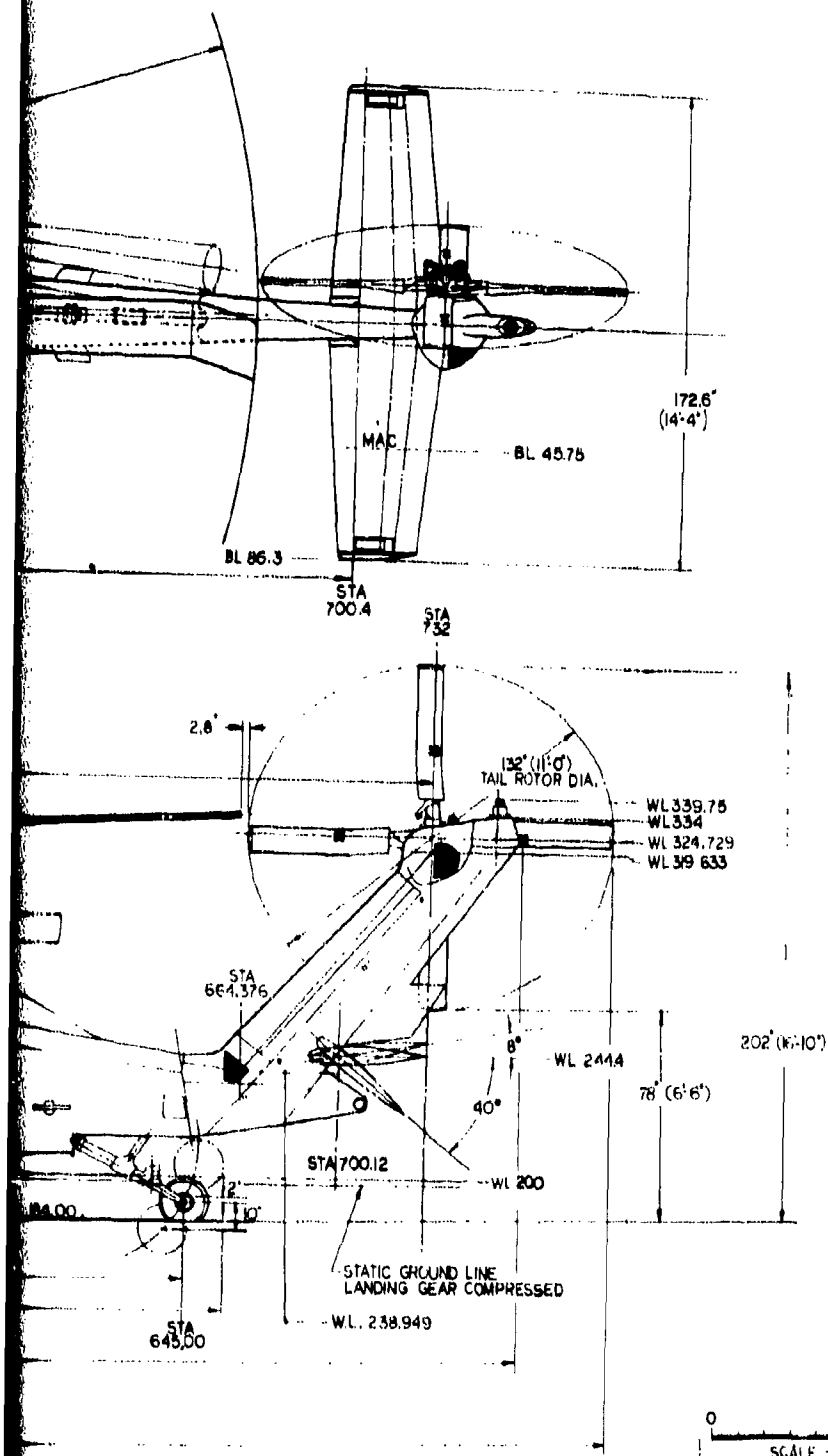


FIGURE 2. GENERAL ARRANGEMENT OF UH60A





MAIN ROTOR DATA

DIAMETER 644' (53' 8")
 BLADES 4
 CHORD 1.73' / 175'
 AIRFOIL SC1095/SC1095R8
 BLADE AREA 1868 FT²
 SOLIDITY 0.826
 TIP SWEEP 20°
 TWIST -18°

TAIL ROTOR DATA

DIAMETER 132' (11' 0")
 BLADES 4
 CHORD .81 FT
 AIRFOIL SC1095
 BLADE AREA 17.82 FT²
 SOLIDITY .875
 TWIST -18°

HORIZONTAL STABILATOR DATA

SPAN 172.6'
 AREA 4.8 FT²
 ROOT CHORD 44 IN
 TIP CHORD 30.5 IN
 SWEEP 1/4 CHORD 0°
 ASPECT RATIO 4.6
 AIRFOIL NACA 0014
 INCIDENCE/DIHEDRAL 0°

VERTICAL STABILIZER DATA

SPAN 98' (8' 2")
 AREA 32.3 FT²
 ROOT CHORD LOWER 72 IN
 TIP CHORD LOWER 58 IN
 ROOT CHORD UPPER 45 IN
 TIP CHORD UPPER 34 IN
 SWEEP 1/4 CHORD 41°
 ASPECT RATIO 1.92
 AIRFOIL (MOD OF) NACA 0021 MODIFIED

LANDING GEAR DATA

	MAIN	TAIL
LOCATION STATION	297.25	645
BUTTLINE	530	0
ROLLING RADIUS	106 IN	6.9 IN
FLAT TIRE RADIUS	7.7 IN	4.5 IN
OUTSIDE DIAMETER	26.00 IN	17.5 IN
TIRE WIDTH	9.5 IN	6.3 IN
TIRE SIZE	26 X 9.5-11	600 X 6

NAME	DATE	REVISION	DATE	REVISION
DESIGNED BY		CHECKED BY		
DRAWN BY		APPROVED BY		
DATE		DATE		
GENERAL ARRANGEMENT				
UH-60A				
Scale: 1/8" = 1'-0"				
78286				

Table 1 shows the total structural weight of each section of the baseline fuselage. Material and labor costs, also shown in Table 1, are given in terms of percentage of the total fuselage cost.

The weight and cost data developed in this study pertain to the fuselages considered. Weight and cost data for complete helicopters resulting from the fuselages are developed by a Helicopter Design Model (HDM) computer program discussed in the Helicopter Design Model section of this report.

TABLE 1. BASELINE UH60A FUSELAGE WEIGHT AND COST DATA

FUSELAGE SECTION	SECTION WEIGHT (LB)	MATERIAL COST (PERCENT)	LABOR COST BREAKDOWN			SECTION COST (PERCENT)
			FABRICATION (PERCENT)	ASSEMBLY (PERCENT)	INSTALLATION (PERCENT)	
Cockpit	330.3	3.1	3.6	2.5	4.8	14.0
Mid-Cabin	995.7	6.8	11.5	8.6	19.1	46.0
Aft-Cabin	295.2	5.7	5.4	5.1	5.8	22.0
Tail Cone	168.0	.6	2.4	.5	2.3	5.8
Pylon	165.0	1.2	1.4	.8	3.1	6.5
Stabilizer	88.6	.3	2.2	.6	2.6	5.7
Total	2042.8					100.0

NOTE: Percent of Total Fuselage

LOW RADAR CROSS SECTION CONFIGURATIONS

Three low radar cross section fuselage configurations for this study were developed by the Applied Technology Laboratory. The first configuration slightly modified the nose section from the baseline configuration; the second configuration changed the fuselage shape along the lines of a truncated triangular prism; the third extended canted flat side shaping throughout the fuselage. The tail surfaces and main rotor pylon fairing were the same as those of the baseline UH60A.

Mold line drawings of the three configurations were used to develop general arrangement drawings for each configuration.

CONFIGURATION 1

The general arrangement of Configuration 1, shown in Figure 3, was developed from mold line drawing No. 20074180. This configuration alters the baseline fuselage forward of the mid-cabin section (the cockpit). Although this configuration is different from the baseline, the internal structure must be compatible with the forward cabin to avoid a heavy joining structure. From Figure 2, the overall length is slightly increased due to this configuration.

CONFIGURATION 2

The general arrangement of Configuration 2, shown in Figure 4, was developed from mold line drawing No. 20074135. This configuration is basically a trapezoidal cross section airframe having sides canted inward 30° and made up of flat exterior structural panels. This configuration is wider at the bottom of the fuselage and narrower at the top of the fuselage than the baseline. This configuration is slightly longer than the baseline UH60A, and its overall height is slightly larger than the baseline. The increased length, width, and height of Configuration 2 does not allow an aircraft of this size to meet the air transportability requirements of the baseline. The narrow upper fuselage causes the pilot and copilot seats to be spaced closer to each other, and shoulder room in the main cabin is decreased. The main cabin floor is approximately 6 inches higher than the baseline from the ground. The increased floor-to-ground height causes difficulties for combat troops to enter or leave the aircraft quickly.

Minor modifications of the mold lines for the transition and tail-cone sections were made to properly house the tail rotor shaft of the baseline UH60A.

CONFIGURATION 3

The general arrangement of Configuration 3, shown in Figure 5, was developed from mold line drawing No. 20074136. This configuration is basically a flat side cross section airframe having sides canted inward 5° and is tapered in width from a narrow cockpit section to a transition section as wide as the baseline UH60A. The tail-cone is a rectangular section which is narrower than the baseline. The narrow cockpit causes the pilot and copilot seats to be spaced closer to each other; space for four-across seating in the main cabin is decreased. The cockpit and main cabin floors are at the same height from the ground as the baseline. The slope of the windshields may cause problems of visibility for the flight crew.

Minor modifications of the mold lines for the transition and tail-cone sections were made to properly house the tail rotor shaft of the baseline UH60A.

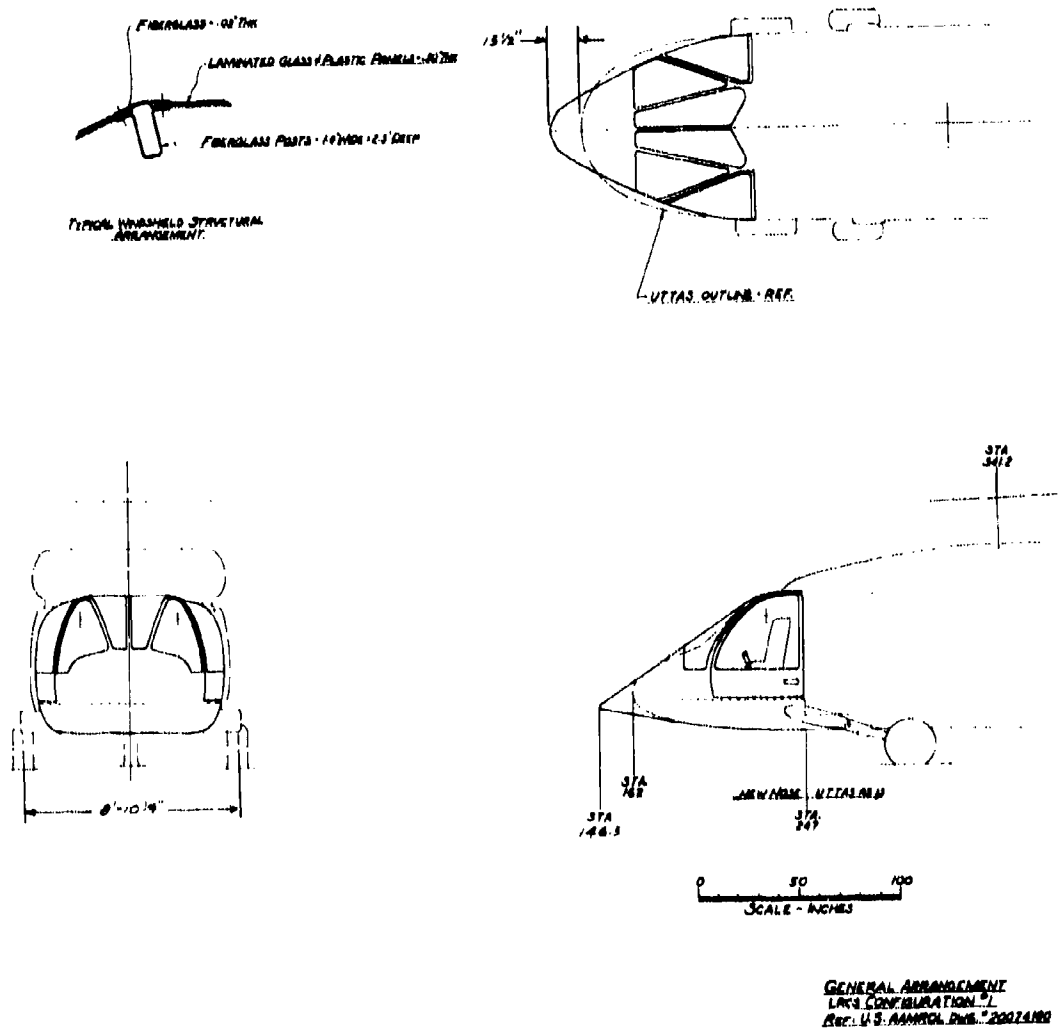


FIGURE 3. GENERAL ARRANGEMENT OF LRC5 CONFIGURATION 1

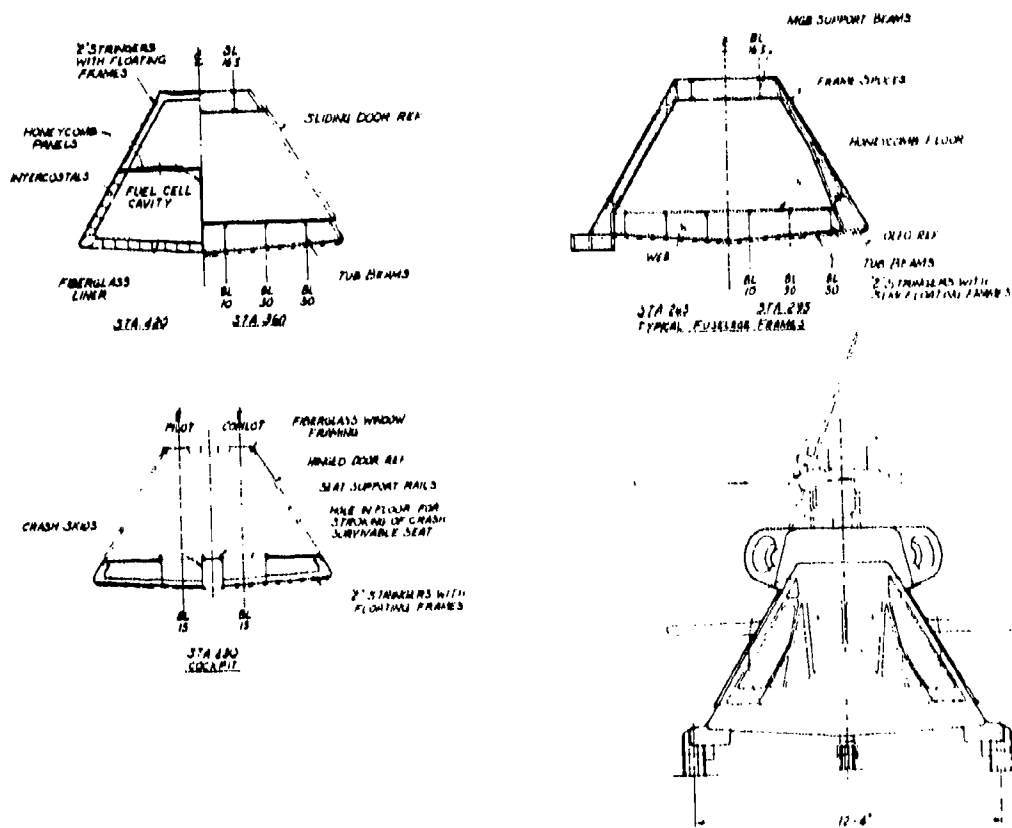
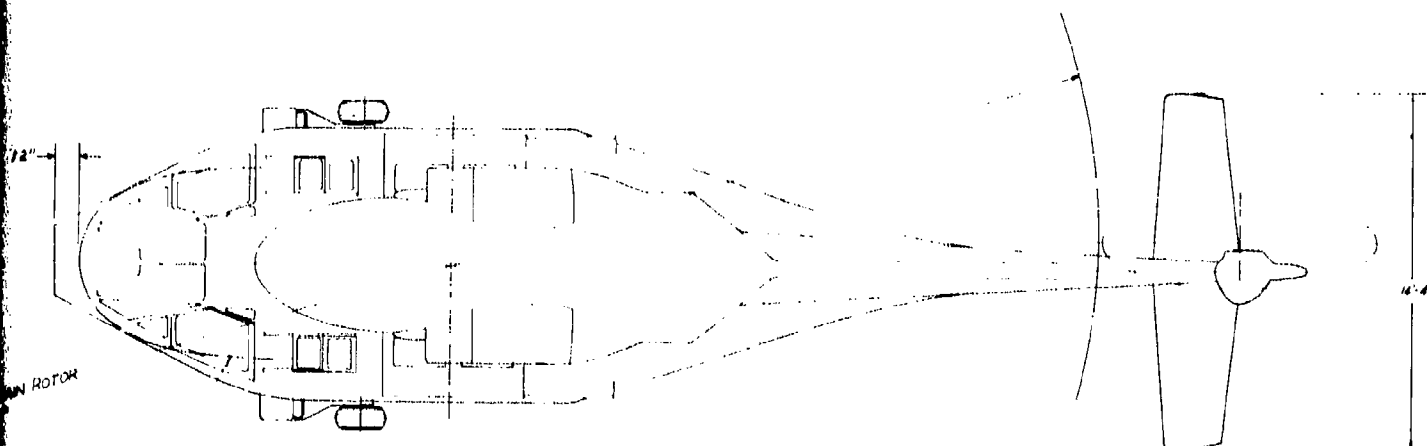
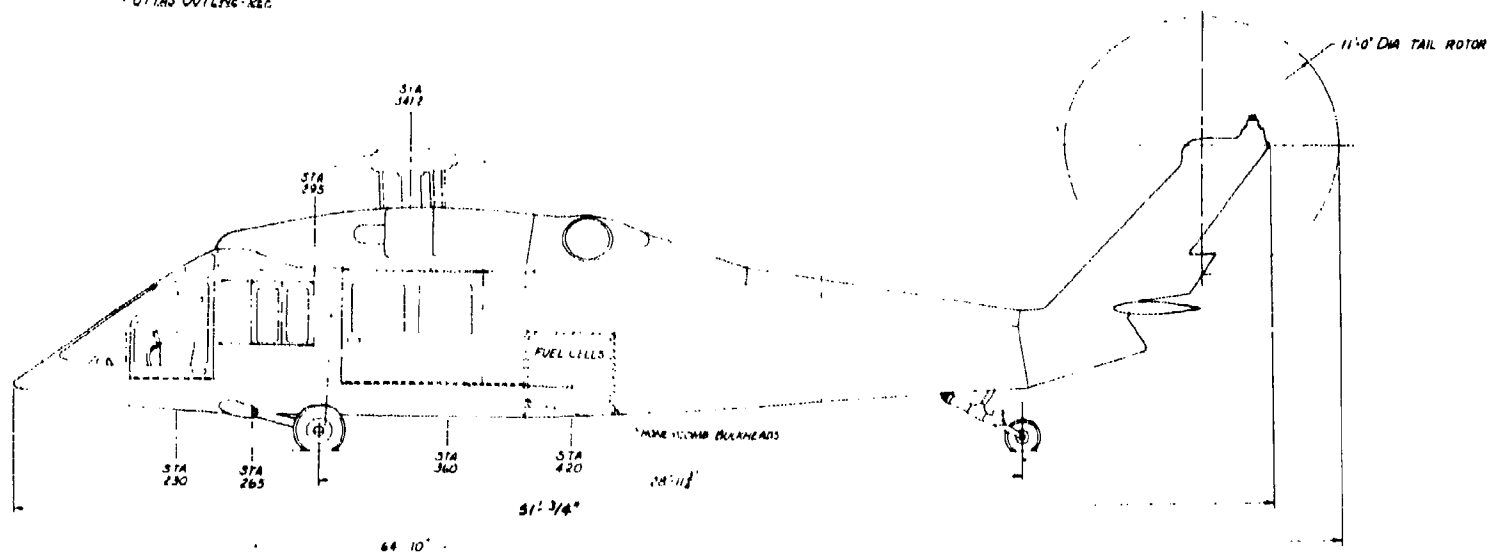


FIGURE 4. GENERAL ARRANGEMENT OF LRCS CONFIGURATION 2



UTTAS OUTLINE - REF



GENERAL ARRANGEMENT
LRCS CONFIGURATION 52
REF: US AMMOL DNR 1988

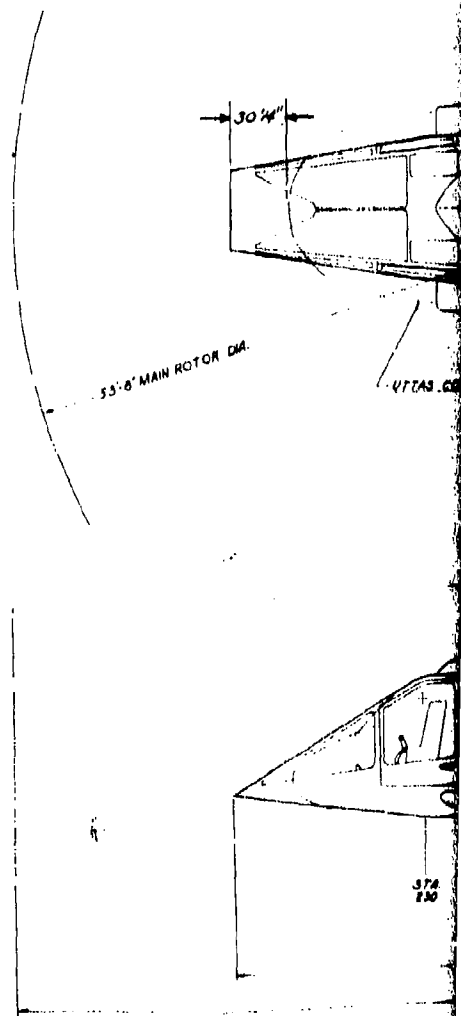
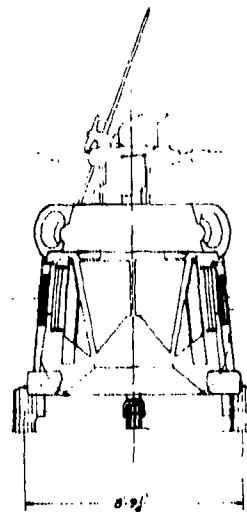
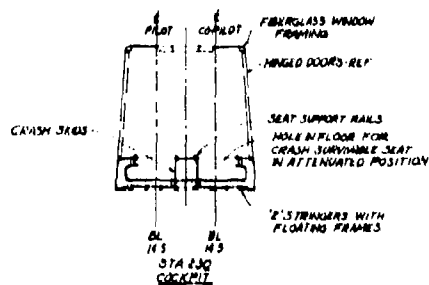
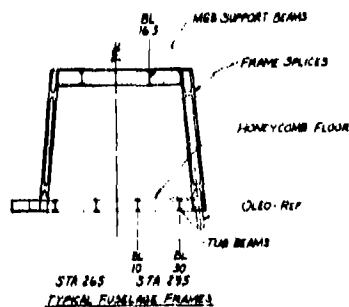
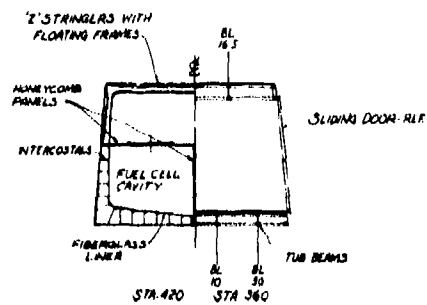
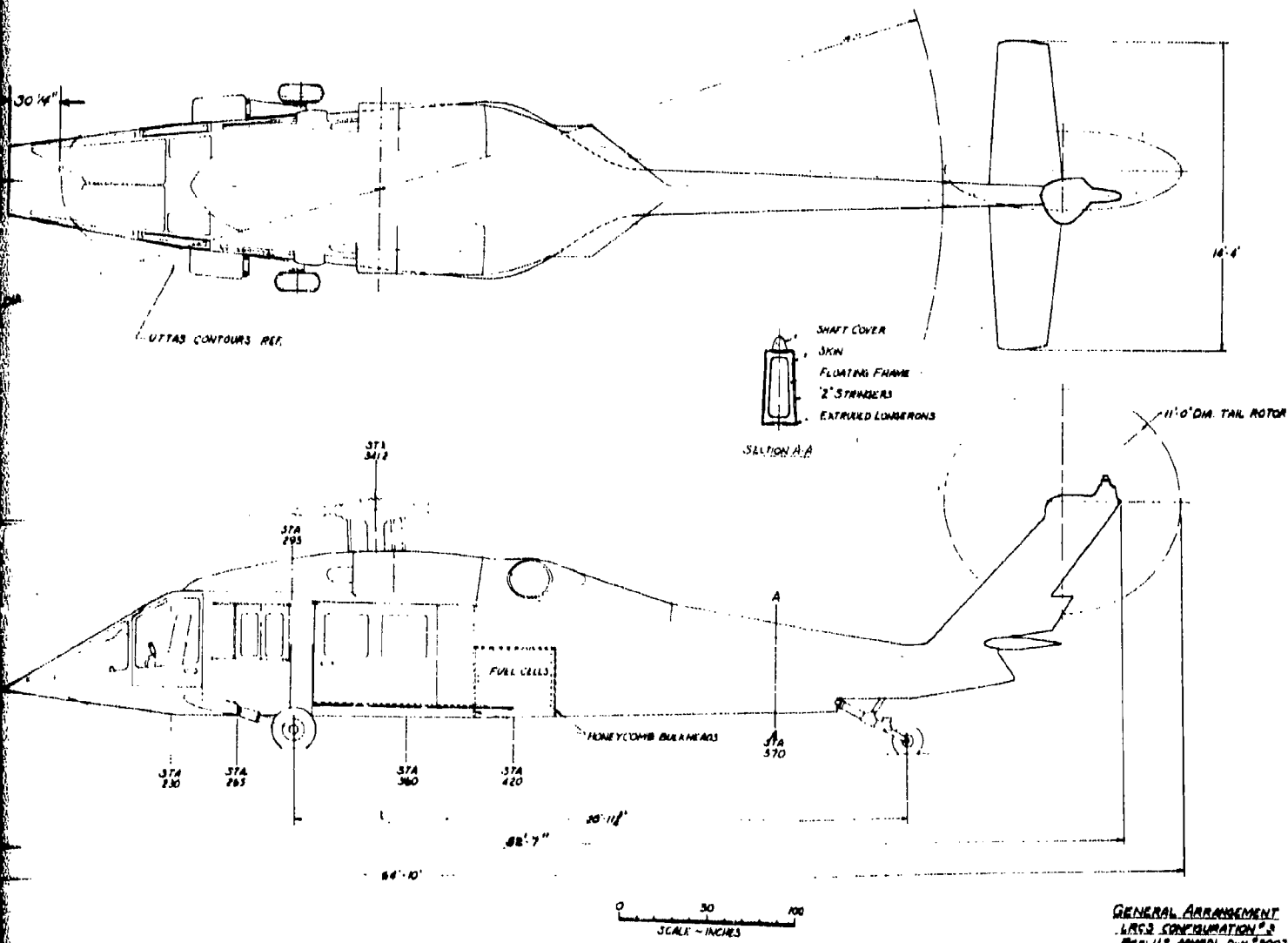


FIGURE 5. GENERAL ARRANGEMENT OF LRCS CONFIGURATION 3



PRELIMINARY DESIGN CONCEPTS
(CONVENTIONAL MATERIALS)

The structural concepts developed are based on current UH60A technology for fuselage construction. The extent of the structural concepts is dependent on the complexity of the RCS shapes. Since the primary purpose of this study was to evaluate the effect on weight and cost resulting from external configurations, it was assumed that the internal structure (beams, frames, bulkheads and intercostals) is of current UH60A design. It was also assumed that no changes occur for the tail pylon and stabilizer.

Four concepts were developed for the three configurations. The first concept was applied to the cockpit canopy framework supporting the windshields of the three configurations. This concept is of molded fiberglass posts and skins as shown in Figure 3 for Configuration 1. This concept is currently used on the UH60A. The other three concepts are applied to the external structure of the lower cockpits of Configurations 1, 2 and 3 and the external structure for the mid-cabin, aft-cabin, and tail cone of Configurations 2 and 3.

Concepts for the external structure are of three designs. The first design is riveted skin/stringer panels on floating frames (Concept A); the second design is riveted skin/stringer panels where the stringer passes through the frames and the skins are riveted to the frames (Concept B). The third design is an external structure of aluminum-faced honeycomb sandwich panels (Concept C) riveted to frames and longerons.

Concepts A, B and C are shown in Figure 6.

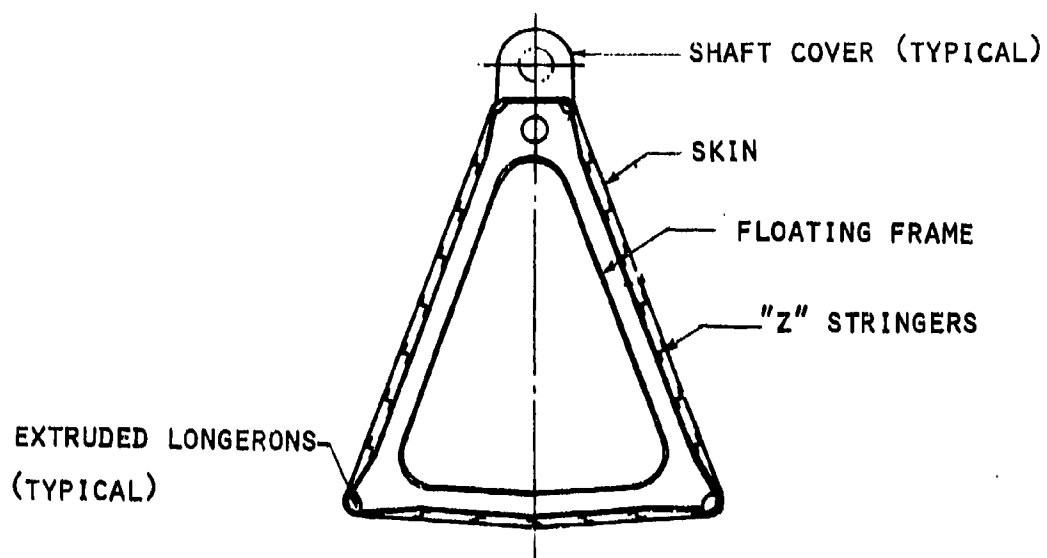
The structural weights for the skin/stringers of Concepts A and B are identical and were predicted using a fuselage shell program.

WEIGHT ANALYSIS

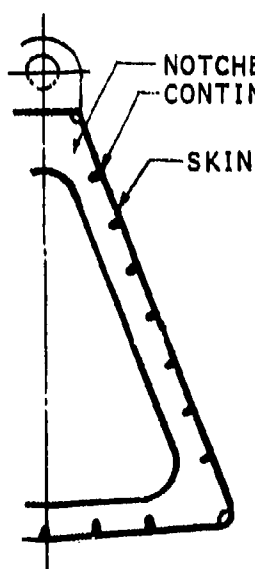
A Fuselage Shell Program (Y076B) was used to predict the weight of skins, stringers, longerons and stabilizing frames of the UH60A and variants of the UH60A for low radar reflectivity. The program uses the following inputs:

1. Shell geometry and frame spacing
2. Loads (shears, moments and torsions)
3. Initial guesses for skin and stringer gages and stringer spacing

With these inputs, the program iterates for the optimum skin and stringer gages, which are assumed to occur when a fully stressed design is reached (applied stresses are equal to the allowable stresses). The output consists of a bay-by-bay breakdown of the skin and stringer gages, as well as weights, for the critical flight and ground load conditions.

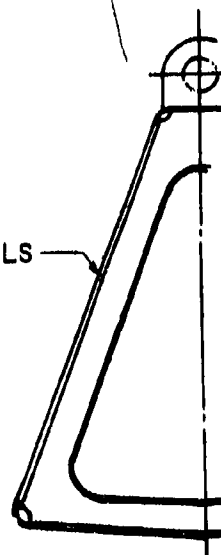


CONCEPT A



CONCEPT B

HONEYCOMB PANELS



CONCEPT C

FIGURE 6. STRUCTURAL CONCEPTS A, B AND C

In its present form, the program can analyze rectangular shell cross sections only. Therefore, when used to predict sizes for the baseline UH60A, a rectangular shell cross section having approximately the same perimeter as the actual cross section is used. Using standard Sikorsky stringers (used on UH60A), the predicted weights for skins, stringers and longerons are then correlated to the latest UH60A weights to obtain non-optimum factors. These factors are then applied to the RCS configurations so that a proper weight comparison for all the fuselage cross sections can be made.

The design of main frames to support local loads requires separate analysis and is not considered in this study. Instead, weight deltas over the UH60A baseline are estimated using frame weights to maintain shell stability obtained from the Fuselage Shell Analysis Program (Y076B) and based on correlated test information on cylindrical shells subjected to torsion and bending. Weight increments for each RCS configuration are obtained by taking the weight difference of stabilizing frames and applying a 10% installation factor. These deltas are +31.8 for RCS Configuration 2 and +0.4 for RCS Configuration 3.

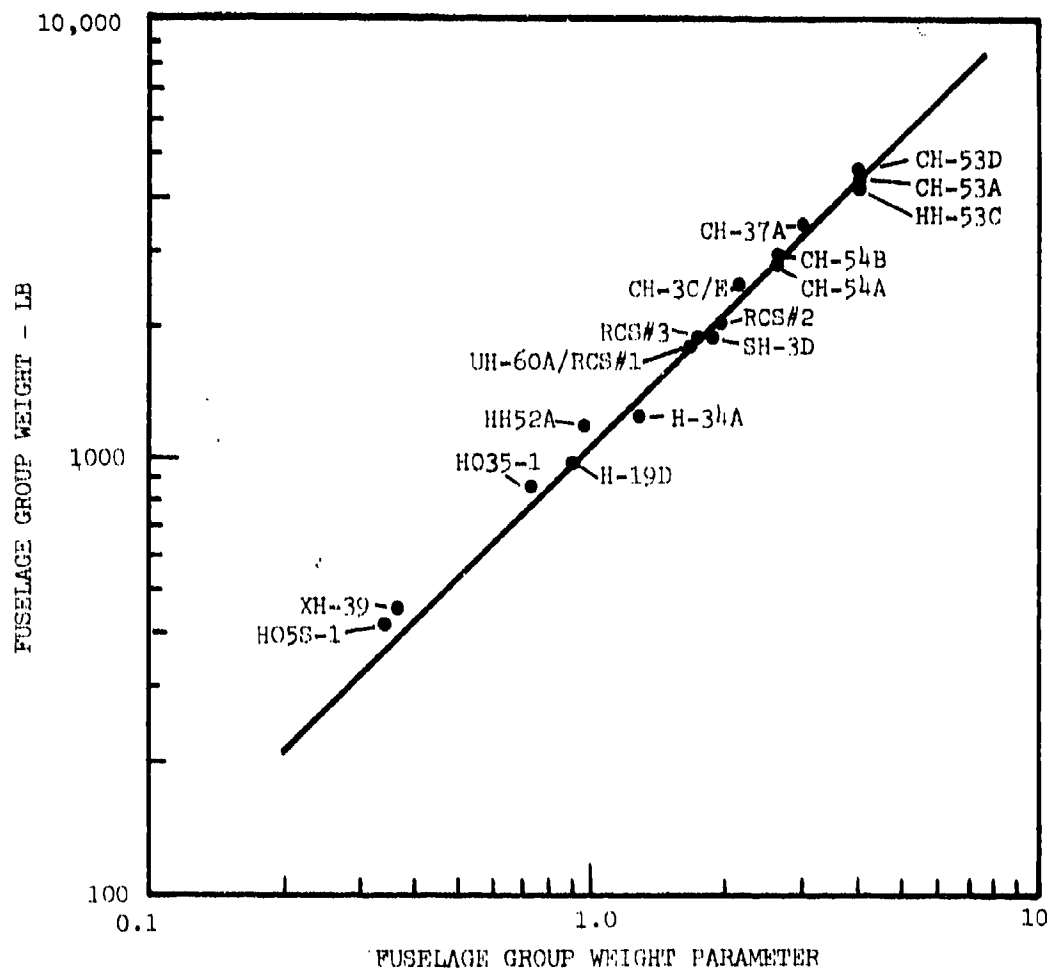
Weight deltas for each cockpit configuration are based on configuration and wetted area changes over the baseline UH60A cockpit which weighs 330.3 lb for 150 ft² of wetted area, or 2.2 psf. Wetted areas for RCS Configurations 1, 2 and 3 are 146, 158 and 157 ft², respectively, yielding weight deltas of -8.8, +17.6 and +15.4 lb, respectively. To verify these statistical deltas and to include effects of configuration changes, a further weight check was made by comparing cockpit component weights for primary structure (skins, stringers, frames), windshield, doors, cockpit enclosure, floor and supports, windows, etc.

Floor panels are treated separately from floor support beams. Weight deltas for floor panels are based on floor area changes for each RCS configuration using 1.014 psf for the personnel portion (Sta. 247-288) and 1.63 psf for the cargo portion (Sta. 288-398), as in the baseline UH60A. Weight deltas for floor support beams are estimated from analytical weight equations derived from stress relationships for beam webs and caps.

To verify the total body group weight deltas for each RCS configuration, a statistical weight derivation was made using the statistical body group equation based on Sikorsky models. The statistical data is shown in Figure 7.

The weight of honeycomb skin panels, Concept C, was determined as follows:

1. The weights of the skins and stringers for the baseline UH60A were obtained from Reference 1 for each section of the fuselage, and a percentage of skin/stringer weight to section weight was derived as shown in Table 2. The percentage of skin/stringer weight for the baseline cockpit was applied to the cockpits of Configurations 2 and 3. The skin/stringer weights for the other sections of Configurations 2 and 3 were obtained from the fuselage shell program and are shown in Tables 3 and 4.



$$\left(\frac{NzSGW}{10,000} \right)^{0.3056} \left(\frac{s}{1000} \right)^{0.875} \left(\frac{1 + \Delta F}{14.7} \right)^{0.33} \left(\frac{q}{100} \right)^{0.05}$$

FIGURE 7. BODY GROUP WEIGHT VERSUS BODY GROUP WEIGHT PARAMETERS

2. From the preliminary weight analysis of Concepts A and B, a minimum skin gage of .025 in. and a minimum stringer gage of .032 in. were obtained. For an aluminum skin/stringer panel 12 in. by 20 in. (aluminum density of 0.1 lb/in.³), the weight is:

$$\text{Skin } 12 \text{ in.} \times 20 \text{ in.} \times .025 \text{ in.} \times .1 \text{ lb/in.}^3 = .58 \text{ lb.}$$

Stringer (2 standard Sikorsky aluminum stringers with a cross-sectional area of .059 in.² each)

$$2 \text{ in.} \times 20 \text{ in.} \times .059 \text{ in.} \times .1 \text{ lb/in.}^3 = .24 \text{ lb.}$$

$$\text{Total } .82 \text{ lb.}$$

3. A review was conducted to determine the minimum sheet facing thickness for the external honeycomb structure. The minimum gages used by Sikorsky Aircraft on military helicopters are .016 in. for the outer face and .008 in. for the inner face. The honeycomb core was considered to be 1/4 in. thick at 4 lb/ft³ (density), the minimum considered practicable from manufacturing considerations. For a 12-in. by 20-in. minimum gage honeycomb skin panel, the weight is:

$$\text{Facings } 12 \text{ in.} \times 20 \text{ in.} \times (.016 \text{ in.} + .008 \text{ in.}) \times .1 \text{ lb/in.}^3 = .576 \text{ lb.}$$

$$\text{Core } \frac{.25 \times 12 \times 20 \times 4}{1728} = .134 \text{ lb.}$$

Adhesive (.06 lb/ft²/surface)

$$\frac{.06 \times 2 \times 12 \times 20}{144} = .200 \text{ lb.}$$

Close out (2 edges - 12 in.)

$$1.25 \text{ in.} \times 12 \text{ in.} \times 2 \text{ in.} \times .008 \text{ in.} \times .1 \text{ lb/in.}^3 = .020 \text{ lb.}$$

$$\text{Total } .930 \text{ lb.}$$

TABLE 2. BASELINE FUSELAGE SKIN/STRINGER WEIGHT
FROM WEIGHT AND BALANCE REPORT

SECTION	TOTAL WEIGHT (LB)	WETTED AREA (FT ²)*	SKIN/STRINGER WEIGHT (LB)	SKIN/STRINGER WEIGHT (PERCENT)
Cockpit	330.3	150	39.6	11.9
Mid-Cabin	995.7	350	137.8	13.8
Aft-Cabin	295.3	180	136.2	46.1
Tail Cone	168.0	139	123.7	73.6
*Tail Surfaces and Miscellaneous 85 Ft ²				

TABLE 3. CONFIGURATION 2A AND 2B SKIN/STRINGER WEIGHT

SECTION	TOTAL WEIGHT (LB)	WETTED AREA (FT ²)*	SKIN/STRINGER WEIGHT (LB)	SKIN/STRINGER WEIGHT (PERCENT)
Cockpit	347.9	158	41.7	11.9
Mid-Cabin	1135.3	385	156.5	13.8
Aft-Cabin	354.8	234	198.5	55.9
Tail Cone	173.9	161	143.3	82.4
*Tail Surfaces and Miscellaneous 118 Ft ²				

TABLE 4. CONFIGURATION 3A AND 3B SKIN/STRINGER WEIGHT

SECTION	TOTAL WEIGHT (LB)	WETTED AREA (FT ²)*	SKIN/STRINGER WEIGHT (LB)	SKIN/STRINGER WEIGHT (PERCENT)
Cockpit	345.7	151	41.4	11.9
Mid-Cabin	1017.0	345	134.8	13.3
Aft-Cabin	324.1	213	173.1	53.4
Tail Cone	168.3	142	126.4	74.6
*Tail Surfaces and Miscellaneous 91 Ft ²				

Therefore, the minimum weight honeycomb skin panel is 13 percent heavier than the minimum skin/stringer panels of Concepts A and B. The honeycomb skin weights are shown in Tables 5 and 6.

The 13 percent increase was applied to each skin/stringer weight of each configuration (Configurations 2 and 3) to obtain a section weight using Concept C. The section baseline weight was subtracted and a Δ weight was obtained for Concept C.

COST ANALYSIS

The estimated change in cost for each configuration and concept was based upon the change in costs of material and labor. The material costs include the cost of sheet stock, raw forgings and extruded or rolled shapes. This cost is then given in terms of cost per pound of structural weight. The labor costs are total labor hours required to fabricate the details from materials, to assemble the details, and then to install the assembly. For this study, labor costs are based on the wetted area of the structure being fabricated.

The changes in cost for each section of Configurations 1, 2 and 3 were estimated as follows:

Change in section cost:

Material cost + labor cost - baseline cost

An example is given as follows:

Configuration 2A mid-cabin (Table 8)

Material cost change:

$$.068 \text{ (Table 1)} \frac{1135.3 \text{ (Table 3)}}{995.7 \text{ (Table 1)}} = .0775 \text{ (Mat'l Cost, \%)}$$

$$\Delta \text{ cost} = .0775 - .068 = .0095 = .95\%$$

Labor cost change:

$$\frac{385 \text{ (Table 3)}}{350 \text{ (Table 2)}} \times (.115 + .86 + .191) \text{ (Table 1)} = .4312 \text{ (Labor Cost, \%)}$$

$$\Delta \text{ cost} = .4312 - .392 = .0392 = 3.92\%$$

Section cost change:

$$.0775 + .4312 = .5087 \text{ (Section Cost, \%)}$$

$$\begin{aligned} \Delta \text{ cost} &= .5087 - .46 \text{ (Table 1)} = .0487 \\ &= 4.87\% \end{aligned}$$

Percent cost Δ from baseline is:

$$.0487 \text{ (.46)} = .0224 = 2.24\%$$

Concept B is the same basic design and weight as Concept A, but it is fabricated by a slightly different method. For Concept B, stringer clips are fabricated, and frame cutouts with joggles are formed during detail fabrication. During assembly, the skin/stringer combination is fitted to the frames.

The material costs of Concept B are the same as those of Concept A. The labor costs are approximately 10 percent greater than Concept A for detail fabrication and assembly. Installation costs were assumed to be equal.

The cost changes for the honeycomb sandwich skins (structural Concept C) were developed for Configurations 2 and 3.

The cost of honeycomb sandwich skins is based on the following:

1. Detail fabrication, assemble and bond, 1.11 hr/ft^2
2. Materials, $\$6.50/\text{ft}^2$

For conventional skin/stringers (Concept A)

1. Detail fabrication, 1 hr/ft^2
2. Assemble and automatic rivet, $.19 \text{ hr/ft}^2$
3. Material, $\$2.14/\text{ft}^2$

TABLE 5. CONFIGURATION 2C HONEYCOMB PANEL SKIN WEIGHT

SECTION	TOTAL WEIGHT (LB)	HONEYCOMB PANEL SKIN WEIGHT (LB)	HONEYCOMB SKIN WEIGHT (PERCENT)
Cockpit	353.3	47.1	13.3
Mid-Cabin	1155.6	176.8	15.2
Aft-Cabin	380.6	224.3	58.9
Tail Cone	192.5	161.9	84.1

TABLE 6. CONFIGURATION 3C HONEYCOMB PANEL SKIN WEIGHT

SECTION	TOTAL WEIGHT (LB)	HONEYCOMB PANEL SKIN WEIGHT (LB)	HONEYCOMB SKIN WEIGHT (PERCENT)
Cockpit	350.9	46.7	13.3
Mid-Cabin	1034.5	152.3	14.7
Aft-Cabin	346.6	195.6	56.4
Tail Cone	185.7	142.8	76.8

Based upon an assumed labor cost of \$22.50 per hour (Reference 2), the cost per square foot of honeycomb is

$$1.11 \times 22.50 + 6.50 = \$31.48$$

For skin/stringer panels

$$(1 + .19) 22.50 + 2.14 = \$28.92$$

The honeycomb panel is 8.8 percent more expensive than the skin/stringer panel to fabricate and assemble. The installation costs are assumed to be equal. The material cost for the honeycomb panels is

$$\$6.50/.93 = \$6.85/lb$$

For skin/stringer panels, the material cost is

$$\$2.14/.82 = \$2.61/lb$$

Material cost for honeycomb panels is 164 percent more than for skin/stringer panels. The increased material costs are due primarily to the honeycomb core, which can be between 3 and 10 dollars per square foot.

Labor costs for honeycomb panels are 7 percent less than skin/stringer panels for the cockpit, aft-cabin and tail-cone sections. The labor costs for honeycomb panels in the mid-cabin section are 5 percent greater than conventional construction due to structural inserts and local reinforcing required to mount the many components attached to the mid-cabin.

APPLICATION OF DESIGN CONCEPTS TO LOW RADAR CROSS SECTION FUSELAGES

CONFIGURATION 1

The structure of Configuration 1 could not be changed since the structure must match the mid-cabin of the baseline and not alter the baseline mid-cabin structure. The change in weight and the percentage change in cost for Configuration 1, from the baseline, are shown in Table 7.

CONFIGURATIONS 2 AND 3

The three structural concepts developed are applicable, as shown in Figures 3, 4 and 5, to the lower cockpit, mid-cabin, aft-cabin and tail cone of Configurations 2 and 3. Tables 8 through 13 show the changes in weight and the percentage change in costs for Configurations 2 and 3 using Concepts A, B and C.

The percentage change of the cost of each section of Configurations 2 and 3 is based on the difference of the sum of material and labor costs from the baseline section cost divided by the baseline section cost.

The percentage change for each configuration fuselage cost is based on the sum of the cost change for each section.

TABLE 7. CONFIGURATION 1. FUSELAGE WEIGHT AND COST DATA

FUSELAGE SECTION	SECTION Δ WEIGHT (LB)	SECTION COST Δ FROM BASELINE			COST Δ TOTAL BASELINE FUSELAGE
		MATERIAL (PERCENT)	TOTAL LABOR (PERCENT)	SECTION COST (PERCENT)	
Cockpit	- 8	- .093	- .353	- .318	- .00063
Mid-Cabin	0	0	0	0	0
Aft-Cabin	0	0	0	0	0
Tail Cone	0	0	0	0	0
Pylon	0	0	0	0	0
Stabilizer	0	0	0	0	0
Total	- 8				- .00063

TABLE 8. CONFIGURATION 2A FUSELAGE WEIGHT AND COST DATA

FUSELAGE SECTION	SECTION Δ WEIGHT (LB)	SECTION COST Δ FROM BASELINE			COST Δ TOTAL BASELINE FUSELAGE (PERCENT)
		MATERIAL (PERCENT)	TOTAL LABOR (PERCENT)	SECTION COST (PERCENT)	
Cockpit	18	.15	.54	.35	.05
Mid-Cabin	140	.95	3.92	4.87	2.24
Aft-Cabin	59	1.15	5.00	6.00	1.32
Tail Cone	6	.02	.62	.64	.04
Pylon	0	0	0	0	0
Stabilizer	0	0	0	0	0
Total	223				3.65

TABLE 9. CONFIGURATION 2B FUSELAGE WEIGHT AND COST DATA

FUSELAGE SECTION	SECTION Δ WEIGHT (LB)	SECTION COST Δ FROM BASELINE			COST Δ TOTAL BASELINE FUSELAGE (PERCENT)
		MATERIAL (PERCENT)	TOTAL LABOR (PERCENT)	SECTION COST (PERCENT)	
Cockpit	18	.15	.56	.36	.05
Mid-Cabin	140	.95	4.13	5.08	2.31
Aft-Cabin	59	1.15	5.32	6.42	1.42
Tail Cone	6	.02	.65	.67	.05
Pylon	0	0	0	0	0
Stabilizer	0	0	0	0	0
Total	223				3.83

TABLE 10. CONFIGURATION 2C FUSELAGE WEIGHT AND COST DATA

FUSELAGE SECTION	SECTION Δ WEIGHT (LB)	SECTION COST Δ FROM BASELINE			COST Δ TOTAL BASELINE FUSELAGE (PERCENT)
		MATERIAL (PERCENT)	TOTAL LABOR (PERCENT)	SECTION COST (PERCENT)	
Cockpit	23	.79	.49	.31	.04
Mid-Cabin	160	2.52	10.00	9.31	4.51
Aft-Cabin	85	7.41	6.85	6.78	1.24
Tail Cone	25	.85	1.08	1.07	.07
Pylon	0	0	0	0	0
Stabilizer	0	0	0	0	0
Total	293				5.86

TABLE 11. CONFIGURATION 3A FUSELAGE WEIGHT AND COST DATA

FUSELAGE SECTION	SECTION Δ WEIGHT (LB)	SECTION COST Δ FROM BASELINE			COST Δ TOTAL BASELINE FUSELAGE (PERCENT)
		MATERIAL (PERCENT)	TOTAL LABOR (PERCENT)	SECTION COST (PERCENT)	
Cockpit	15	.15	.04	.14	.02
Mid-Cabin	21	.14	- .52	- .39	- .18
Aft-Cabin	29	.55	2.99	3.54	.78
Tail Cone	.3	.08	.09	.10	0
Pylon	0	0	0	0	0
Stabilizer	0	0	0	0	0
Total	65.3				.62

TABLE 12. CONFIGURATION 3B FUSELAGE WEIGHT AND COST DATA

FUSELAGE SECTION	SECTION Δ WEIGHT (LB)	SECTION COST Δ FROM BASELINE			COST Δ TOTAL BASELINE FUSELAGE (PERCENT)
		MATERIAL (PERCENT)	TOTAL LABOR (PERCENT)	SECTION COST (PERCENT)	
Cockpit	15	.15	.05	.27	.04
Mid-Cabin	21	.14	- .48	- .35	- .17
Aft-Cabin	29	1.25	3.01	4.35	.80
Tail Cone	.3	.08	.10	.11	0
Pylon	0	0	0	0	0
Stabilizer	0	0	0	0	0
Total	65.3				.67

TABLE 13. CONFIGURATION 3C FUSELAGE WEIGHT AND COST DATA

FUSELAGE SECTION	SECTION Δ WEIGHT (LB)	SECTION COST Δ FROM BASELINE			COST Δ TOTAL BASELINE FUSELAGE (PERCENT)
		MATERIAL (PERCENT)	TOTAL LABOR (PERCENT)	SECTION COST (PERCENT)	
Cockpit	20	.79	1.17	.96	.14
Mid-Cabin	39	1.65	9.17	8.47	4.04
Aft-Cabin	51	7.33	3.83	3.91	.71
Tail Cone	18	.91	- .14	.01	0
Pylon	0	0	0	0	0
Stabilizer	0	0	0	0	0
Total	128				4.89

DESCRIPTION OF EVALUATION FOR FAIL-SAFETY,
SAFETY AND MAINTAINABILITY

FAIL-SAFETY

The three configurations meet the following fail-safety requirements of the baseline UH60A:

1. The ability to sustain limit load with the loss of a single structural component.
2. Ease of access for inspection of the fuselage.

CRASH SAFETY/SAFETY

A relative evaluation was made of each configuration for crash safety and safety. For crash safety the criteria were:

1. Noseover due to plowing
2. Rollover
3. High impact on landing
4. Side impact

For safety:

1. Crew visibility
2. Egress
3. Hazards to protrusion

MAINTAINABILITY

An evaluation of maintainability was made for Configurations 1, 2 and 3 based on the ease of maintaining the fuselages due to the overall shape and size.

For Configuration 1 (cockpit only), the following is noted:

1. The number of window pieces is reduced from 9 to 6 compared to the baseline; this should improve maintainability slightly.
2. There is a slight narrowing of the nose section which may cause relocation of components or reduce spacing between components. This may reduce access and degrade maintainability.

The overall ranking is 5.

For Configuration 2, the following is noted:

1. The number of window pieces in the cockpit is reduced from 9 to 8 compared to the baseline; however, some panels are larger than the baseline which may cause them to be more susceptible to cracking.

The maintainability is decreased compared to the baseline.

2. Relocation of all electrical/avionics components from the cockpit section is necessary. The wider fuselage should provide good space for access, and possibly shorter wiring harnesses may result. The maintainability is judged to be equal to the baseline.
3. Deeper tub section may provide space for components with better in-place access. Access to the tub section will depend on the design. The maintainability is judged to be equal to the baseline.
4. Reduced volume in the cockpit above the floor may reduce access in a crowded area. This is a negative effect on maintainability.
5. The cabin side windows may have less chance to fall out, thus fewer maintenance actions compared to the baseline.
6. The fuselage has a larger skin area; however, flat panels are perhaps easier to repair compared to the slightly curved panel of the baseline.

The overall ranking is 5.

For Configuration 3, the following is noted:

1. The number of window pieces in the cockpit is reduced from 9 to 6 compared to the baseline. However, a few panels are larger than those of Configuration 2 and the baseline. The larger panels have a negative effect on maintainability.
2. Reduced cockpit space allows less access compared to the baseline.
3. Relocation of electrical/avionics from the cockpit section into a more restricted fuselage will probably reduce access.
4. Reduced tail-cone width reduces access to controls and components in this area.

The overall ranking is 4.2.

The ranking method used was the same as that described in Reference 2. The results are summarized in Tables 14 and 15.

Table 15 is a summary of weight and percentage cost changes compared to the baseline fuselage. Also shown are total wetted fuselage areas and ranking for fail-safety, safety and maintainability.

TABLE 14. SAFETY AND CRASH-SAFETY RANKING

	BASELINE	CONFIGURATION 1	CONFIGURATIONS 2A, B, C	CONFIGURATIONS 3A, B, C
<u>Safety</u>				
Crew Visibility	5	4	3	4
Egress	5	5	3	5
Hazards	<u>5</u>	<u>5</u>	<u>3</u>	<u>6</u>
	5	4.6	3	5
<u>Crash Safety</u>				
Maneuver	5	4	3	4
Rollover	5	5	3	4
Impact Landing (Gear)	5	5	4	5
Side Impact	<u>5</u>	<u>5</u>	<u>6</u>	<u>3</u>
	5	4.75	3.2	3.2
Overall Safety	5	4.6	3.1	4.1

TABLE 15. SUMMARY OF FUSELAGE WEIGHT AND COST DATA OF CONVENTIONAL CONSTRUCTION

CONFIGURATION	WEIGHTED AREA (FT ²)	Δ WEIGHT (LB)	A COST (PERCENT)	FAIL-SAFETY	SAFETY	MAINTAINABILITY
Baseline	904	0	0	5	5	5
1	900	- 8	- .00063	5	4.6	5
2A	1056	223	3.65	5		
2B	1056	223	3.83	5	3.1	5
2C	1056	293	5.86	5		
3A	942	65.3	.62	5		
3B	942	65.3	.67	5	4.1	4.2
3C	942	128	4.89	5		

MODIFICATION OF CONFIGURATION 2

A study was made to determine the effect of lowering the cabin floor and ceiling 6 inches. Lowering the floor 6 inches placed the floor at the same waterline as the baseline fuselage; lowering the ceiling 6 inches maintained the same cargo door and opening as the baseline and Configuration 2. The change in weight due to lowering the floor is shown in Table 16 for the lower floor of Configuration 2 and the original floor of Configuration 2.

TABLE 16. FLOOR WEIGHT COMPARISON FOR CONFIGURATION 2

STRUCTURE	CONFIGURATION 2 Δ WEIGHT (LB)	LOWER FLOOR Δ WEIGHT (LB)
Floor Panels	41.7	69.3
Beams & Supports	5.5	2.1
Total	47.2	71.4

Based upon the data of Table 16, lowering the floor 6 inches increases the fuselage weight of Configuration 2. Material and labor costs would be increased due to the increase of floor weight and area. As a result of increased weight and costs, Configuration 2 was not changed for this study.

SELECTED CONCEPTS

Based upon the summary of Fuselage Weight and Cost (Table 15), Concept A was selected for further evaluation. Concept A (floating frame concept) is the lowest in cost, compared to Concepts B and C; also, the weight of Concept A is equal to or less than that of Concepts B and C.

ADVANCED MATERIAL APPLICATION

Advanced composite materials can be used in the construction of the three fuselage shapes considered in this study. Studies, as reported in References 2 and 3, have shown that the use of composite materials can reduce both fuselage weight and cost. The fuselages of this study are relatively lightly loaded compared to fixed-wing aircraft. To efficiently use advanced materials in the fuselages, very light composite skins are used in the post-buckled stress state. Frames and stringers of the fuselages would be constructed of stabilized composites to develop the full-strength capabilities of the materials.

The stabilized composite structural members and the thin composite skins can be molded as a single structural assembly such as sides, top and bottom to form a fuselage section. The fuselages constructed of advanced materials are shown in Figures 8 and 9 for Configurations 2 and 3.

The cockpits of Configurations 1, 2 and 3 are constructed from two assemblies, the cockpit enclosure and the lower cockpit tub. The cockpit enclosure is the framework and skins that support the windshields and windows. The lower tub supports the seats, controls and equipment.

The enclosure framework is constructed of advanced materials using 75 percent Kevlar and 25 percent graphite/epoxy to replace the fiberglass/epoxy used for conventional construction. The weight savings is 22 percent as shown in Reference 2.

A structural weight breakdown for the conventional cockpit structures is shown in Table 17.

Tables 18, 19, and 20 compare the structural weight of the cockpit of the three configurations for conventional construction and advanced material.

FRAMES

There are two basic types of frames used in airframe structure. One type of frame is used to provide the shape of the cross section and to support the stringers. This type of frame is usually of thin gage aluminum formed as a "C" section. The other type of frame is used to transfer high concentrated load to the fuselage shell. This type of frame is made up of forged sections, or built up from extruded members.

The tail cones are made up of the formed frames. The cabin and transition sections are constructed of the built-up frames.

-
3. Rich, M. J., Ridgley, G. F., and Lowry, D. W., APPLICATION OF COMPOSITES TO HELICOPTER AIRFRAME AND LANDING GEAR STRUCTURES, Sikorsky Aircraft Div., NASA Technical Report CR-112333, National Aeronautics and Space Administration, NASA-Langley Research Center, Hampton, Virginia, June 1973.

The weight of a formed frame is .0128 lb/in. (Reference 2). A foam stabilized frame, which must match the stiffness of a formed aluminum frame, weighs .0115 lb/in. (Reference 2). The weight savings for the tail cone frames is 10%.

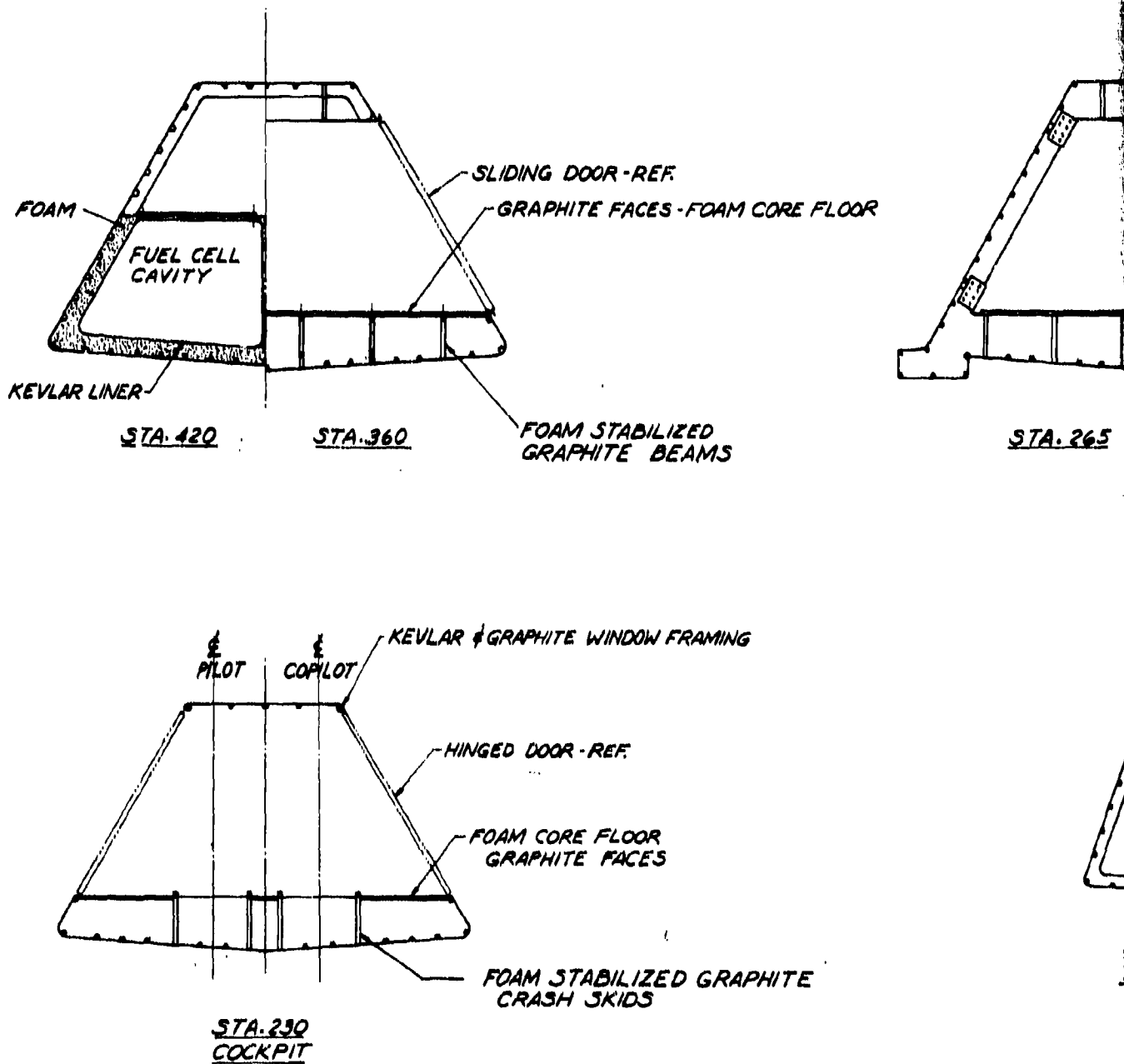
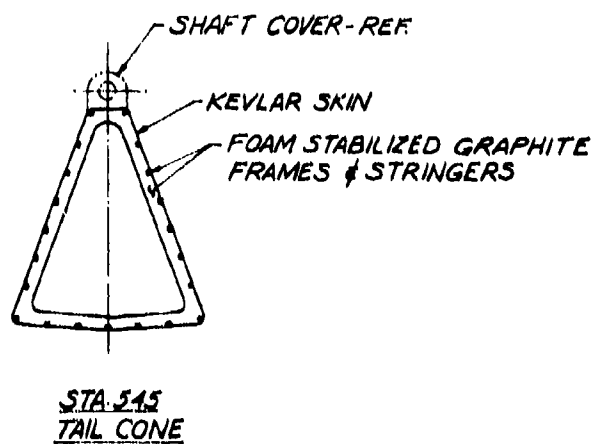
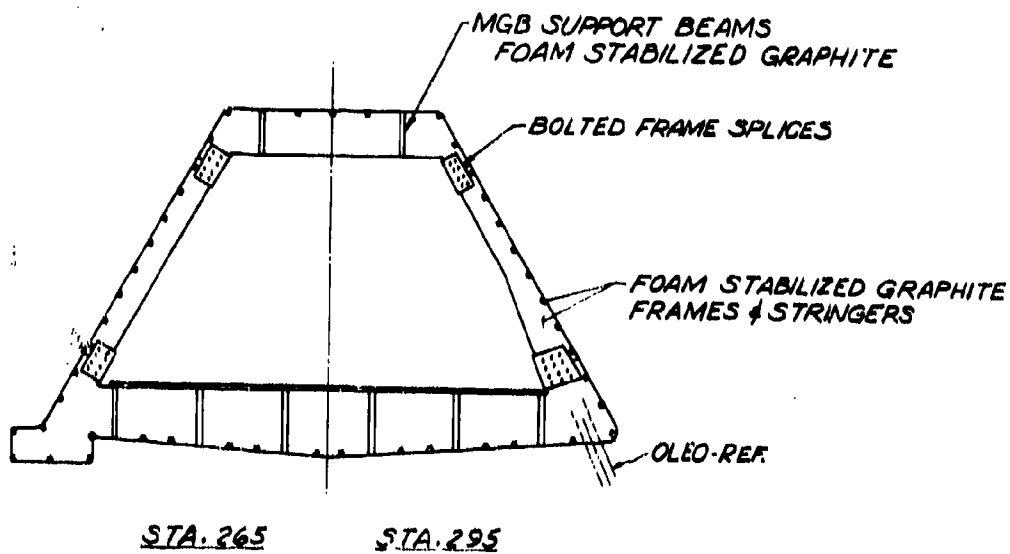


FIGURE 8. ADVANCED MATERIALS APPLICATION FOR CONFIGURATION 2



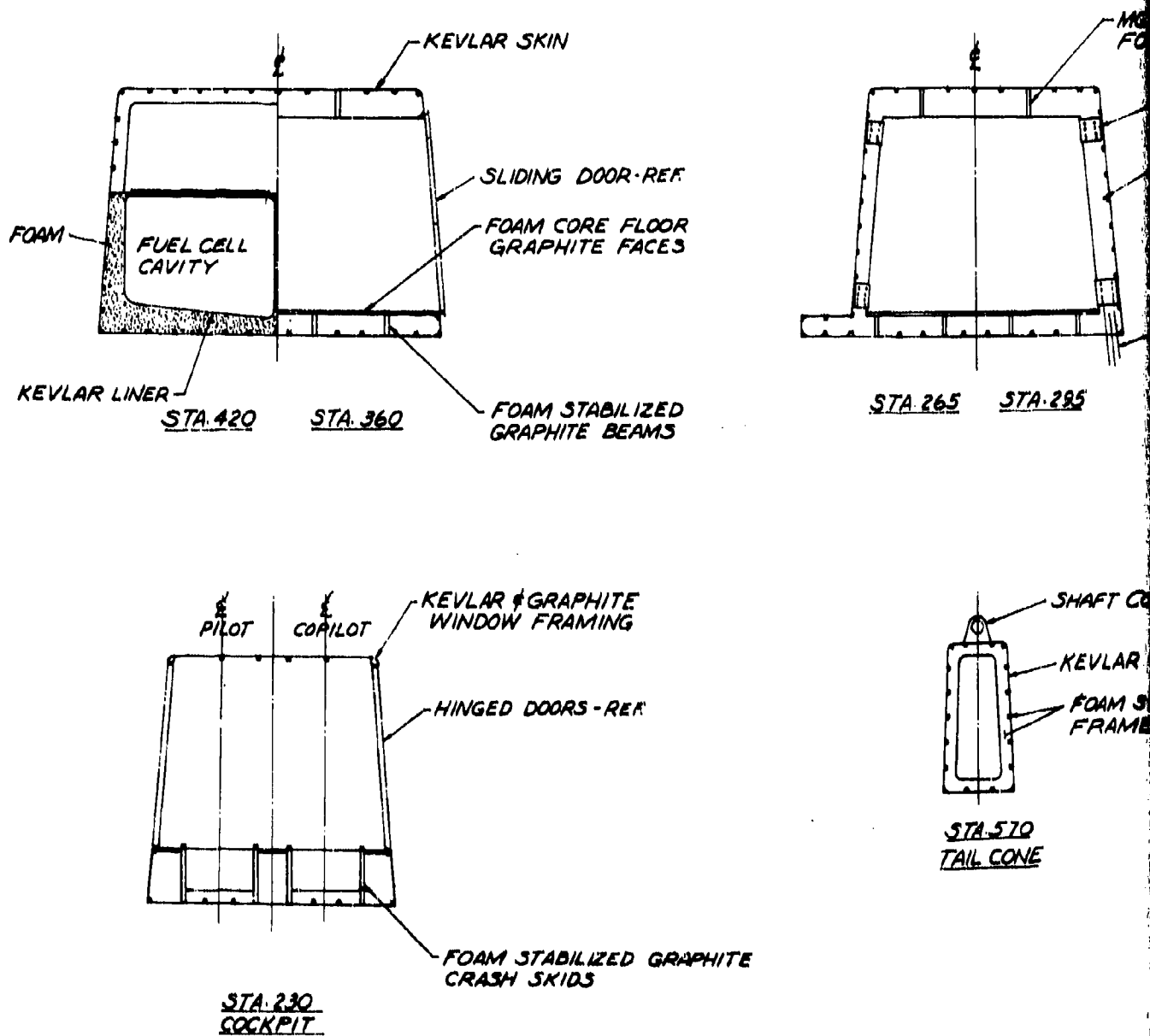


FIGURE 9. ADVANCED MATERIALS APPLICATION FOR CONFIGURATION 3

R SKIN

SLIDING DOOR-REF

FOAM CORE FLOOR
GRAPHITE FACES

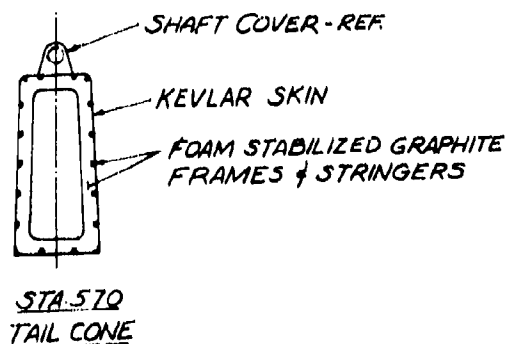
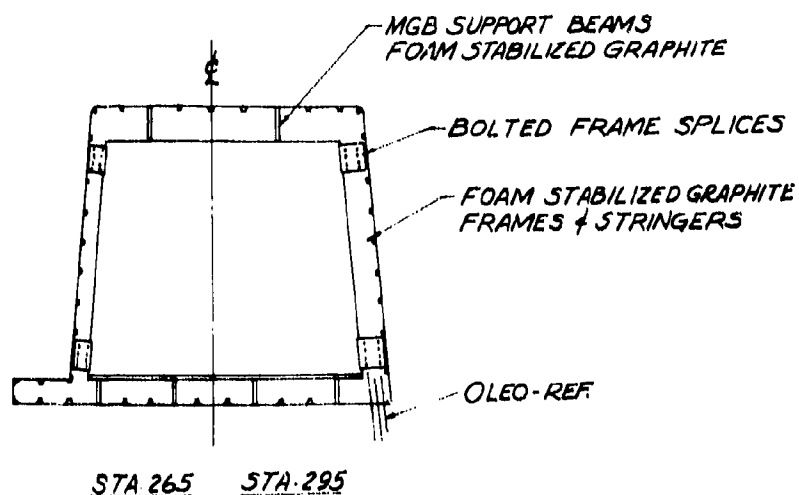
FOAM STABILIZED
GRAPHITE BEAMS

R & GRAPHITE
LOW FRAMING

D DOORS-REF

STABILIZED GRAPHITE
H SKIDS

ION FOR CONFIGURATION 3



For highly loaded frames in the cabin and transition section, the weight savings, using foam stabilized composite frames, is 33% (Reference 3).

BEAMS AND INTERCOSTALS

Beams are similar in construction to heavy frames. The weight savings for composite beams is the same as that for composite frames.

Intercostals are similar in construction to bent-up frames.

SKINS

Minimum skin gage is .025 in. aluminum

$$q_{ult} = 500 \text{ lb/in. } 2024\text{-T } 6 \text{ in. stringer}$$

$$F_{su} = 24000 \text{ psi for woven Kevlar fabric at } \pm 45^\circ$$

25% Reduction for Environment (.75 Design Factor)

$$F_{s \text{ Design}} = 24000 \text{ psi} \times .75 \text{ Design Factor} = 18000 \text{ psi}$$

$$t_{req.} = 500/18000 = .0277 \text{ in.}$$

A layup of $\pm 45^\circ$ Kevlar 4 ply is minimum skin requirement (.010 in. / ply, .050 lb/in.³). Percentage weight savings is:

$$\left(1 - \frac{\text{Kevlar skin thickness} \times \text{Kevlar density}}{\text{Aluminum skin thickness} \times \text{Aluminum density}} \right) / 100$$

$$\left(1 - \frac{.04_K \times .050_K}{.025_A \times .010_A} \right) / 100 = 20\% \text{ weight savings for skins}$$

STRINGERS

The original composite stringers considered in Reference 3 were of uni-directional graphite and foam. The stringer weight was .0056 lb/in. for a 3000-lb load capability. The composite stringer designed and tested as discussed in Reference 4 contained 2 ply at $\pm 45^\circ$ of Kevlar to provide shear capability for the stringer. The weight of the stringer with the Kevlar resulted in a composite stringer being of equal weight with a conventional stringer. These composite stringers are used to stabilize the Kevlar skins and to provide axial load capabilities for the airframe.

ADVANCED MATERIAL APPLICATION COSTS

The costs for advanced materials were based on the material costs of Reference 2. These costs are as follows:

Graphite/Epoxy	\$20/lb
Kevlar-49/Epoxy	\$10/lb
Foam	\$ 3/lb

The cost of materials for nonaffected and miscellaneous structures was that for materials of the baseline fuselage sections.

Labor costs for the fabrication of each section using advanced material were based on total labor costs for each section of conventional construction. The conventional labor costs were reduced 17-1/2 percent to give the labor costs for the advanced materials. The reduction was based on the following:

- . Current studies indicate that cockpit doors and cargo doors constructed of advanced material would reduce labor hours by 39 to 42 percent when compared to built-up sheet metal doors.
- . Studies conducted under a NASA program show that labor hours for production are reduced 25 percent with composites (Reference 4).
- . Earlier studies (References 2 and 3) showed a reduction of 13 to 14 percent for production composite fuselage labor costs compared to conventional.

The results of the study using advanced material for each configuration are given in Tables 21, 22 and 23. These results are based on the structural concept A for fuselage construction of conventional materials.

A summary comparison of fuselage weight and cost changes for both concept A and advanced materials is presented in Table 24.

-
4. Adams, K. M., and Lucas, J. J., STUDY TO INVESTIGATE DESIGN, FABRICATION AND TEST OF LOW COST CONCEPTS FOR LARGE HYBRID COMPOSITE HELICOPTER FUSELAGE - PHASE II, Sikorsky Aircraft Div., NASA Technical Report CR-145167, National Aeronautics and Space Administration, NASA-Langley Research Center, Hampton, Virginia, April 1977.

TABLE 17. COCKPIT STRUCTURAL WEIGHT*

STRUCTURE	BASELINE WEIGHT (LB)	CONFIG. 1 WEIGHT (LB)	CONFIG. 2A WEIGHT (LB)	CONFIG. 3A WEIGHT (LB)
Frames	43.0	41.8	45.3	46.3
Skins	32.9	32.3	34.6	34.7
Stiffeners	10.5	10.2	11.4	10.0
Floor & Support	18.9	18.4	19.9	11.8
Crash Beams	33.6	32.7	35.3	31.7
Seat Beams	13.3	12.9	14.0	11.4
Cockpit				
Enclosure	32.2	31.3	33.9	28.6
Windshield	57.5	55.9	60.5	80.8
Windows	15.8	15.4	16.6	13.9
Door	64.8	63.1	68.2	69.5
Steps	.3	.3	.3	.3
Paint	2.4	2.3	2.5	2.3
Sealant	5.1	4.9	5.4	4.8
	330.3	321.5	347.9	346.1
*Conventional Material				

TABLE 18. COCKPIT STRUCTURAL WEIGHT
OF CONFIGURATION 1A OF
CONVENTIONAL MATERIALS
AND ADVANCED MATERIALS

STRUCTURE	CONFIG. 1A CONVENTIONAL WEIGHT (LB)	CONFIG. 1 ADVANCED MATERIAL WEIGHT (LB)
Frame	41.8	38.2
Skins	32.3	26.1
Stiffeners	10.2	10.2
Floor & Supports	18.8	16.4
Crash Beams	32.7	22.5
Seat Beams	12.9	8.9
Cockpit		
Enclosure	31.3	24.8
Windshield	55.9	55.9
Windows	15.4	15.4
Doors	63.1	48.4
Steps	.3	.3
Paint	2.3	2.3
Sealant	4.9	4.9
	<u>321.5</u>	<u>274.3</u>
The material weight for Configuration 1 Advanced is:		
Graphite/Epoxy	53.0	
Kevlar	92.9	
Foam	39.9	
Misc.	9.7	
Windshield	55.9	
Nonaffected	<u>22.9</u>	
	274.3	

TABLE 19. COCKPIT STRUCTURAL WEIGHT
OF CONFIGURATION 2A OF
CONVENTIONAL MATERIALS AND
ADVANCED MATERIALS

STRUCTURE	CONFIG. 2A CONVENTIONAL WEIGHT (LB)	CONFIG. 2 ADVANCED MATERIAL WEIGHT (LB)
Frames	45.3	41.3
Skins	34.6	27.7
Stiffeners	11.4	11.4
Floor & Supports	19.9	17.5
Crash Beams	35.3	24.1
Seat Beams	14.0	9.6
Cockpit		
Enclosure	33.9	26.8
Windshield	60.5	60.5
Windows	16.6	16.6
Doors	68.2	51.2
Steps	.3	.3
Paint	2.5	2.5
Sealant	5.4	5.4
	<u>347.9</u>	<u>294.8</u>

The material weight for Configuration 2 Advanced is:

Graphite/Epoxy	55.7
Kevlar	98.4
Foam	44.9
Misc.	10.5
Windshield	60.5
Nonaffected	24.8
	<u>294.8</u>

TABLE 20. COCKPIT STRUCTURAL WEIGHT
OF CONFIGURATION 3A OF
CONVENTIONAL MATERIALS AND
ADVANCED MATERIALS

STRUCTURE	CONFIG. 3A CONVENTIONAL WEIGHT (LB)	CONFIG. 3 ADVANCED MATERIAL WEIGHT (LB)
Frames	46.3	41.7
Skins	34.7	27.8
Stiffeners	10.0	10.0
Floor & Supports	11.8	9.4
Crash Beams	31.7	20.9
Seat Beams	11.4	7.5
Cockpit		
Enclosure	28.6	22.3
Windshield	80.8	80.8
Windows	13.9	13.9
Doors	69.5	51.5
Steps	.3	.3
Paint	2.3	2.3
Sealant	4.8	4.8
	<u>346.1</u>	<u>291.8</u>

The material weight for Configuration 3 Advanced is:

Graphite/Epoxy	52.6
Kevlar	86.6
Foam	41.0
Misc.	9.5
Windshield	80.8
Nonaffected	21.3
	<u>291.8</u>

TABLE 21. CONFIGURATION 1 ADVANCED MATERIALS
FUSELAGE WEIGHT AND COST DATA

FUSELAGE SECTION	SECTION Δ WEIGHT (LB)	SECTION COST Δ FROM BASELINE			COST Δ TOTAL BASELINE FUSELAGE (PERCENT)
		MATERIAL (PERCENT)	TOTAL LABOR (PERCENT)	SECTION COST (PERCENT)	
Cockpit	- 56	61.0	- 17.5	- 6.5	- .91
Mid-Cabin	0	0	0	0	0
Aft-Cabin	0	0	0	0	0
Tail Cone	0	0	0	0	0
Pylon	0	0	0	0	0
Stabilizer	0	0	0	0	0
Total	- 56				- .91

TABLE 22. CONFIGURATION 2 ADVANCED MATERIALS
FUSELAGE WEIGHT AND COST DATA

FUSELAGE SECTION	SECTION Δ WEIGHT (LB)	SECTION COST Δ FROM BASELINE			COST Δ TOTAL BASELINE FUSELAGE (PERCENT)
		MATERIAL (PERCENT)	TOTAL LABOR (PERCENT)	SECTION COST (PERCENT)	
Cockpit	- 36	72.3	- 17.1	- 3.7	- .53
Mid-Cabin	- 50	44.8	- 13.2	- 7.3	-3.51
Aft-Cabin	- 18	547.9	- 11.3	1.1	.20
Tail Cone	- 14	208.2	- 16.8	- .7	- .04
Pylon	0	0	0	0	0
Stabilizer	0	0	0	0	0
Total	-118				-3.88

TABLE 23. CONFIGURATION 3 ADVANCED MATERIALS
FUSELAGE WEIGHT AND COST DATA

FUSELAGE SECTION	SECTION Δ WEIGHT (LB)	SECTION COST Δ FROM BASELINE			COST Δ TOTAL BASELINE FUSELAGE (PERCENT)
		MATERIAL (PERCENT)	TOTAL LABOR (PERCENT)	SECTION COST (PERCENT)	
Cockpit	- 37	93.0	- 17.2	- .74	- .12
Mid-Cabin	-153	8.97	- 17.8	-15.10	-7.20
Aft-Cabin	- 41	541.0	- 13.8	- 1.50	- .28
Tail Cone	- 25	196.5	- 17.4	- 2.10	- .13
Pylon	0	0	0	0	0
Stabilizer	0	0	0	0	0
Total	-256				-7.73

TABLE 24. SUMMARY OF WEIGHT AND COST DATA FOR
CONCEPT A AND ADVANCED MATERIALS

CONFIGURATION	CONCEPT A		ADVANCED MATERIALS	
	Δ WEIGHT (LB)	PERCENT COST Δ	Δ WEIGHT (LB)	PERCENT COST Δ
Configuration 1	- 8	- .00063	- 56	- .91
Configuration 2	223	3.65	- 118	-3.88
Configuration 3	65	.62	- 256	-7.73

HELICOPTER DESIGN MODEL

INTRODUCTION

The design attributes of six aircraft designs, incorporating the six fuselage concepts, were developed using the Sikorsky Helicopter Design Model (HDM) computer program described in Reference 2. The design attributes were based on the following parameters:

1. Fixed payload
2. Fixed hover performance
3. Fixed range
4. Estimate of vertical and forward drag

Two tasks were performed using the weight and cost changes for six fuselages shown in Table 24 and preliminary estimates of forward and vertical drag shown in Table 25.

HDM RESULTS

The HDM was used to determine the payload/range of six aircraft at the takeoff gross weight (TOGW) using the dynamic components of the baseline UH-60A aircraft. Table 26 shows the results for weight empty, fuel, payload, maximum cruise performance, vertical rate of climb, range, and the ratio of flyaway cost to baseline flyaway cost. The payload range of the six LRCS aircraft is plotted in Figure 10. The baseline UH-60A was not shown because it coincides nearly with LRCS Configuration 1.

Table 26 also shows that Configuration 2, at the same takeoff gross weight as the baseline UH-60A (16,450 pounds), has the lowest rate of vertical climb and the lowest cruise speed. This is a result of the aerodynamic drag characteristics of a wide fuselage with sharp corners.

The HDM was again used to develop design attributes trending solutions of six aircraft that meet all UH-60A performance requirements except cruise speed. Table 27 shows the results for takeoff gross weight at a constant payload of 2644 pounds, weight empty, fuel, main rotor size, main gearbox design horsepower, maximum cruise speed, and the ratio of flyaway cost to baseline flyaway cost.

Table 27 also shows that Configuration 2, at the same payload as the baseline UH-60A (2644 pounds), results in an aircraft with the largest gross weight, empty weight, and fuel weight, which meets the baseline performance requirements.

The significant differences in the attributes of Configurations 2 and 3 of conventional or advanced materials, compared to the baseline, are due to the aerodynamic characteristics of the configurations. The weight savings gained by the use of advanced materials has little effect on the design/performance attributes when compared to the greater effects of aerodynamic design.

TABLE 25. PRELIMINARY DRAG ESTIMATE

CONFIGURATION	FORWARD DRAG AT 0 ANGLE OF ATTACK, D/q (FT^2)	VERTICAL DRAG GROSS WEIGHT LESS TAIL ROTOR LIFT (PERCENT)
Baseline	26.13	3.37
Configuration 1	27.20	3.37
Configuration 2	35.52	7.20
Configuration 3	34.20	5.60

TABLE 26. HELICOPTER DESIGN MODEL CONSTANT GROSS WEIGHT RESULTS

CONFIGURATION	TAKE OFF GROSS WEIGHT (LB)	WEIGHT EMPTY (LB)	FUEL (LB)	PAYLOAD (LB)	MAXIMUM CRUISE SPEED (KT)	VERTICAL RATE OF CLIMB (FT/MIN)	RANGE (NAUTICAL MILES)	FLYAWAY COST BASE FLYAWAY COST
Baseline	16450	10596	1975	2644	147	450	244	1.
Config. 1		10888	1994	2628	145	450	244	1.00008
Config. 2		11119	2107	2257	133	66	234	1.011
Config. 3		10961	2107	2417	135	226	237	1.005
Config. 1 Adv.		10840	1994	2677	145	450	244	.999
Config. 2 Adv.		10778	2107	2599	133	66	234	.997
Config. 3 Adv.	16450	10640	2107	2737	135	226	237	.992

Note: Main Rotor Radius = 26.88 Ft
Main Gear Box Design Power = 2852 HP

TABLE 27. HELICOPTER DESIGN MODEL TRENDING RESULTS

CONFIGURATION	TAKEOFF GROSS WEIGHT (LB)	WEIGHT EMPTY (LB)	FUEL (LB)	MAIN ROTOR RADIUS (FT)	MAIN GEAR BOX DESIGN POWER (HP)	MAXIMUM CRUISE SPEED (KT)	FLYAWAY COST BASE FLYAWAY COST
Baseline	16450	10896	1975	26.83	2852	147	1.
Config. 1	16488	10916	1997	26.85	2858	145	1.002
Config. 2	18019	12113	2331	28.05	3269	142	1.095
Config. 3	17334	11532	2227	27.52	3086	140	1.053
Config. 1 Adv.	16382	10819	1988	26.77	2840	145	.996
Config. 2 Adv.	17224	11385	2265	27.43	3129	139	1.048
Config. 3 Adv.	16614	10869	2168	26.95	2962	137	1.0097

Note: Payload = 2644 lb

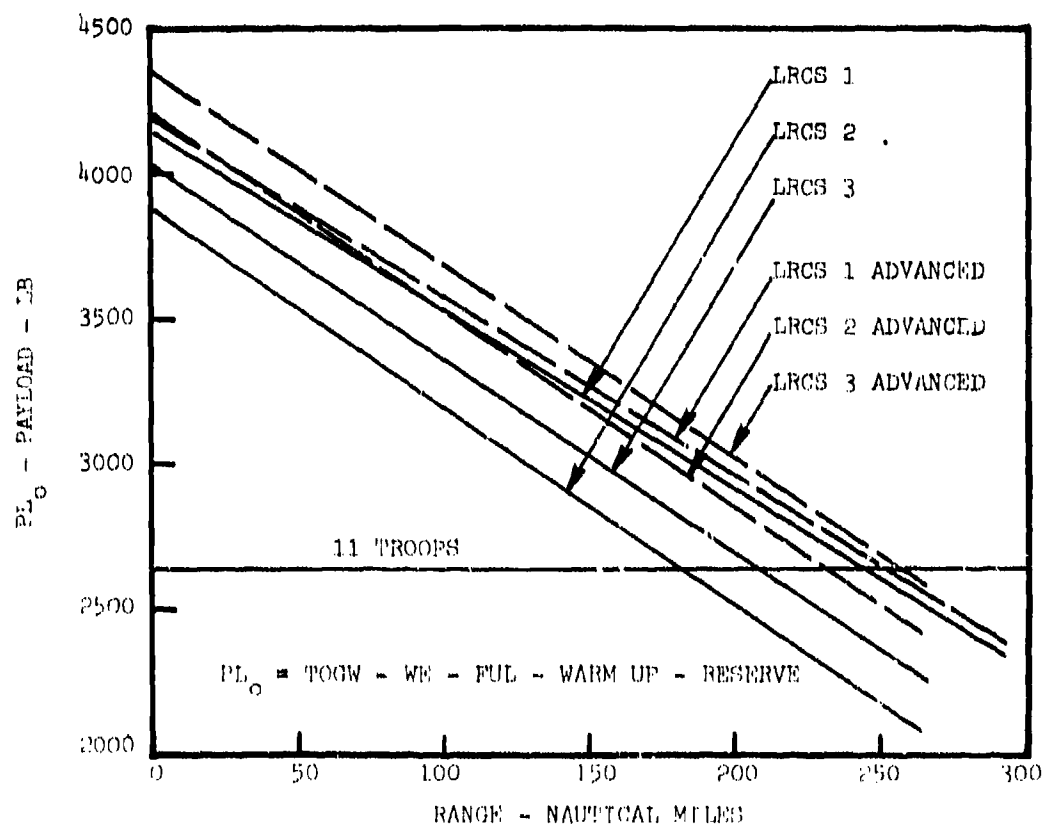


FIGURE 10. PAYLOAD AND RANGE FOR LOW RADAR CROSS SECTION HELICOPTERS

TECHNICAL RISKS

The three configurations of conventional construction offer no technical risks for design and manufacturing.

The use of advanced materials such as graphite, Kevlar and foam for fuselage construction offer a few technical risks, such as:

- . In absence of proper protective coatings, a possible decrease in strength properties of up to 10 percent for graphite and up to 25 percent for Kevlar due to environmental effects of temperature and humidity can occur.
- . A foam capable of curing temperatures of up to 350°F will be required for foam stabilized structures.
- . Design data is required for:
 1. Interaction strength of composite skin/stringer panels.
 2. Crippling strength of composite flanges.
 3. Effect of local stress concentration in primary structure for routing of equipment, initial design and retrofit.
- . Behavior of composite fuselage structure during a crash.
- . Repair of damaged composite structure.
- . Wire mesh in the Kevlar skins or external radar reflective coatings may be required for lightning protection and to reduce radar reflection of internal structure under the skins.

CONCLUSIONS

Based on the results of this study, the following conclusions are made:

1. The use of advanced materials can result in both weight and cost savings over the baseline fuselage, even with the most severe change in LRCS configurations presented.
2. Without the use of advanced materials, the LRCS Configurations 2 and 3 significantly increase both weight and cost of the total aircraft compared to the baseline UH60A.
3. Minor changes to the nose section of Configuration 1 result in negligible fuselage difference to the weight and cost of the fuselage.
4. Consideration of the total aircraft attributes show that vertical drag penalties appear to be of greater magnitude than the structural weight changes involved with the fuselages of Configurations 2 and 3. Even with the use of advanced materials, the vertical drag penalty exceeds any weight savings .

Further conclusions from the detailed aerodynamic analysis presented in Appendix A shows:

1. The forward drag estimates for LRCS Configurations 2 and 3 were found to be higher than the values obtained through the use of the detailed and more sophisticated aerodynamic analysis presented. The higher values were the result of the unavailability of prior test data of the representative shapes of the two configurations for comparison purposes. Also, interference factors which were applied to the original estimates to account for interference of the two shapes and the main rotor pylon may have been exaggerated.
2. The detailed aerodynamic analysis increased the cruise speed of Configuration 2 from 133 knots to 140 knots and the cruise speed of Configuration 3 from 135 knots to 136 knots.
3. Vertical drag estimates were not significantly changed by the detailed aerodynamic analysis, and the low vertical rates of climb for Configuration 2 and 3, presented in Table 26, were substantiated.

REFERENCES

1. UH-60A VOLUME 3, PART 1-III WEIGHT AND BALANCE dated September 27, 1976.
2. Rich, M. J., INVESTIGATION OF ADVANCED HELICOPTER STRUCTURAL DESIGNS, VOLUME 1 - ADVANCED STRUCTURAL COMPONENT DESIGN CONCEPTS STUDY, Sikorsky Aircraft Div., USAAMRD-L-TR-75-59A, U.S. Army Air Mobility Research and Development Laboratory, Fort Eustis, Va. 23604, May 1976, AD A026246.
3. Rich, M. J., Ridgley, G. F., and Lowry, D. W., APPLICATION OF COMPOSITES TO HELICOPTER AIRFRAME AND LANDING GEAR STRUCTURES, Sikorsky Aircraft Div., NASA Technical Report CR-112333, National Aeronautics and Space Administration, NASA-Langley Research Center, Hampton, Virginia, June 1973.
4. Adams, K. M., and Lucas, J. J., STUDY TO INVESTIGATE DESIGN, FABRICATION AND TEST OF LOW COST CONCEPTS FOR LARGE HYBRID COMPOSITE HELICOPTER FUSELAGE - PHASE II, Sikorsky Aircraft Div., NASA Technical Report CR-145167, National Aeronautics and Space Administration, NASA-Langley Research Center, Hampton, Virginia, April 1977.
5. Sheehy, T. W., and Clark, D.R., A METHOD FOR PREDICTING HELICOPTER HUB DRAG, USAAMRD-L-TR-75-48, Eustis Directorate, U. S. Army Air Mobility R&D Laboratory, Ft. Eustis, Virginia, January 1976, AD A021201.
6. Keys, Charles, and Weisner, Robert, GUIDELINES FOR REDUCING PARASITE DRAG, Boeing Vertol Company, Journal of the American Helicopter Society, January 1975.
7. Delaney, Noel K., and Sorenson, Norman E., LOW SPEED DRAG OF CYLINDERS OF VARIOUS SHAPES, NACA TN-3038, November 1953.
8. Hoerner, Dr. Ing S. F., FLUID DYNAMIC DRAG, Second Edition, Bricktown, New Jersey, Hoerner Fluid Dynamics, 1965.
9. Werner, J. V., and Flemming, R. J., YUH-60A QUARTER SCALE WIND TUNNEL TEST REPORT, Sikorsky Aircraft, SER-70531, May 1, 1973.
10. Barnard, R. S., YUH-60A/T700 ENGINE IR SUPPRESSOR FULL SCALE PROTOTYPE TEST REPORT, Sikorsky Aircraft, SER-70094, June 18, 1976.
11. Prime Item Development Specification for UH-60A Utility Tactical Transport Aircraft System OPQ, RFQ, DAAJ01-77-C-0001 (PGA), Part 1, U. S. Army Aviations Systems Command, St. Louis, Missouri, November 1976.

APPENDIX A - AERODYNAMIC ANALYSIS OF LOW
RADAR CROSS SECTION CONFIGURATIONS

INTRODUCTION

An analytical investigation of the aerodynamic loads, vertical drag and mission performance of three proposed low radar cross section configurations has been performed.

The Sikorsky Wing and Body Aerodynamic Technique (WABAT), in combination with the Sikorsky Automated Paneling Technique (APT), and empirical methods were employed in the analysis of the aerodynamic loads. WABAT is a three-dimensional potential flow analysis which is capable of calculating the aerodynamic flow and surface pressures about arbitrary lifting bodies. This enables the aerodynamicist to predict body airloads and regions of high dynamic pressure and permits the evaluation of concepts to minimize drag.

The strip analysis method used to calculate the airframe vertical drag is a semi-empirical approach based on experimental drag coefficients and rotor wake flow surveys. This method establishes the flow environment around elements of the airframe to yield element drags which are then summed to yield total airframe drag.

Aircraft performance was based on the Aircraft Trim Adjusted Performance Analysis (ATAP), which uses nondimensional main and tail rotor performance, fuselage attitude, airframe lift and drag data, system losses and powerplant data to compute system power requirements and range characteristics.

PROCEDURES

Using section coordinates from the Government-furnished mold lines and drawings prepared under Task I, the representative geometric models of the three LRCS configurations and the baseline UH-60A were developed with the use of the Automated Paneling Technique (Figures A-1 thru A-8). The panel geometries thus generated were input to the WABAT program which calculated the potential flow solution for each configuration, yielding the surface pressure and forces and pitching moments for each body panel. The geometry and aerodynamic methods and computer programs are described in greater detail in Reference 5.

-
5. Sheehy, T. W. and Clark, D. R., A METHOD FOR PREDICTING HELICOPTER HUB DRAG, USAAMRDL TR-75-48, Eustis Directorate, U. S. Army Air Mobility R & D Laboratory, Ft. Eustis, Virginia, January 1976.

The lift, drag and pitching moment of each LRCS configuration were calculated based on the element surface forces generated by WABAT. The variation of lift with angle of attack was determined by calculating the difference between the total body lift of each LRCS configuration and the total body lift of the basic UH-60A at each angle of attack. This difference was then applied to the total body lift of the UH-60A configuration obtained from test data. The same procedure was applied to the calculation of pitching moment.

The total body drag of each LRCS configuration was computed as an increment to the basic UH-60A. The total body drag increment is defined as the sum of the drag increments due to changes in forebody drag, pylon drag, drag as a result of contraction in the transition region, and drag as a result of wetted area. The drag increment due to contraction was based on data presented in Reference 6. The variation of drag with angle of attack was also based on data presented in Reference 6.

The vertical drag of each LRCS configuration was generated using the strip analysis method. The method requires three basic sets of data to provide the necessary information for the calculation of drag: airframe element areas, drag coefficients and cylindrical coordinates describing the location of each of the airframe centroids. Two-dimensional drag coefficients based on References 7 and 8 were used for this calculation. In some instances, three-dimensional drag coefficients were used for those elements exhibiting three-dimensional effects.

Using the airframe lift and drag results and the baseline UH-60A powerplant data in combination with the Aircraft Trim Adjusted Performance Analysis program, the mission performance of each LRCS configuration was generated.

SUMMARY OF DATA PRESENTED

Surface pressures generated by WABAT for the proposed LRCS configurations have been compared to the baseline UH-60A surface pressures over a range of angles of attack ($-8^\circ \leq \alpha \leq +8^\circ$) along the top ($\alpha_g = 0^\circ$), bottom ($\alpha_g = 180^\circ$), and lateral ($\alpha_g = 90^\circ$) centerlines at waterline 219 and are presented in Figures A-9 thru A-53.

-
6. Keys, Charles, and Weisner, Robert, GUIDELINES FOR REDUCING PARASITE DRAG, Boeing Vertol Company, Journal of the American Helicopter Society, January 1975.
 7. Delaney, Noel K., and Sorenson, Norman E., LOW SPEED DRAG OF CYLINDERS OF VARIOUS SHAPES NACA TN-3038, November 1953.
 8. Hoerner, Dr. Ing S. F., FLUID DYNAMIC DRAG, Second Edition, Bricktown, New Jersey, Hoerner Fluid Dynamics, 1965.

Lifts, drags, and pitching moments for each of the LRCS configurations have been compared to the baseline lift, drag and pitching moment over a range of angles of attack ($-8^\circ \leq \alpha \leq +8^\circ$) and are presented in Figure A-54 thru A-56. The UH-60A lift and drag data were based on wind tunnel test data obtained from References 9 and 10.

The comparison of the body lifts, without empennage, for the UH-60A and the three LRCS concepts shown in Figure A-54 demonstrates that both the LRCS2 and LRCS3 configurations produce approximately 4 square feet of additional download at representative cruise angles of attack (-2° to -5°). The LRCS1 configuration demonstrates no significant change in lift compared to the UH-60A. While the additional download generated by the LRCS2 and LRCS3 configurations is not insignificant, the primary impact on mission performance is the increased drag of these configurations shown in Figure A-55. The data shown in this figure include the drag of the empennage, all external protuberances, and momentum losses.

The drag increase with angle of attack variation for the LRCS2 and LRCS3 configurations is greater because of their difference in cross-sectional shape compared to the UH-60A or the LRCS1. Although the LRCS1 shows no significant change in drag from the UH-60A, the LRCS2 and LRCS3 demonstrate minimum drag values 11% and 17%, respectively, greater than the baseline UH-60A.

The predicted pitching moments of the three LRCS configurations are compared with the baseline UH-60A (without empennage) in Figure A-56. The pitching moment of both the LRCS1 and LRCS3 configurations are not significantly changed from the UH-60A. The LRCS2 pitching moment trend, however, demonstrates an increase in slope resulting in approximately an 83% increase in basic fuselage instability.

In addition to the unfavorable impact of the LRCS3 configuration on stability, the increased drag of both the LRCS2 and LRCS3 configurations will have an unfavorable effect on the dynamic pressure loss in the empennage region and consequently on the horizontal tail effectiveness. This impact has been estimated by assuming that the dynamic pressure loss of the LRCS2 and LRCS3 configurations compared to the UH-60A is proportional to the increased drag of the basic configuration not including the empennage drag or the drag due to momentum losses. Based on this, the tail effectiveness compared to the UH-60A is reduced by 21% for the LRCS2 and by 28% for the LRCS3.

9. Werner, J. V., and Flemming, R. J., YUH-60A QUARTER SCALE WIND TUNNEL TEST REPORT, Sikorsky Aircraft, SER-70531, May 1, 1973.

10. Barnard, R. S. YUH-60A/T700 ENGINE LR SUPPRESSOR FULL SCALE PROTOTYPE TEST REPORT, Sikorsky Aircraft, SER-70094, June 18, 1976.

Based on the calculated fuselage pitching moment results and the assessment of tail effectiveness, the LRCS2 and LRCS3 configurations will demonstrate a substantial reduction in static stability compared to the UH-60A and will require redesign of the horizontal stabilator. The LRCS3 would therefore be penalized by the requirement for increased horizontal stabilator area and the associated weight and drag penalty.

The vertical drag of each LRCS concept and of the baseline UH-60A are presented in Tables A-1 thru A-4. The VOR/LOC and FM homing antennas of the baseline UH-60A were included in the calculation of vertical drag for each of the LRCS configurations for the purpose of comparison. Drag coefficients were estimated on the basis of data presented in References 7 and 8. The vertical drag and parasite drags of each configuration are summarized in Table A-5.

The mission performance for each of the LRCS configurations was generated on the basis of the lift and drag variations shown in Figure A-53 and A-54 and the T700-GE-700 powerplant data used for the baseline UH-60A. The performance was computed with the use of the Aircraft Trim Adjusted Performance program and is presented in Table A-6. Maximum cruise speed was determined by using the maximum continuous power rating at a pressure altitude of 4000 feet for a 95°F day. The hover and one engine in-operative (OEI) service ceilings were calculated for a 95°F day using 95% of the intermediate rated power and 100% of the intermediate rated power, respectively. Endurance was calculated on the basis that the fuel capacity of the three LRCS configurations remains the same as the UH-60A fuel capacity. The endurance mission included the following four categories: 8 minutes at ground idle power, 20 minutes at maximum continuous power, cruise at 145 knots, and 30 minute reserve at 145 knots. The endurance was calculated at a pressure altitude of 4000 feet for a 95°F day. Calculations were based on a gross weight of 16,450 lb. The baseline mission performance was obtained from Reference 11.

CONCLUSIONS

Comparison of the UH-60A attributes with the calculated results for the three proposed low radar cross section configurations indicate that:

1. A change in the UH-60A configuration to reflect the LRCS1 configuration caused a decrease in the drag of the UH-60A at $\alpha = 0^\circ$. This decrease was reflected through a range of angles of attack ($+8^\circ \leq \alpha \leq -8^\circ$) with the exception of angles of attack of $+8^\circ$ and -8° respectively, where no change in drag was exhibited.

-
11. Prime Item Development Specification for UH-60A Utility Tactical Transport Aircraft System OPQ, RFQ, DAAJ01-77-C-0001 (PGA), Part I, U.S. Army Aviations Systems Command, St. Louis, Missouri, November 1976.

Configuration changes reflecting the LRCS2 and LRCS3 configuration showed increases of 11% and 17% respectively, of the UH-60A drag at $\alpha = 0^\circ$ and as high as 21% and 29%, respectively, at angles of attack of $+8^\circ$ and -8° . These changes do not reflect the required increase in stabilator size which would result in an additional drag penalty.

2. The LRCS1 configuration produces an insignificant change in lift compared to the UH-60A while the LRCS2 and LRCS3 configurations reflect an additional download of 40% of the UH-60A download at $\alpha = -4^\circ$.
3. Compared to the UH-60A, the LRCS2 and LRCS3 configurations demonstrate a substantial reduction in static stability which will require a re-design of the horizontal stabilator. This is primarily due to a reduction in tail effectiveness and an increase in fuselage instability. The reduction in tail effectiveness was estimated as 21% for the LRCS2 concept and 28% for the LRCS3 configuration. Minor changes in the pitching moment of the LRCS1 and LRCS3 configurations, compared to the UH-60A were calculated, however, the LRCS2 trend demonstrated an increase in slope resulting in an 83% increase in basic fuselage instability.
4. The three proposed LRCS configurations demonstrated an increase in vertical drag of 27% for the LRCS1, 106% for the LRCS2, and 70% for the LRCS3, of the basic UH-60A vertical drag. This increase in vertical drag is a direct result of the additional cross sectional area and sharp edges presented to the downwash of the main rotor by the LRCS2 configuration. In the case of the LRCS3 configuration, the wedge type of cross sectional area of the cockpit, the additional area of the main landing gear support structure and the presence of sharp edges presented to the main rotor downwash resulted in an increase in vertical drag as indicated. Finally, the increase in vertical drag for the LRCS1 configuration is a direct result of the wedge type cross sectional area of the cockpit.
5. In comparison to the UH-60A, no change in the maximum cruise speed and endurance of the LRCS1 configuration was observed, however, a loss of 217 feet in hover ceiling and 12 feet in OEI service ceiling was exhibited. The performance of the LRCS2 and LRCS3 configurations did not meet the performance requirements of the basic UH-60A. Decreases of 7 and 11 knots in maximum cruise speed, 805 and 520 feet in hover ceiling, 248 and 740 feet in OEI service ceiling, and 0.14 and 0.19 hour in endurance were calculated for the LRCS2 and LRCS3 configurations respectively.

TABLE A-1. UH-60A VERTICAL DRAG CALCULATION

			THRUST			16593.3			RHO			.001920		
			CT			.007276			TIP SPEED			724.7		
			RADIUS			26.83			THRUST RECRY			.0052		

TABLE A-2. LRCS1 VERTICAL DRAG CALCULATION

[illegible]

TABLE A-3. LRCS2 VERTICAL DRAG CALCULATION

ELEMENT	X/R	H/R	CD	V FACTOR	AREA	VEL	Q	DRAW	RHO	TIP SPEED	.001920
										724.7	
										THRUST RECRY	.0052
1	.590	.340	2.080	1.000	.56	75.89	5.53	12.9			
2	.540	.300	1.890	1.050	12.67	71.25	4.87	233.8			
3	.440	.230	1.450	1.000	21.22	47.06	2.13	130.8			
4	.340	.160	1.370	1.000	30.39	38.78	1.44	120.2			
5	.250	.110	1.400	1.000	36.67	28.92	.80	82.4			
6	.150	.090	1.430	1.000	33.44	6.20	.04	3.5			
7	.050	.070	2.000	1.000	10.83	2.67	.01	.3			
8	.050	.070	2.000	1.000	10.83	2.67	.01	.3			
9	.150	.090	1.430	1.000	33.44	6.20	.04	3.5			
10	.250	.110	1.460	1.000	35.00	28.92	.80	82.1			
11	.340	.140	1.450	1.000	26.67	38.50	1.42	110.1			
12	.440	.180	1.270	1.000	19.17	46.00	2.03	98.9			
13	.550	.220	1.160	1.000	14.28	53.77	2.78	92.0			
14	.640	.250	.990	1.000	8.72	76.43	5.61	96.8			
15	.750	.280	.860	1.000	6.94	74.37	5.31	63.4			
16	.850	.300	.870	1.000	4.56	52.86	2.68	21.3			
17	.310	.300	1.680	1.000	4.61	40.17	1.55	24.0			
18	.270	.370	.680	1.000	3.33	36.35	1.27	5.7			
19	.761	.363	1.250	1.000	.83	52.80	2.68	5.6			
20	.326	.161	1.680	1.000	.36	37.53	1.35	1.6			
MISC	--	--	--	--	--	--	--	21.0			

TABLE A-4. LRCS3 VERTICAL DRAG CALCULATION

ELEMENT	Z/R	H/R	C/D	V FACTOR	AREA	VEL	Q	DRAG	NOSE	COCKPIT	FWD CABIN	AFT CABIN	TRANSITION	TAIL BOOM	LAND-GEAR STRUT	TIRES	VOR/LOC	FM HOMING ANTENNAS	MISCELLANEOUS
1	.630	.310	2.180	1.000	6.14	75.79	5.51	147.6											
2	.540	.260	2.380	1.000	10.72	54.49	2.85	145.4											
3	.440	.200	2.050	1.000	13.33	46.00	2.03	111.0											
4	.340	.150	1.970	1.000	15.44	38.92	1.42	86.2											
5	.240	.110	2.100	1.000	17.89	26.28	.66	49.8											
6	.140	.090	2.130	1.000	25.00	5.67	.03	3.3											
7	.040	.070	2.000	1.000	10.44	2.34	.01	.2											
8	.050	.080	2.000	1.000	10.83	2.62	.01	.3											
9	.150	.090	1.970	1.000	26.11	6.16	.04	3.7											
10	.250	.110	1.990	1.000	22.58	28.75	.79	71.3											
11	.350	.140	1.640	1.000	16.67	39.16	1.47	80.5											
12	.450	.190	1.330	1.000	8.84	46.75	2.10	49.2											
13	.550	.220	1.280	1.000	5.36	53.46	2.74	37.6											
14	.640	.250	1.280	1.000	4.72	75.99	5.54	67.0											
15	.740	.280	1.320	1.000	4.11	74.39	5.31	57.6											
16	.840	.300	1.350	1.000	3.69	54.59	2.86	28.5											
17	.940	.320	1.450	1.000	3.33	2.20	.00	.0											
18	.310	.330	2.180	1.000	5.75	38.89	1.45	36.4											
19	.250	.350	.500	1.000	3.06	33.67	1.09	3.3											
20	.220	.350	.450	1.000	3.89	29.94	.86	3.0											
21	.761	.363	1.250	1.000	.83	52.49	2.65	5.5											
22	.326	.161	1.680	1.000	.36	37.32	1.34	1.6											
MISC	--	--	--	--	--	--	--	21.0											
TOTAL DRAG (POUNDS)	1010.3																		
			16972.0		16050.0														
								5.78											

TABLE A-5. SUMMARY OF PARASITE AND VERTICAL DRAG

CONFIGURATION	PARASITE DRAG, f @ $\alpha = 0$, $ft.$	VERTICAL DRAG % GW
UH-60A	26.58	3.40
LRCS1	26.32	4.33
LRCS2	29.49	7.02
LRCS3	31.86	5.78

TABLE A-6. PRIMARY MISSION PERFORMANCE SUMMARY

Configuration	Maximum Cruise Speed (Knots - True Airspeed) (1)	Hover Ceiling (Feet) (2)	OEI Service Ceiling (Feet) (3)	Total Mission Time Including Reserve (Hours) (4)
UH-50A UTTAS	147	4700	5100	2.30
LRC51 Concept	147	4483	5038	2.30
LRC52 Concept	140	3895	4852	2.16
LRC53 Concept	136	4171	4360	2.11

Notes:

1. Cruise at maximum continuous power, 4000 ft, 95°F, GW = 16,450 lb.
2. Hover at 95% of intermediate rated power, 95°F, GW = 16,450 lb.
3. 100% of intermediate rated power, 95°F, GW = 16,450 lb.
4. Endurance Mission
 - a. 8 minutes at ground idle
 - b. 20 minutes at MCP
 - c. Takeoff GW = 16,450 lb.
 - d. Cruise at 145 knots
 - e. 30-minute reserve at 145 knots

Mission calculations computed at pressure altitude of 4000 ft for 95°F day.

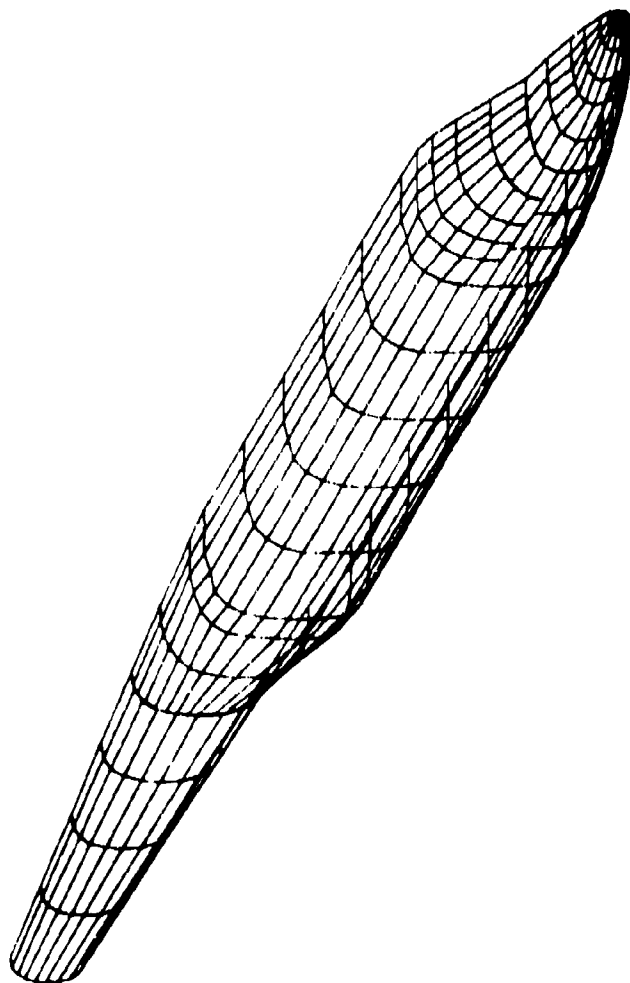


Figure A-1. GEOMETRICAL REPRESENTATION OF THE UH-60A UTTAS FUSELAGE (BASELINE.)

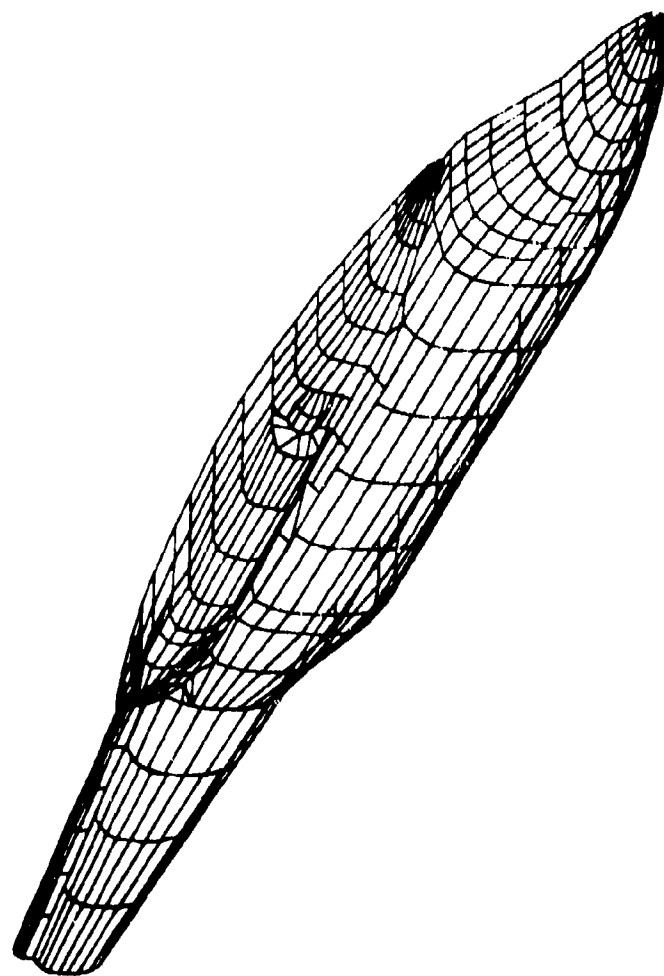


Figure A-2 . GEOMETRICAL REPRESENTATION OF THE UH-60A UTTAS WITH MAIN ROTOR PYLON (BASELINE)

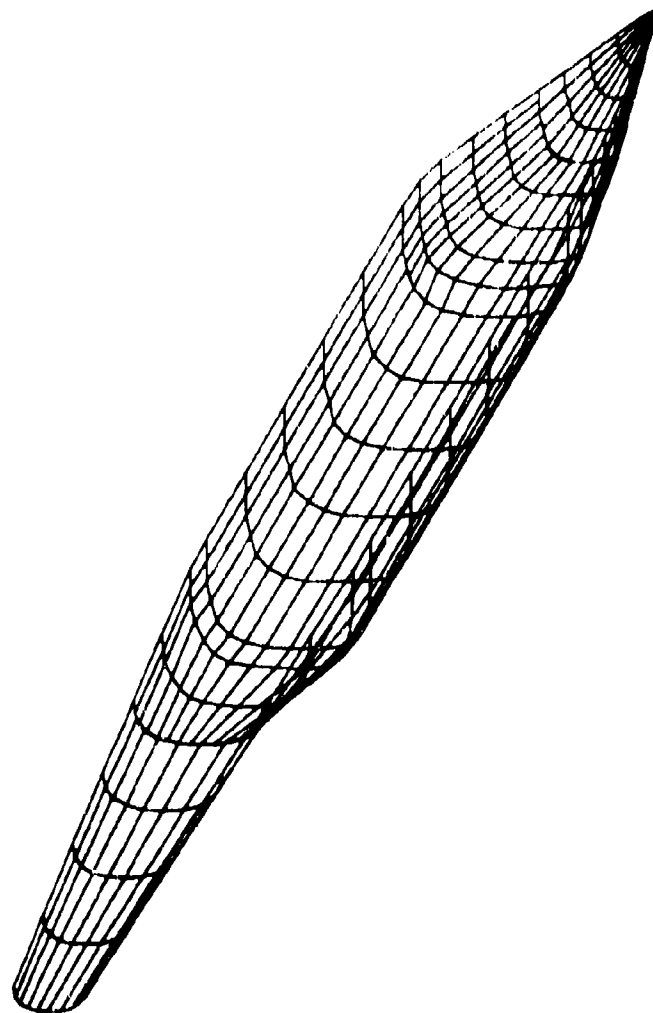


Figure A-3. GEOMETRICAL REPRESENTATION OF THE LRCS1 FUSELAGE

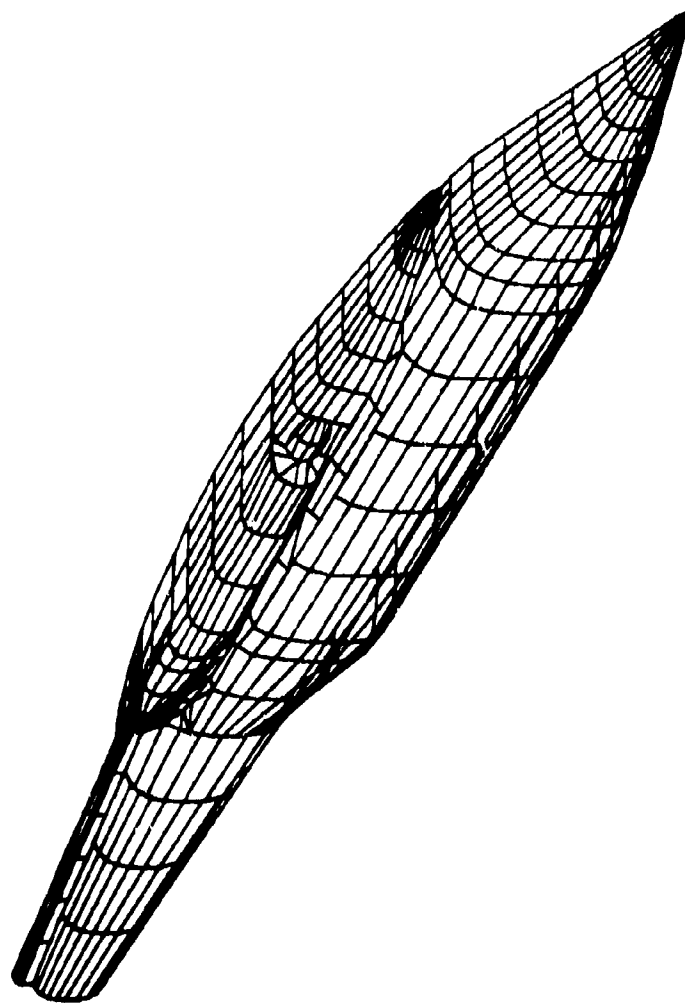


Figure A-4 • GEOMETRICAL REPRESENTATION OF THE LRCS1 FUSELAGE WITH BASELINE MAIN ROTOR PYLON

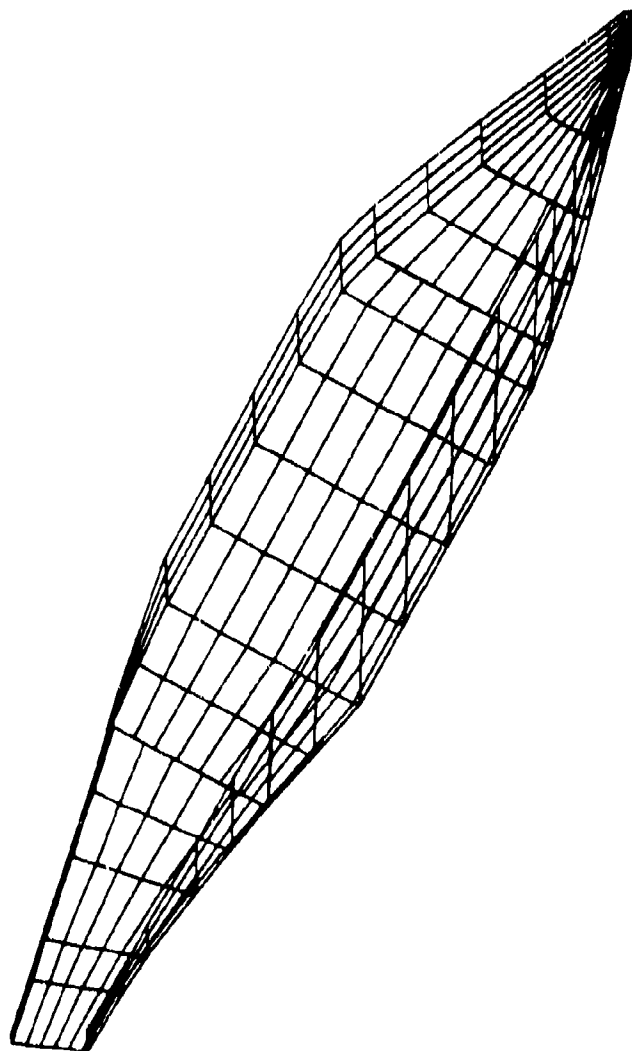


Figure A-5 • GEOMETRICAL REPRESENTATION OF THE LRCS2 FUSELAGE

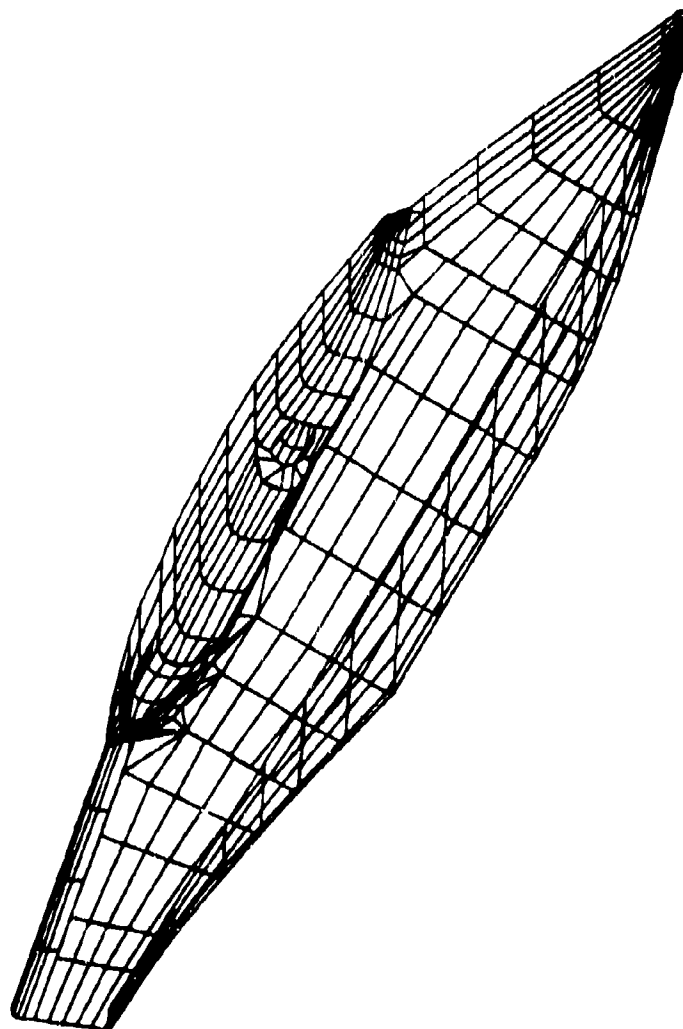


Figure A-6 • GEOMETRICAL REPRESENTATION OF THE LRCS2 FUSELAGE WITH
BASELINE MAIN ROTOR PYLON

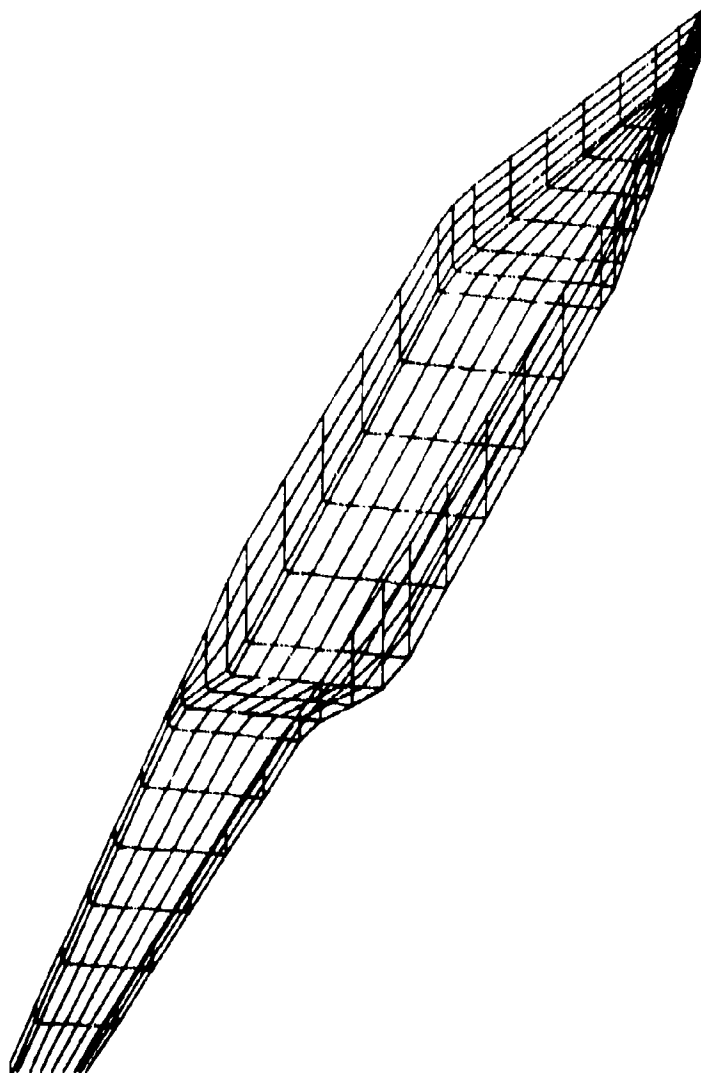


Figure A-7. GEOMETRICAL REPRESENTATION OF THE LRCS3 FUSELAGE

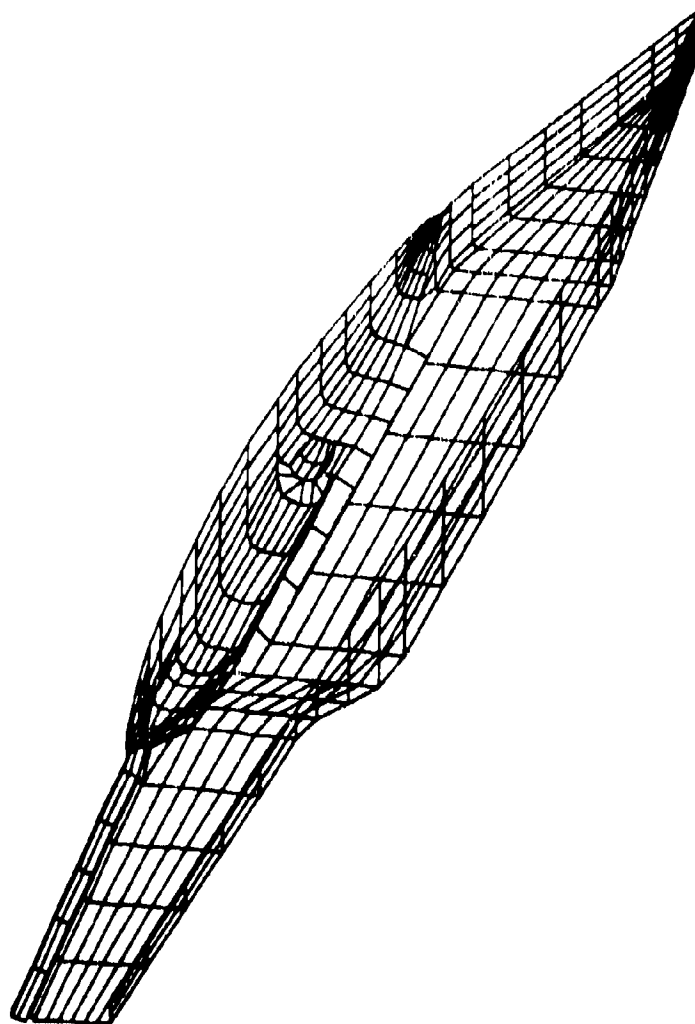


Figure A-8 · GEOMETRICAL REPRESENTATION OF THE LRCs 3 FUSELAGE WITH
BASELINE MAIN ROTOR PYLON

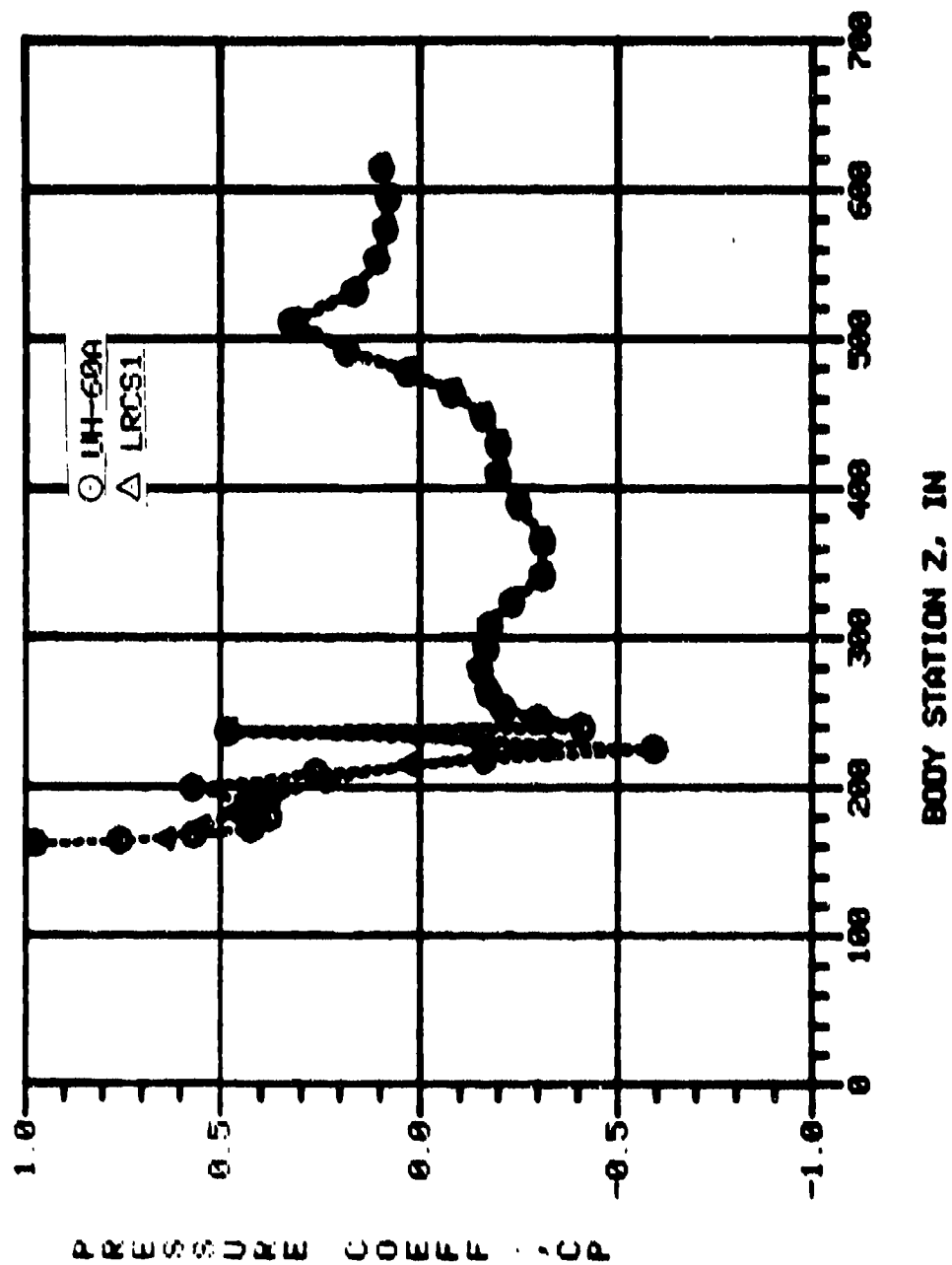


Figure A-9 - COMPARISON OF THE UH-60A UTAS AND LRCS1 CALCULATED SURFACE PRESSURES, TOP CENTERLINE, $\alpha = 0^\circ$, $\psi = 0^\circ$

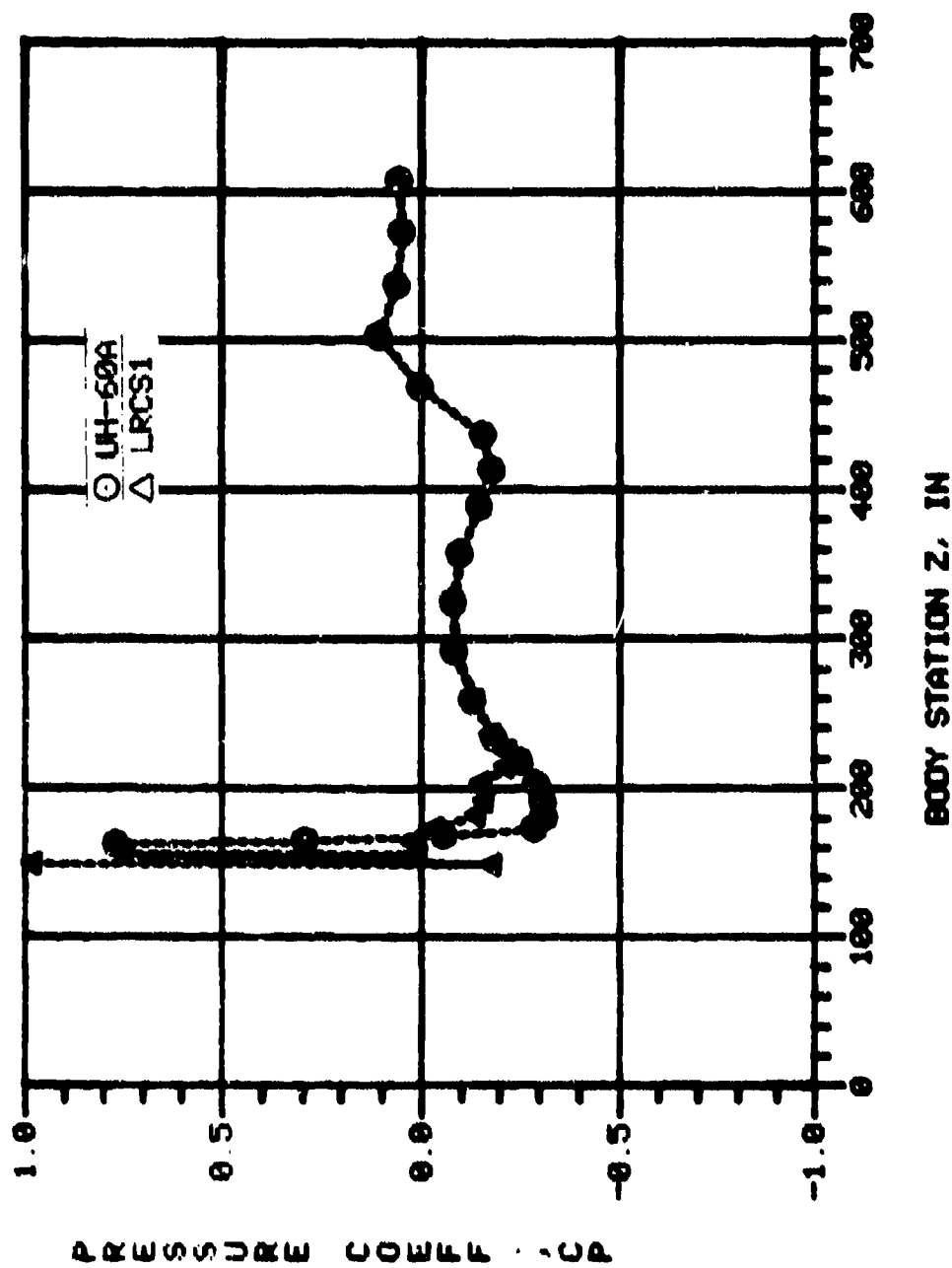


Figure A-10. COMPARISON OF THE UH-60A UTAS AND LRCS1 CALCULATED SURFACE PRESSURES, BOTTOM CENTERLINE, $\alpha = 0^\circ$, $\psi = 0^\circ$

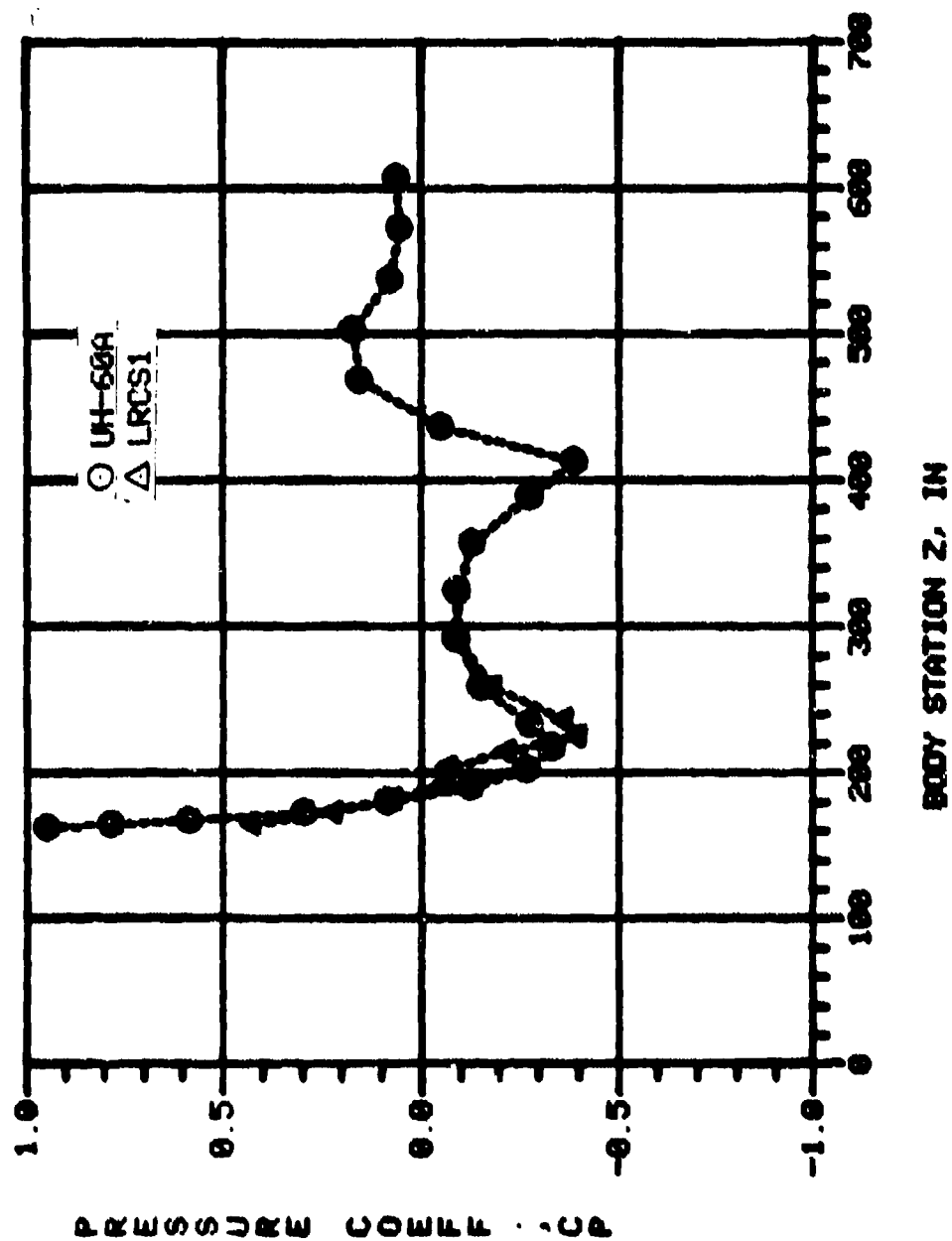


Figure A-11. COMPARISON OF THE UH-60A UTAS AND LRCS1 CALCULATED SURFACE PRESSURES, LATERAL CENTERLINE, $\alpha = 0^\circ$, $\psi = 0^\circ$

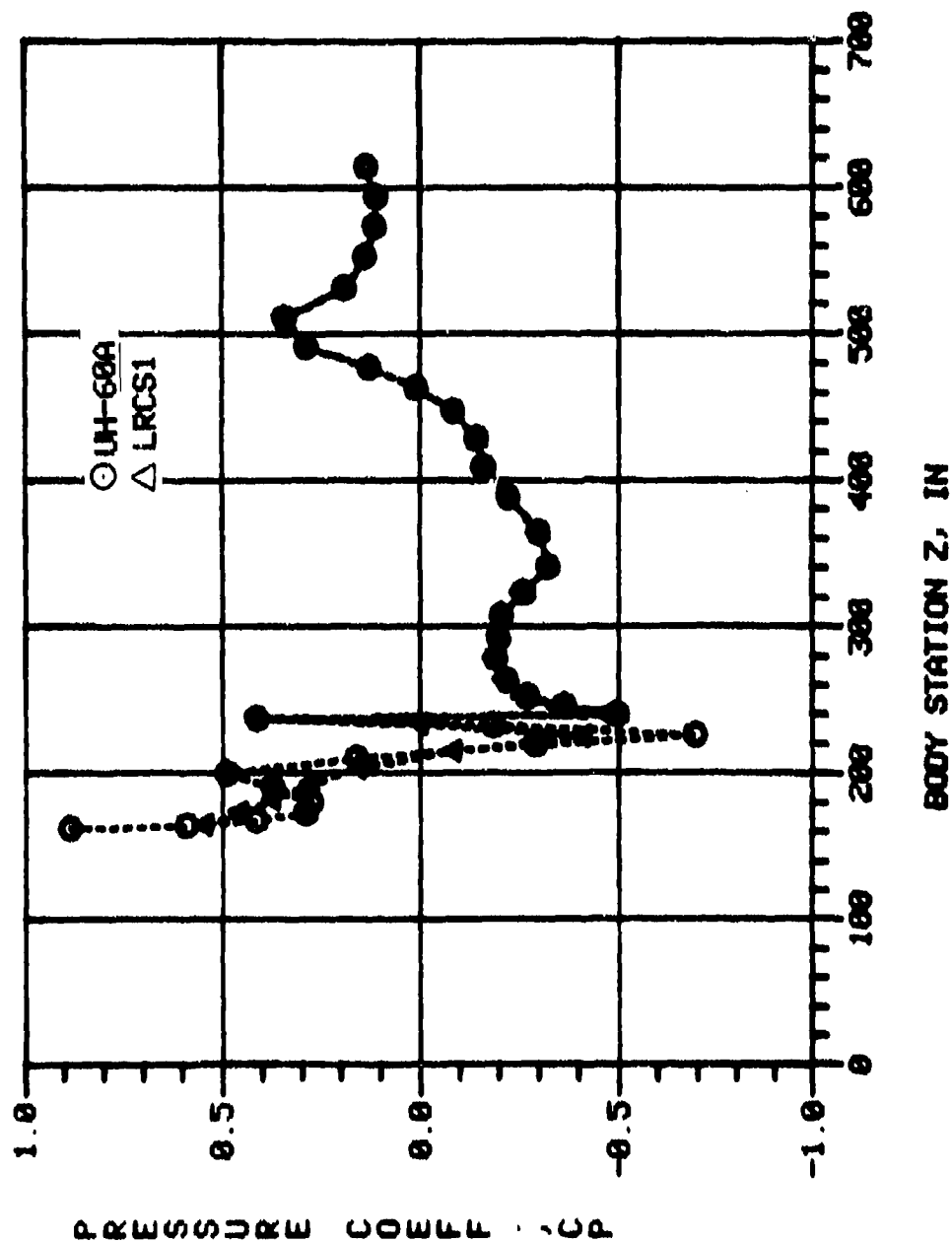


Figure A-12. COMPARISON OF THE UH-60A UTAS AND LRCS1 CALCULATED SURFACE PRESSURES, TOP CENTERLINE, $\alpha = 4.0^\circ$, $\psi = 0^\circ$

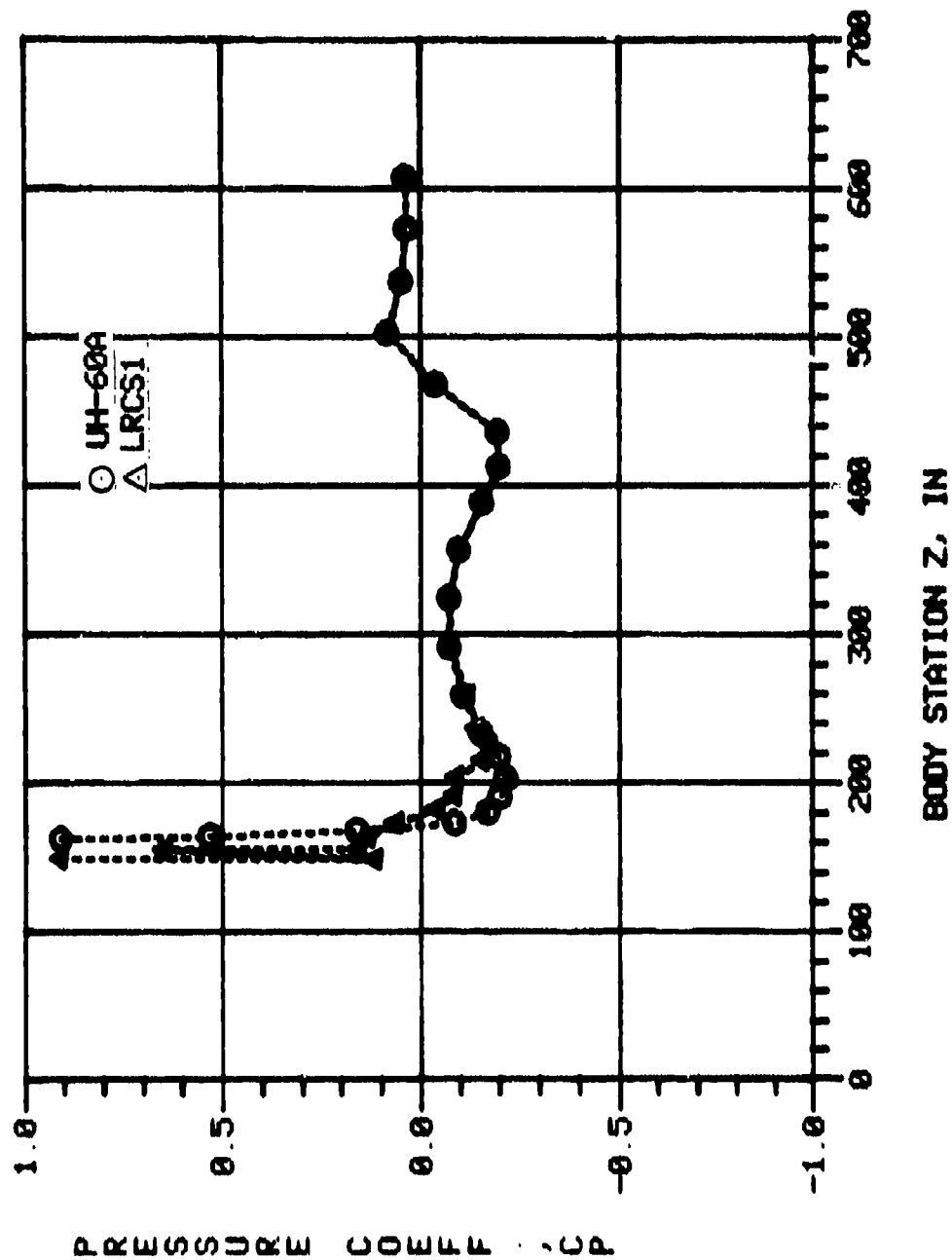


Figure A-13. COMPARISON OF THE UH-60A UTAS AND LRCS1 CALCULATED SURFACE PRESSURES, BOTTOM CENTERLINE, $\alpha = 4^\circ$, $\psi = 0^\circ$

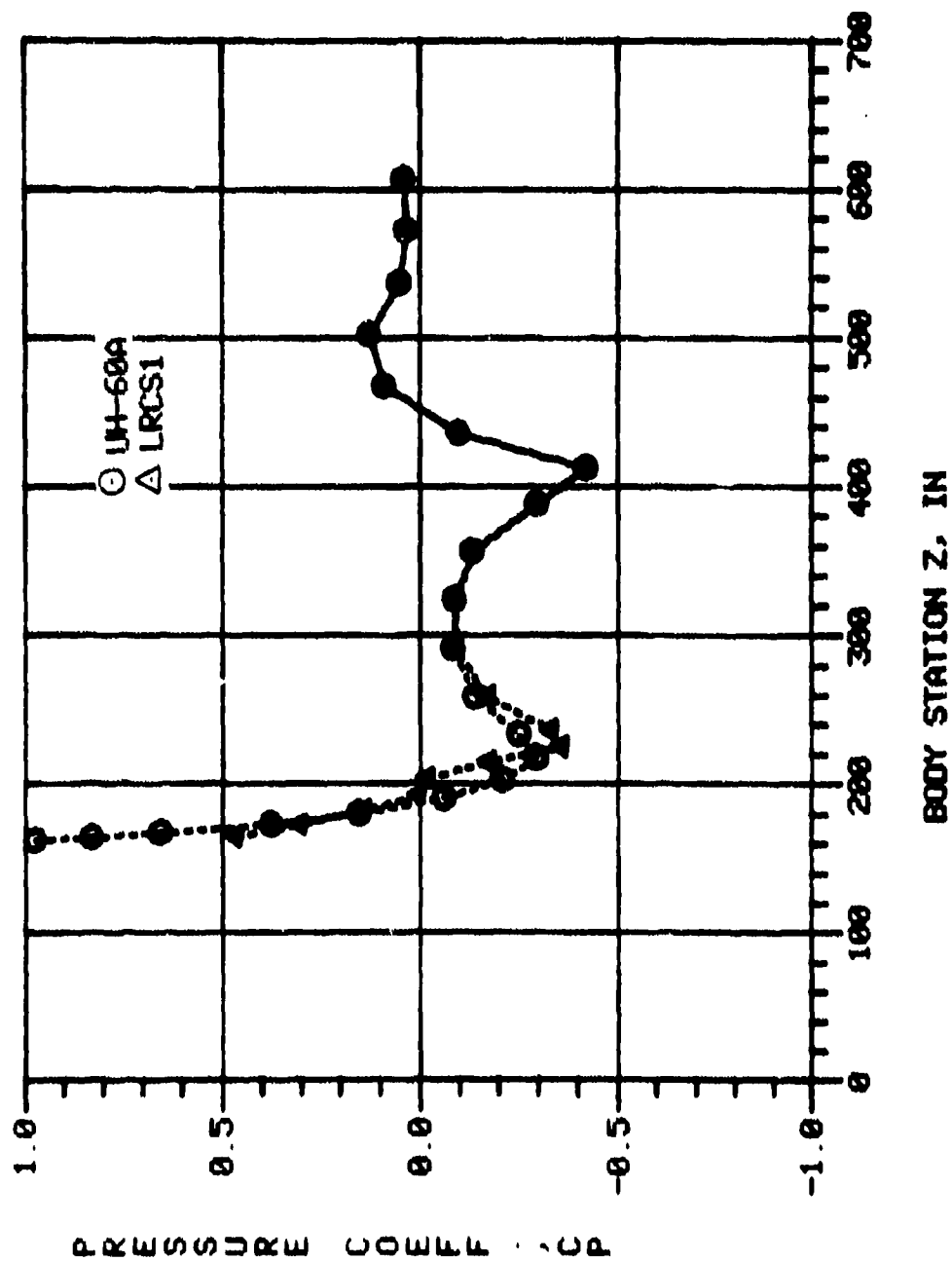


Figure A-14. COMPARISON OF THE UH-60A UTTAS AND LRCS1 CALCULATED SURFACE PRESSURES, LATERAL CENTERLINE, $\alpha = 4^\circ$, $\psi = 0^\circ$

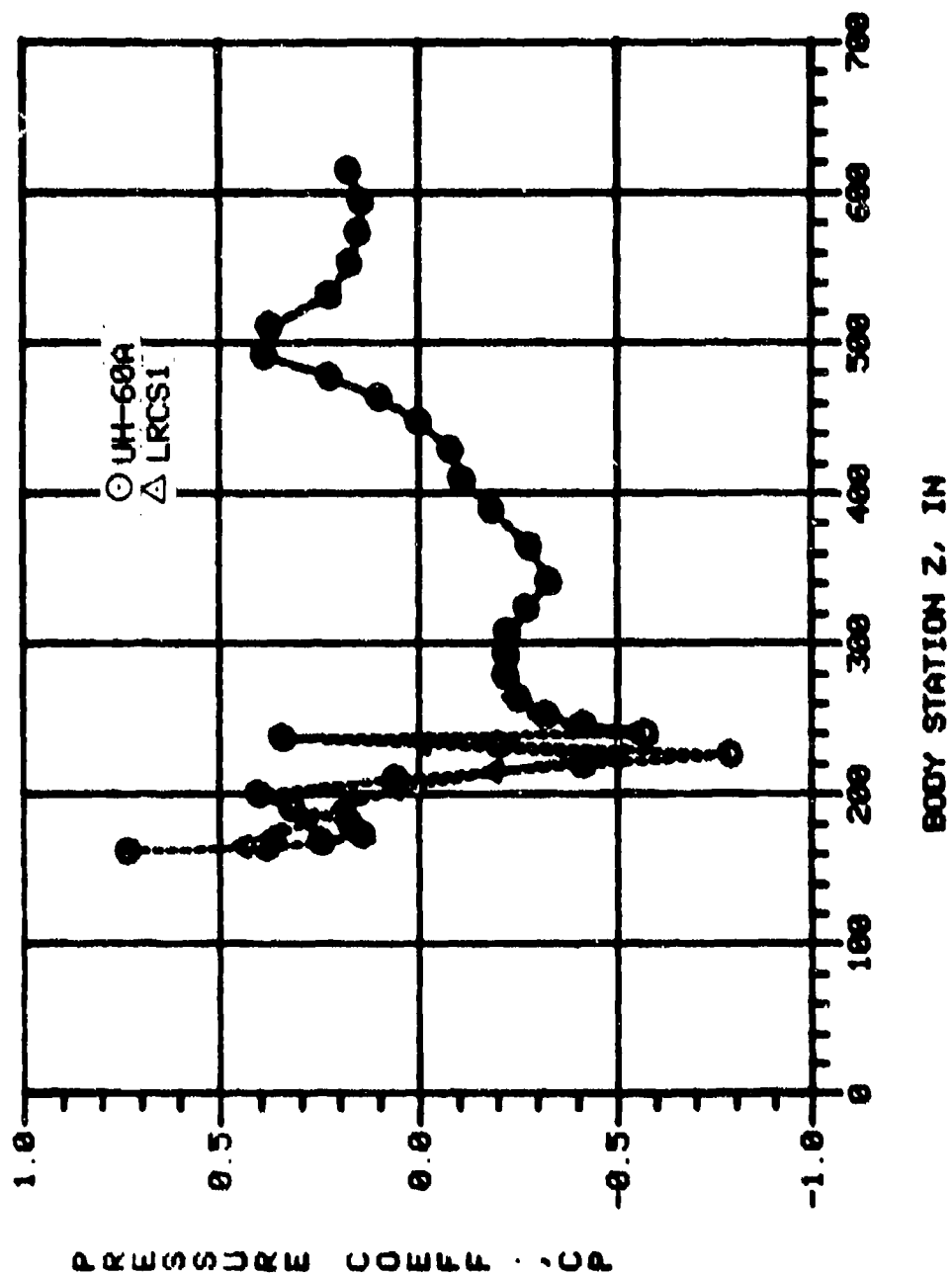


Figure A-15. COMPARISON OF THE UH-60A UTAS AND LRCS1 CALCULATED SURFACE PRESSURES, TOP CENTERLINE, $\alpha = 8^\circ$, $\psi = 0^\circ$

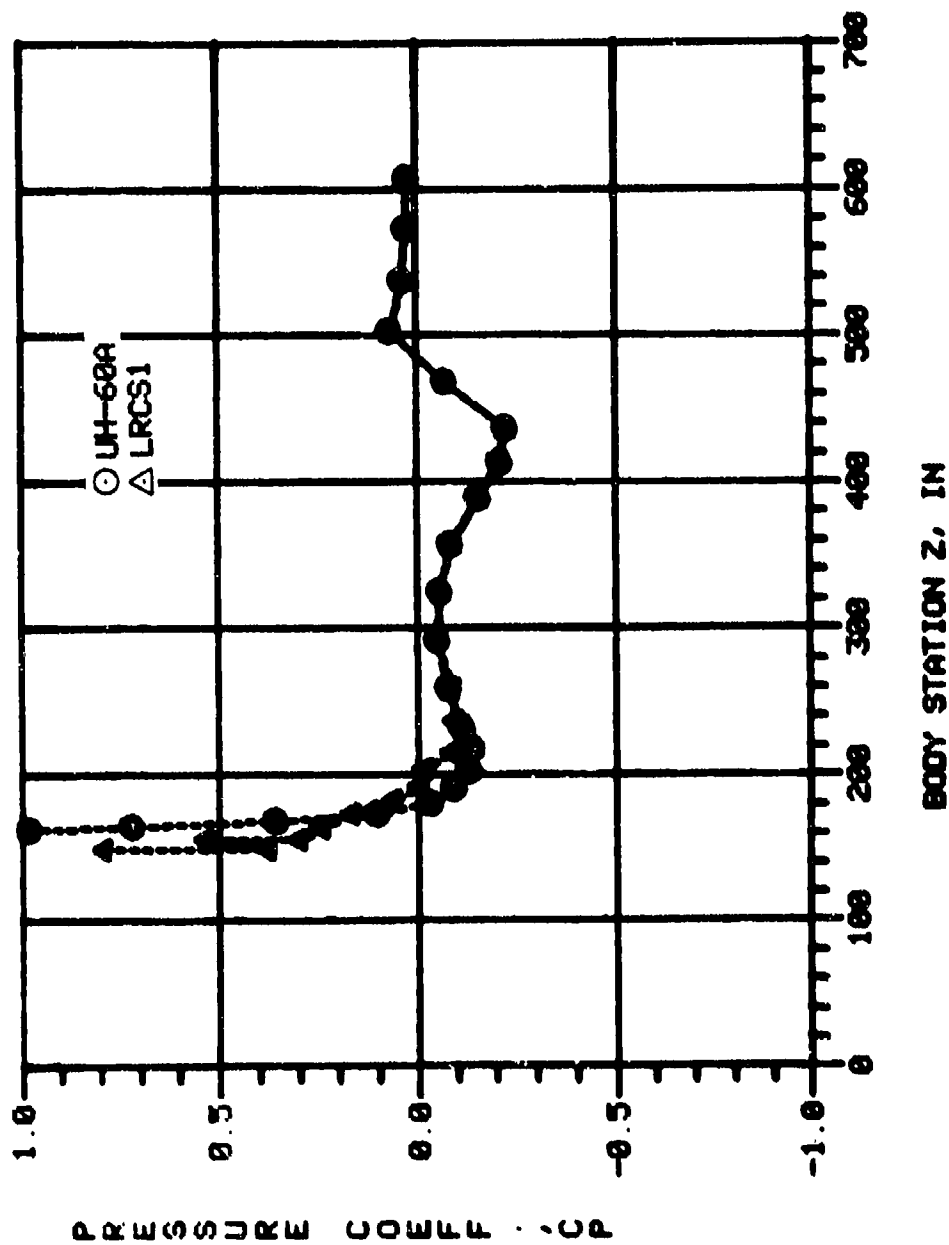


Figure A-16. COMPARISON OF THE UH-60A UTTAS AND LRCS1 CALCULATED SURFACE PRESSURES, BOTTOM CENTERLINE, $\alpha = 8^\circ$, $\psi = 0^\circ$

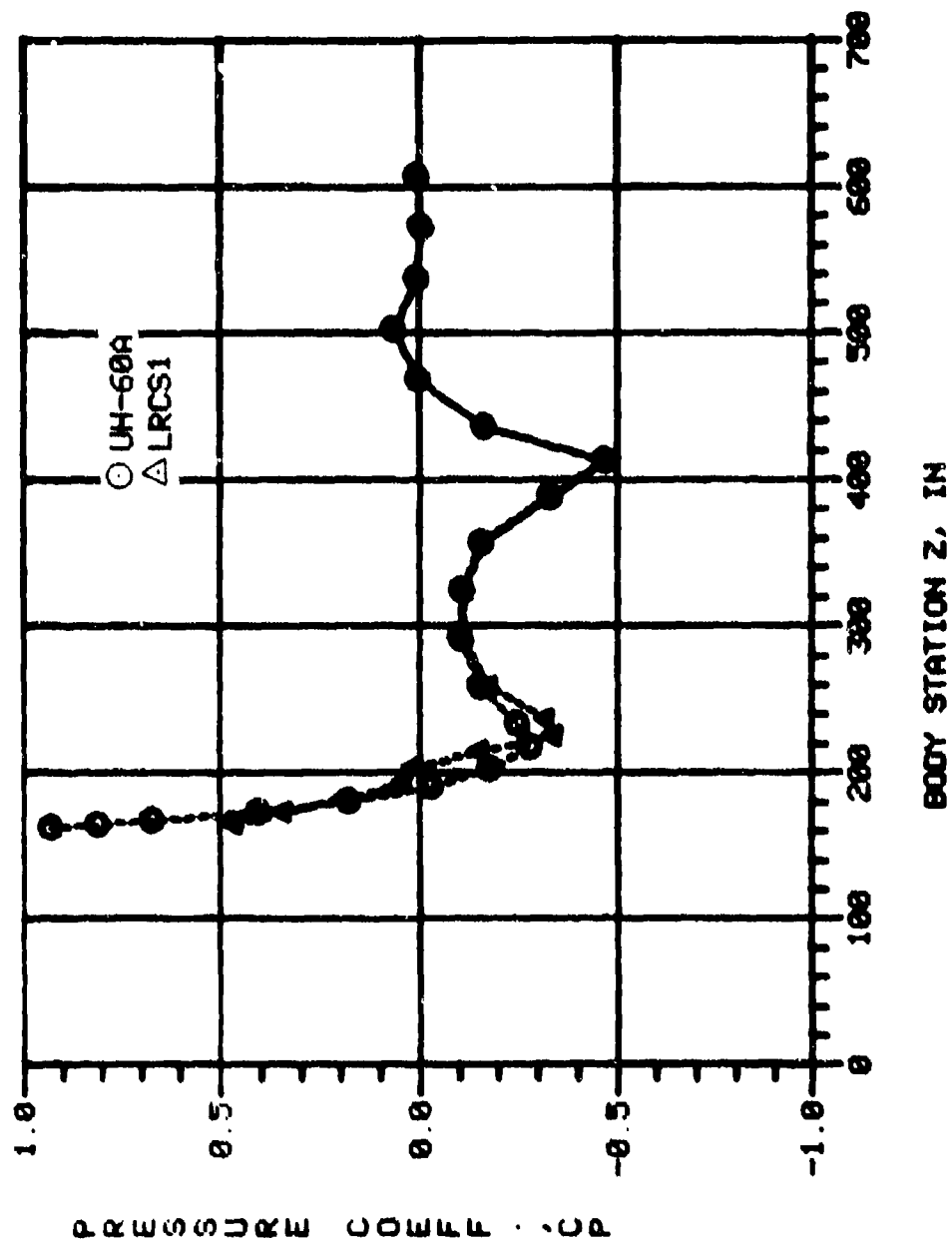


Figure A-17. COMPARISON OF THE UH-60A UTIAS AND LRCS1 CALCULATED SURFACE PRESSURES, LATERAL CENTERLINE, $\alpha = 80^\circ$ $\psi = 0^\circ$

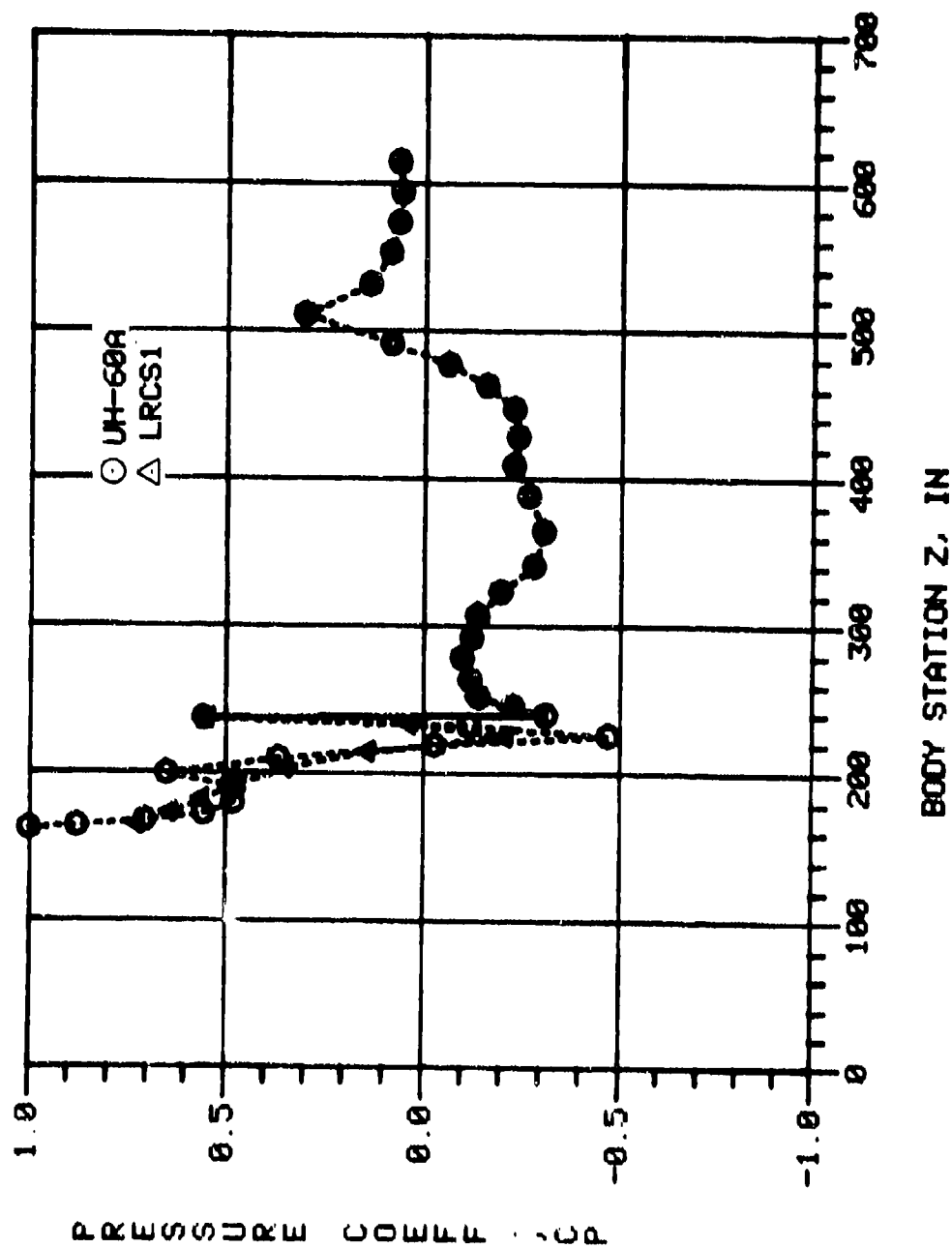


Figure A-18. COMPARISON OF THE UH-60A UTMAS AND LRCS1 CALCULATED SURFACE PRESSURES, TOP CENTERLINE, $\alpha = 14^\circ$, $\psi = 0^\circ$

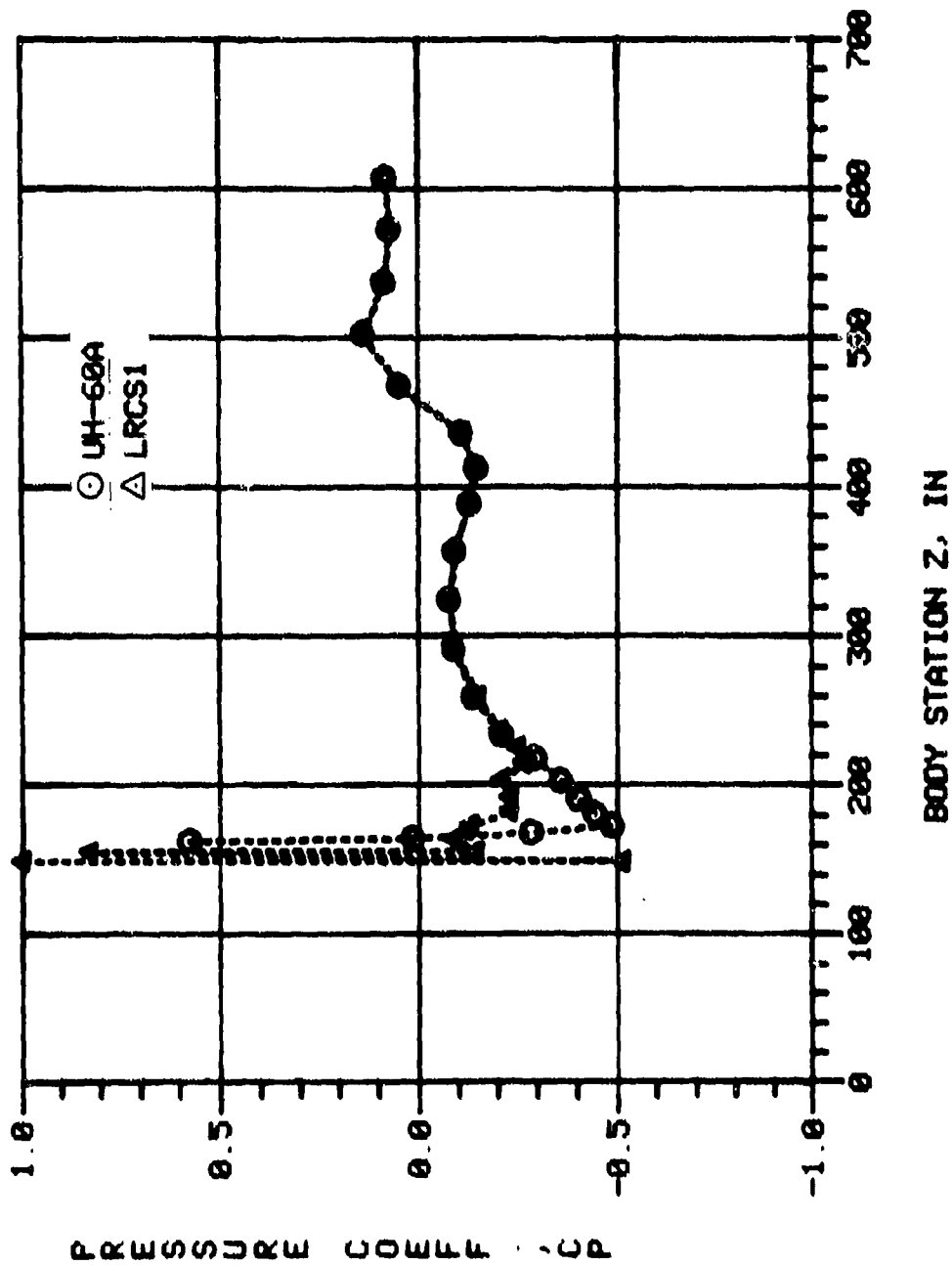


Figure A-19. COMPARISON OF THE UH-60A UHTAS AND LRCS1 CALCULATED SURFACE PRESSURES, BOTTOM CENTERLINE, $\alpha = -4^\circ$, $\psi = 0^\circ$

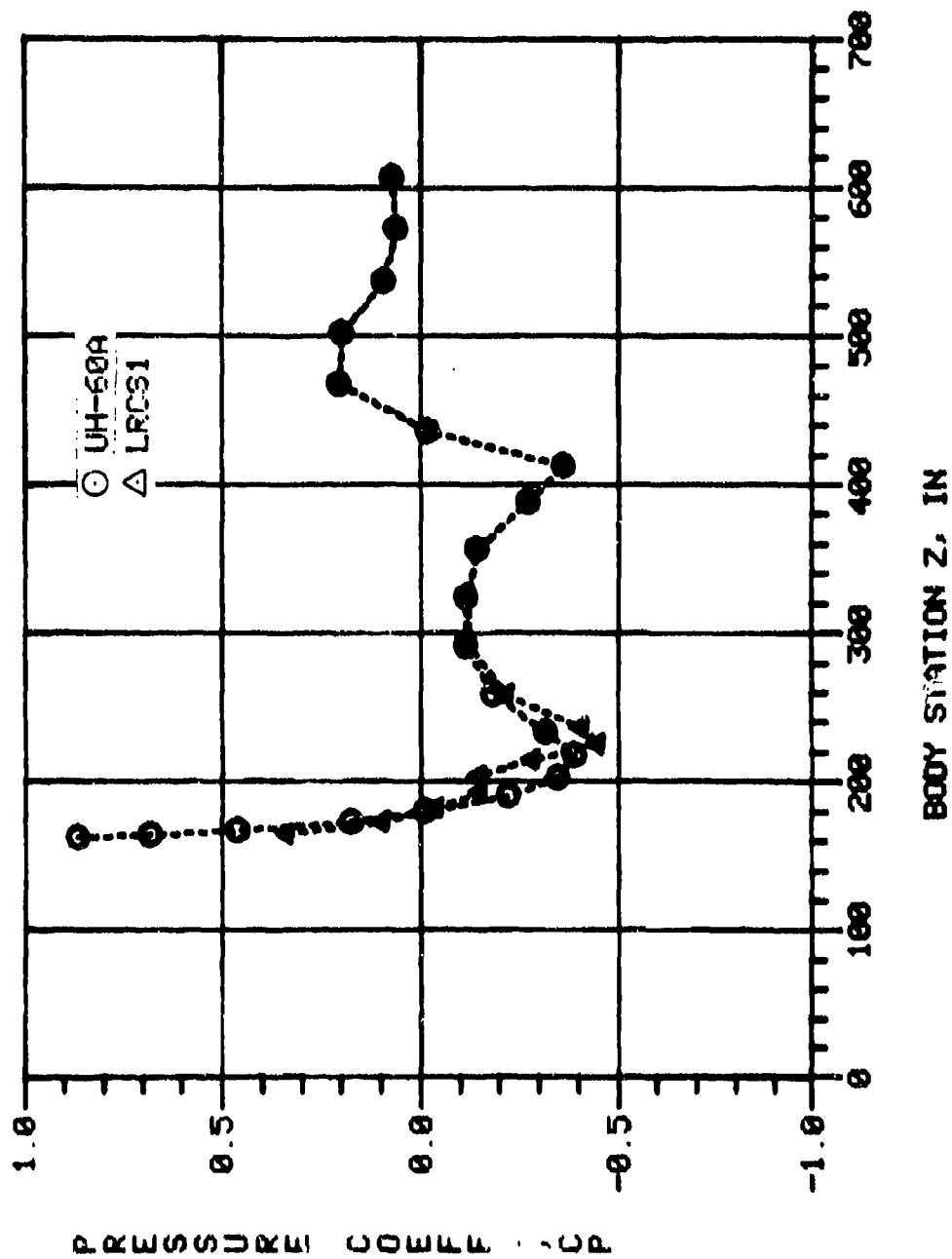


Figure A-20. COMPARISON OF THE UH-60A UTAS AND LRCS1 CALCULATED SURFACE PRESSURES, LATERAL CENTERLINE, $\alpha = -4^\circ$, $\psi = 0^\circ$

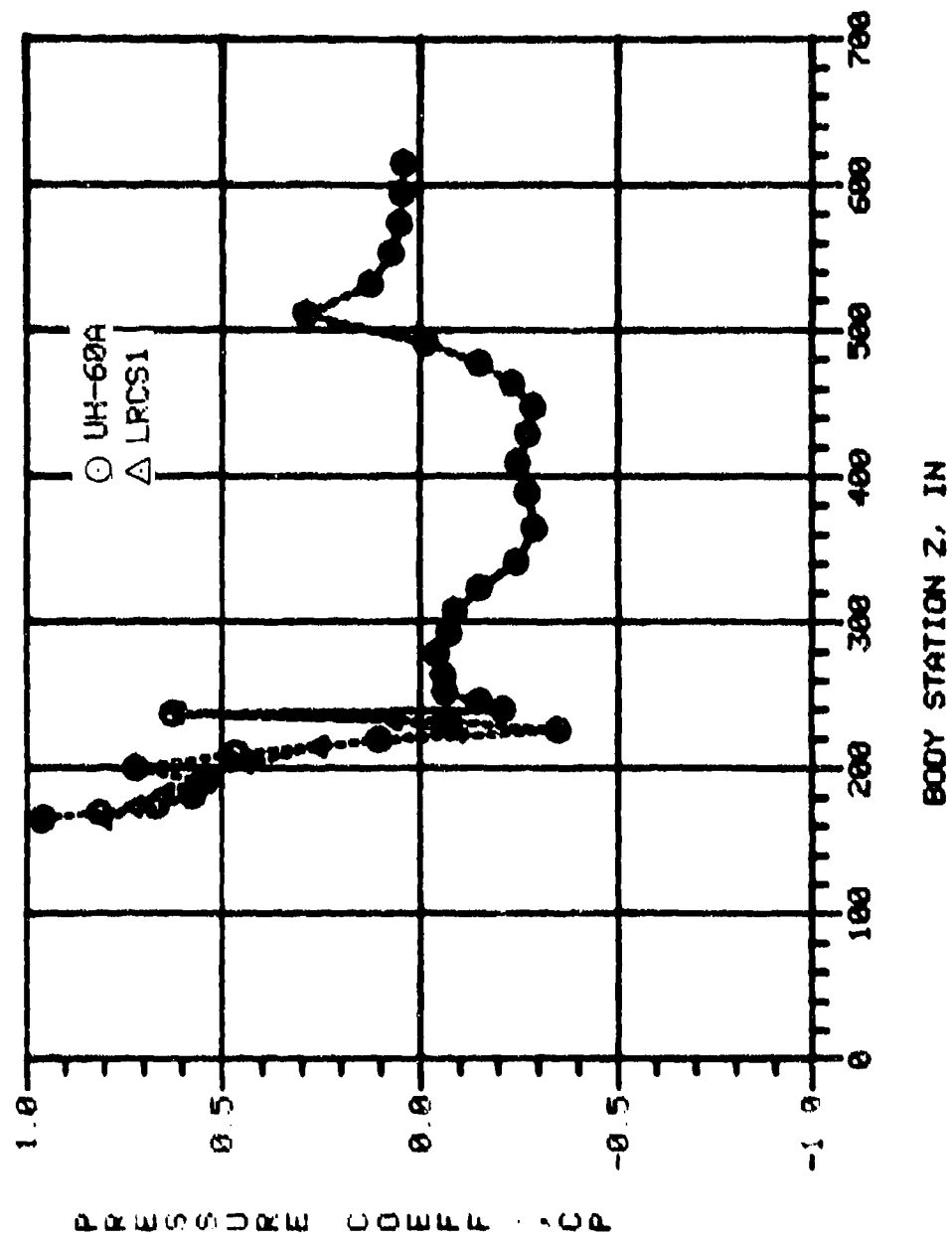


Figure A-21. COMPARISON OF THE UH-60A UFTAS AND LRCS1 CALCULATED SURFACE PRESSURES, IN CENTERLINE, $\alpha = -8^\circ$, $\psi = 0^\circ$

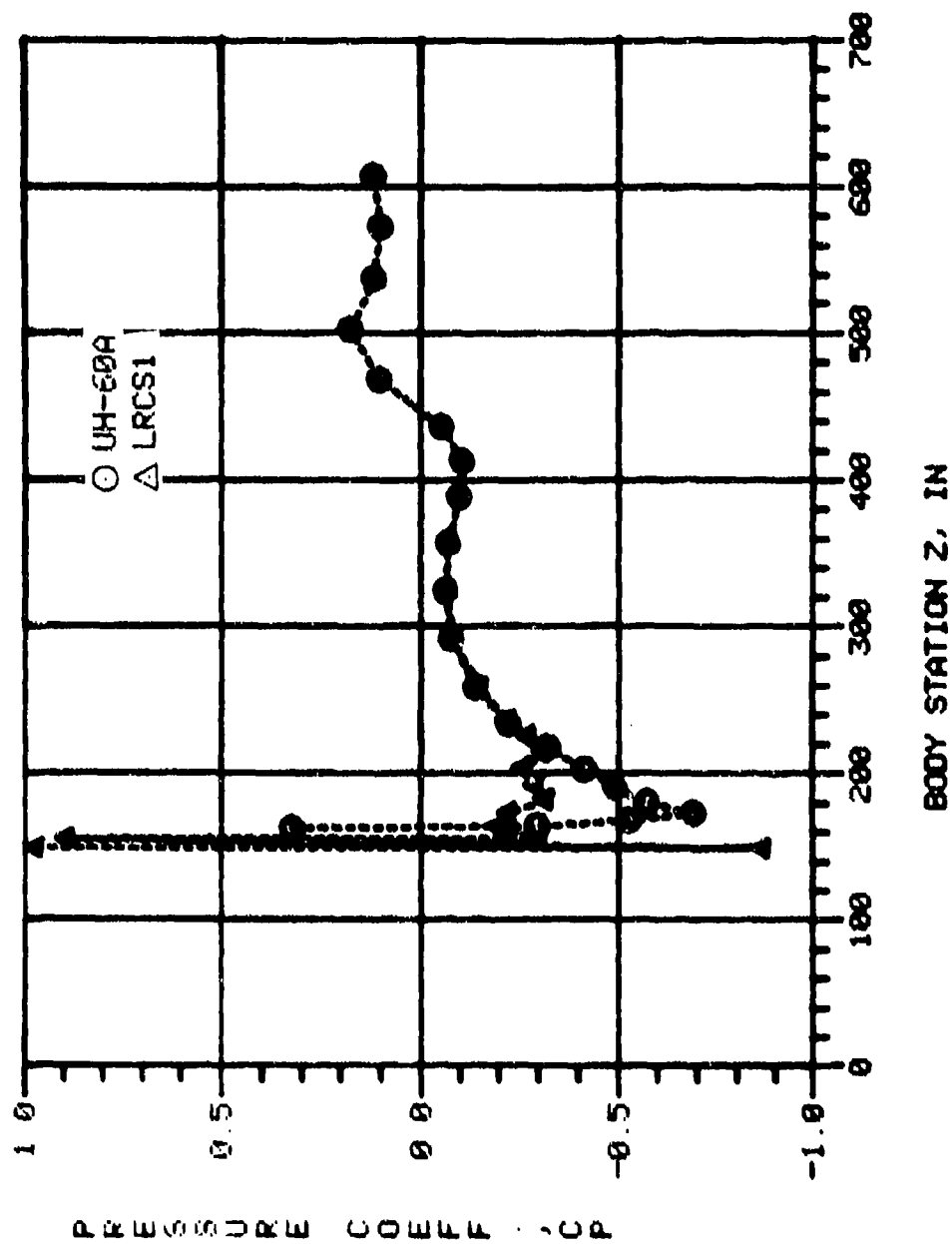


Figure A-22. COMPARISON OF THE UH-60A UTMAS AND LRCS1 CALCULATED SURFACE PRESSURES, BOTTOM CENTERLINE, $\alpha = -8^\circ$, $\psi = 0^\circ$

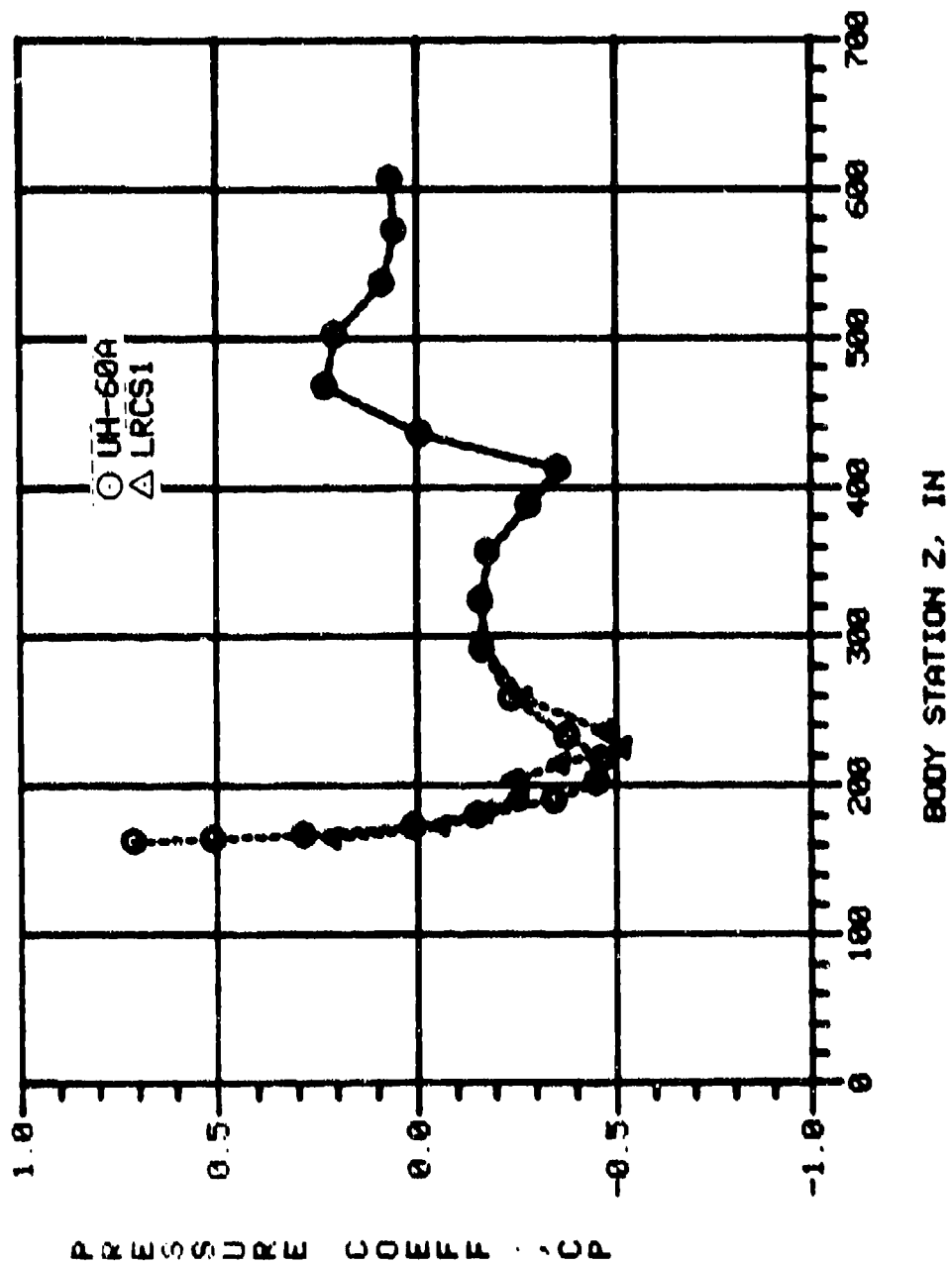


Figure A-23. COMPARISON OF THE UH-60A UTIAS AND LRCS1 CALCULATED SURFACE PRESSURES, LATERAL CENTERLINE, $\alpha = -8^\circ$, $\psi = 0^\circ$

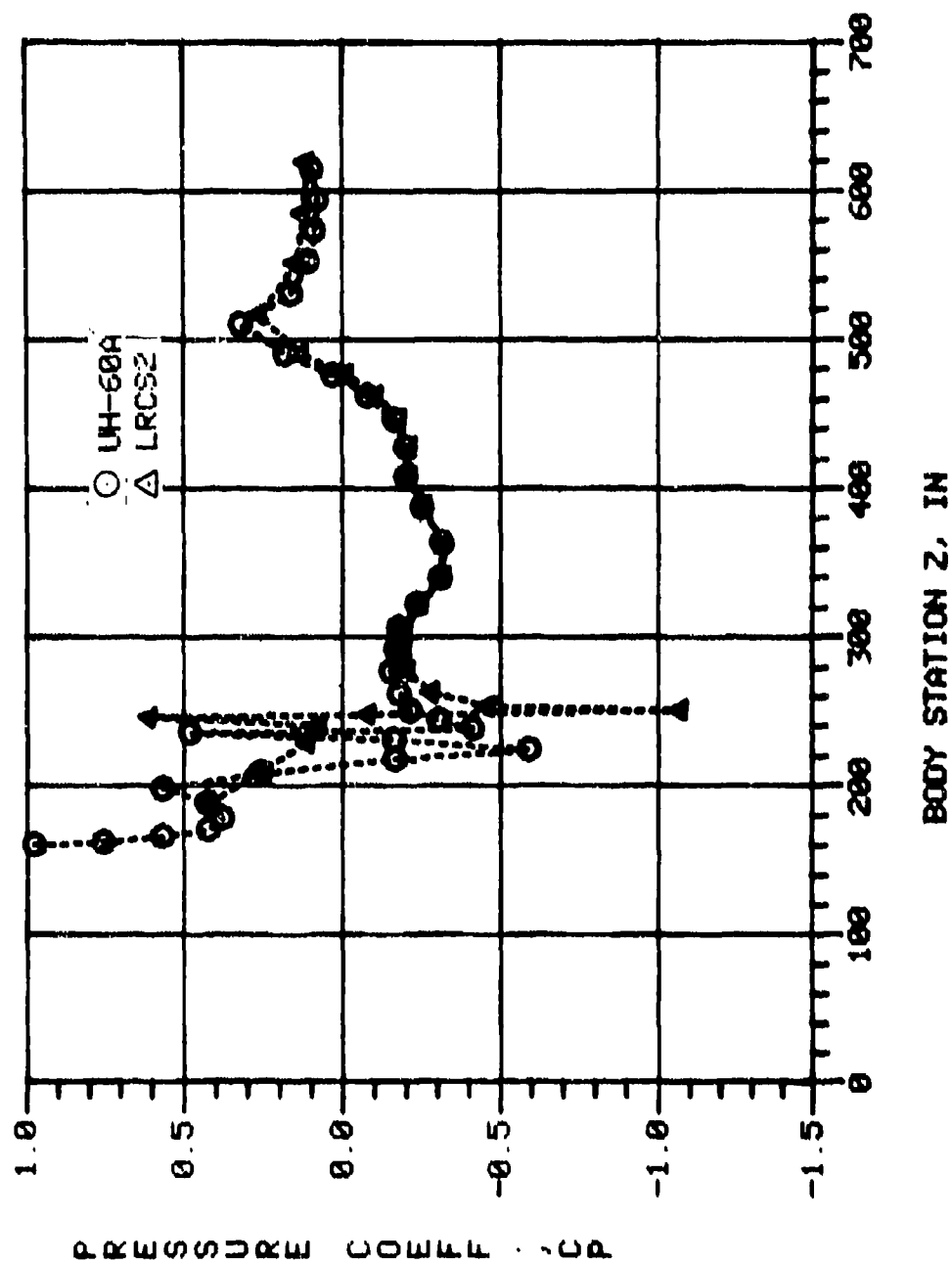


Figure A-24. COMPARISON OF THE UH-60A UTAS AND LRCS2 CALCULATED SURFACE PRESSURES, TOP CENTERLINE, $\alpha = 0^\circ$, $\psi = 0^\circ$

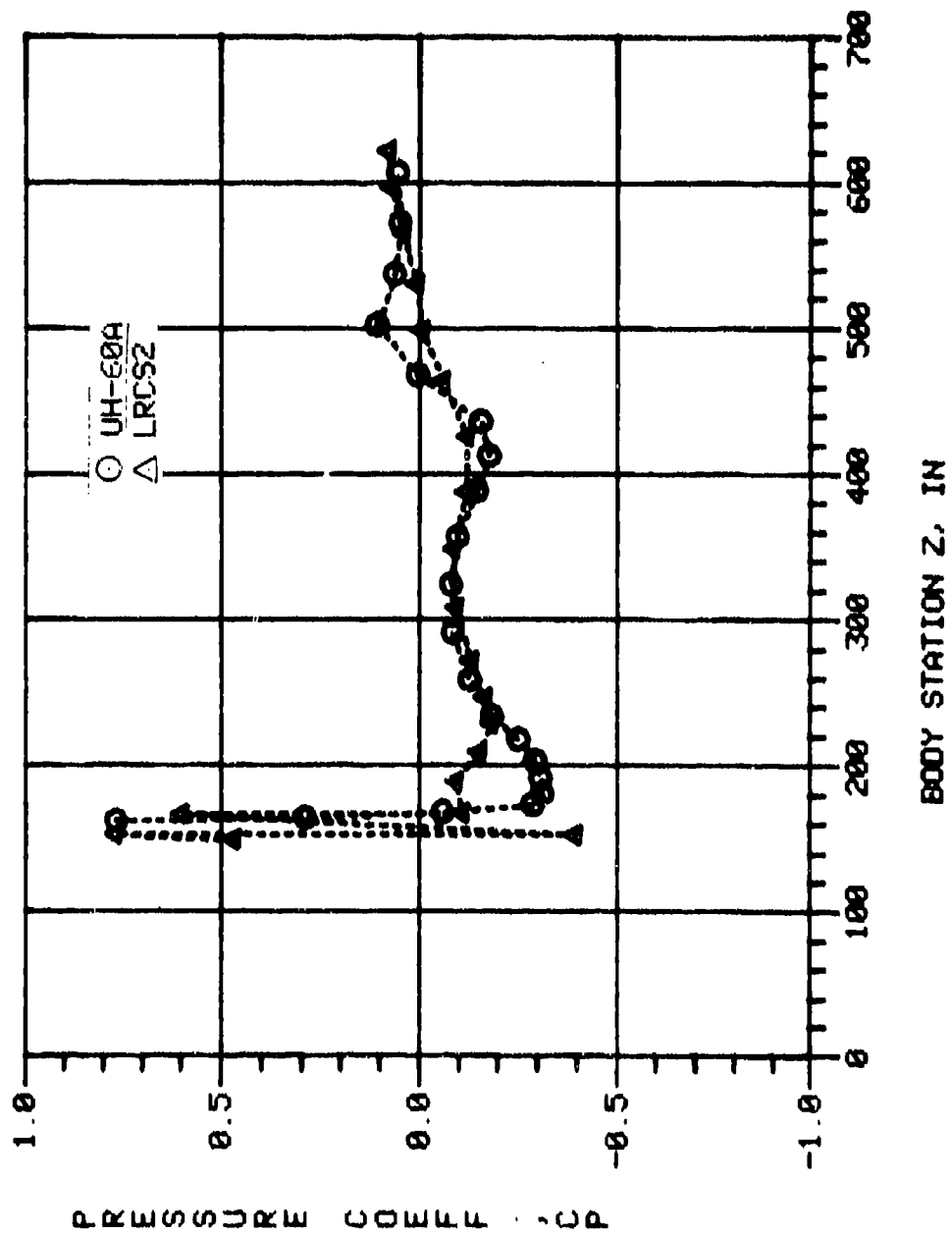


Figure A-25. COMPARISON OF THE UH-60A UTIAS AND LRCS2 CALCULATED SURFACE PRESSURES, BOTTOM CENTERLINE, $\alpha = 0^\circ$, $\psi = 0^\circ$

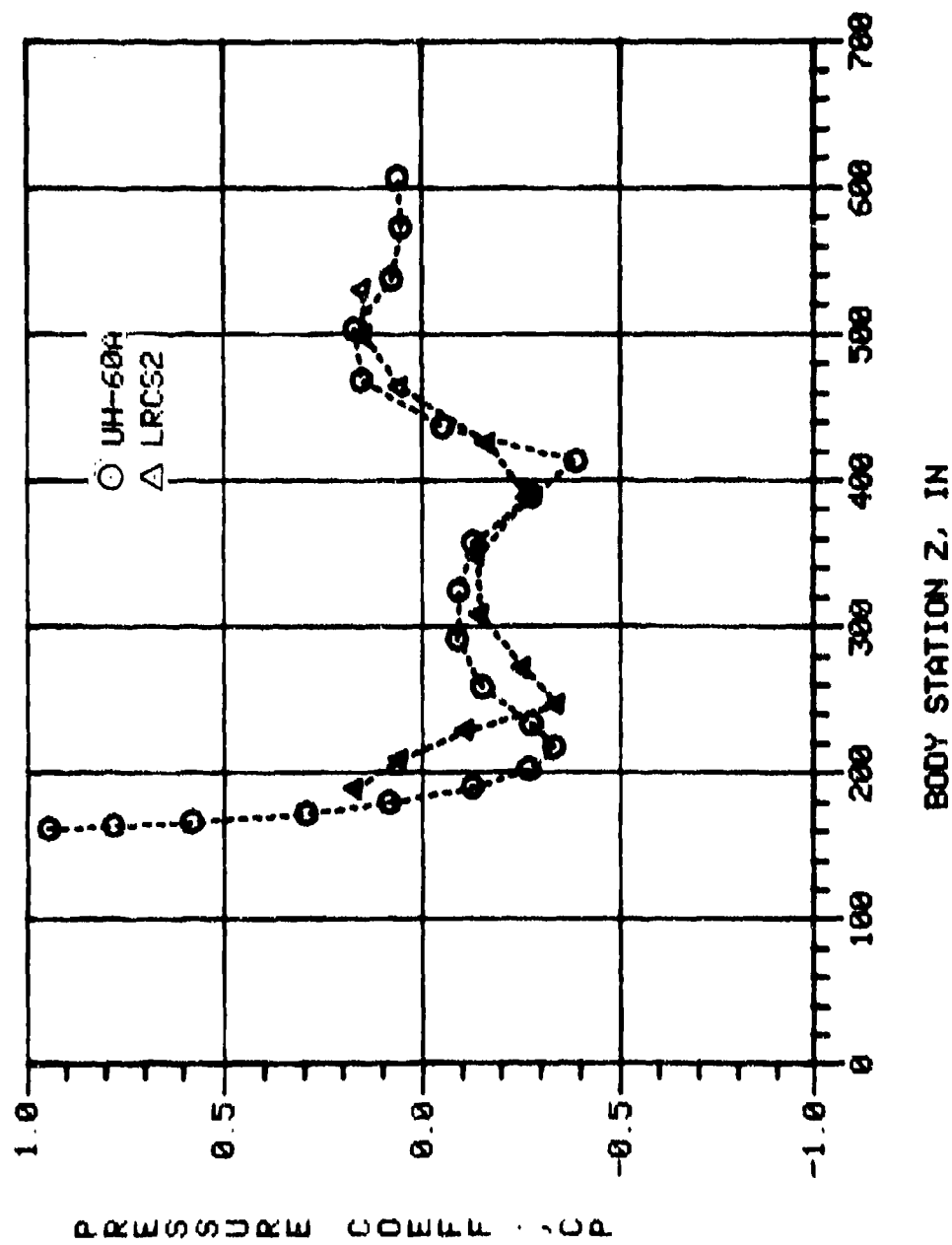


Figure A-26. COMPARISON OF THE UH-60A UNTAS AND LRCS2 CALCULATED SURFACE PRESSURES, LATERAL CENTERLINE, $\alpha = 0^\circ$, $\psi = 0^\circ$

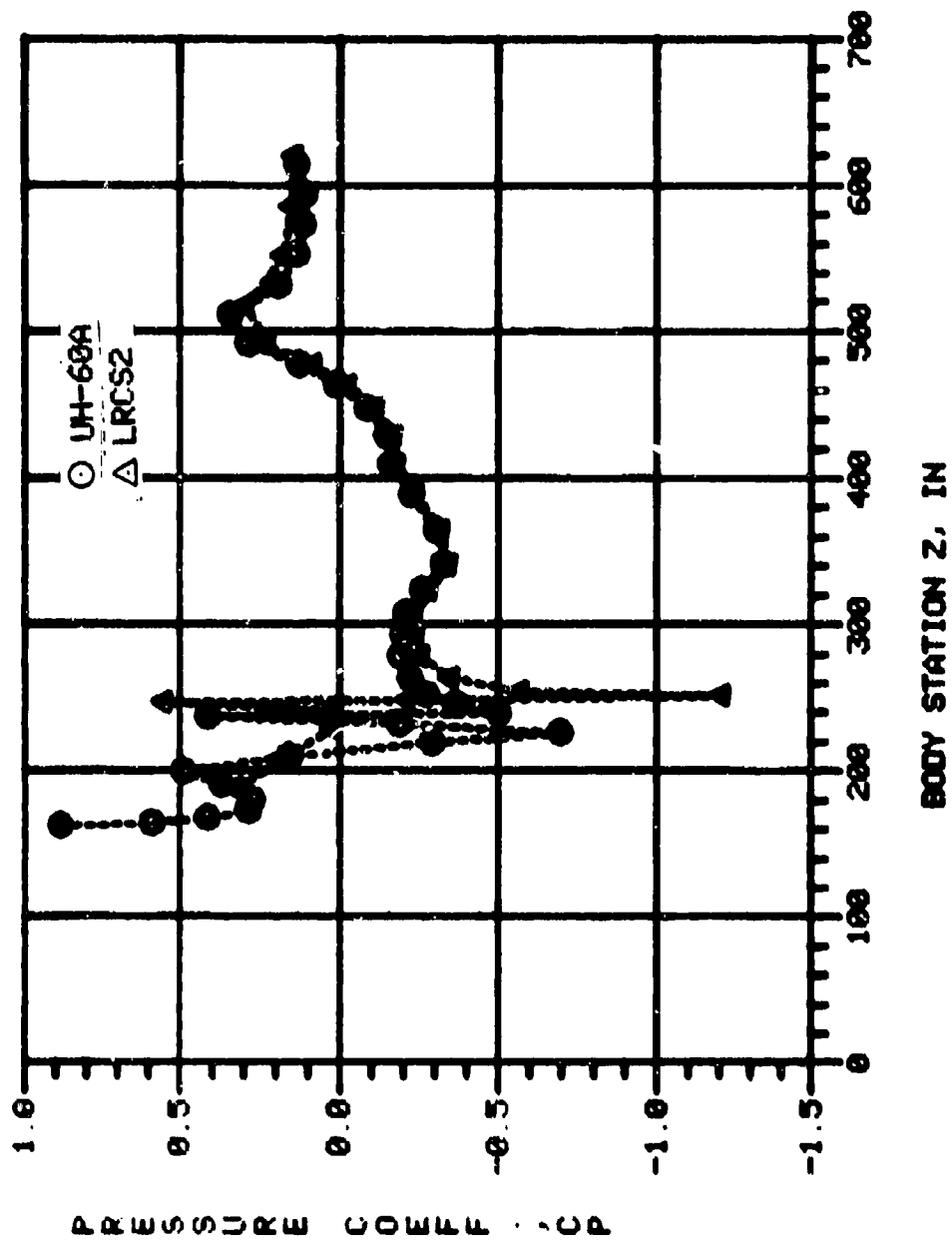


Figure A-27. COMPARISON OF THE UH-60A UTTAS AND LRCS2 CALCULATED SURFACE PRESSURES, TOP CENTERLINE, $\alpha = 4^\circ$, $\psi = 0^\circ$

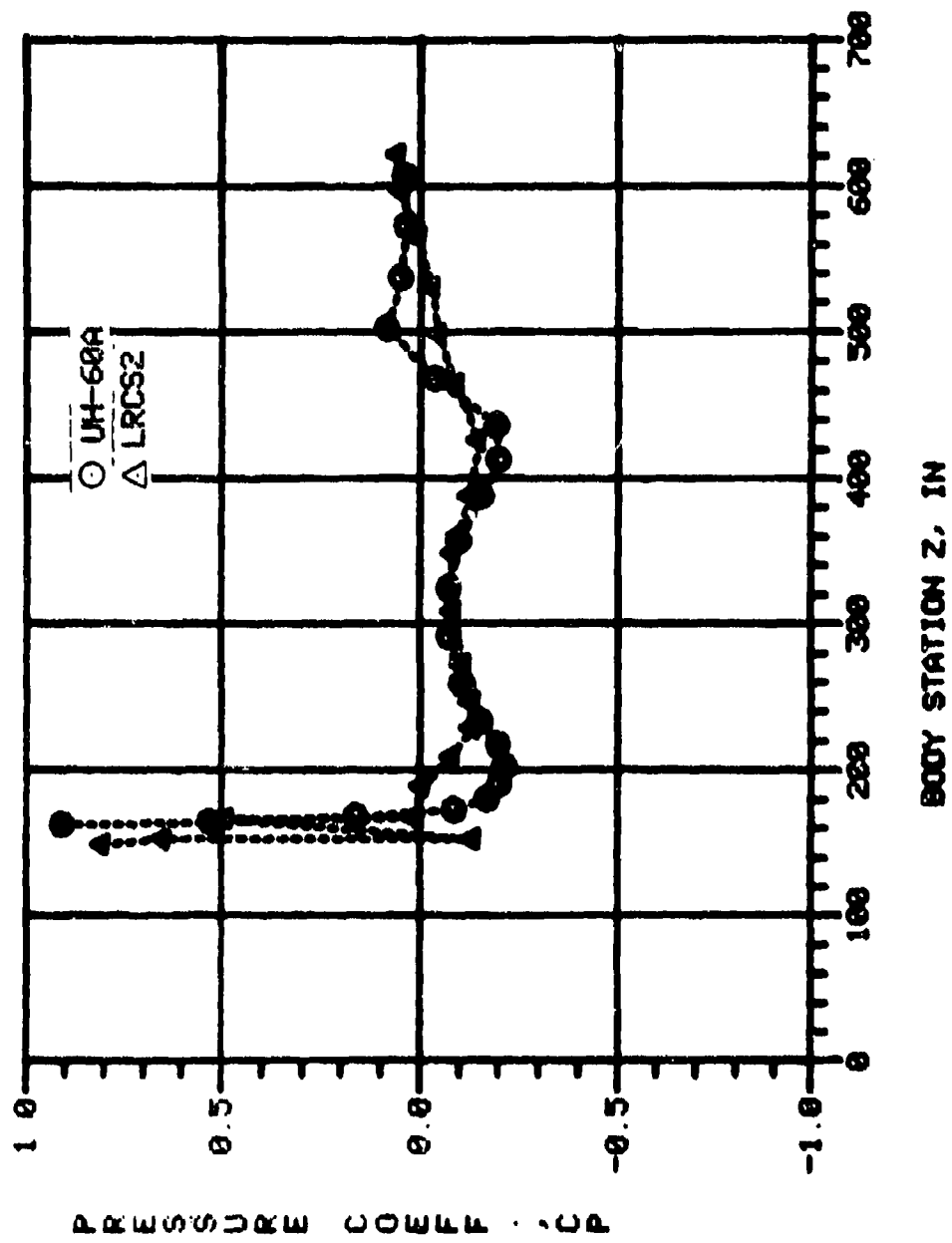


Figure A-28. COMPARISON OF THE UH-60A UTIAS AND LRC52 CALCULATED SURFACE PRESSURES, BOTTOM CENTERLINE $\alpha = 4^\circ$ $\psi = 0^\circ$

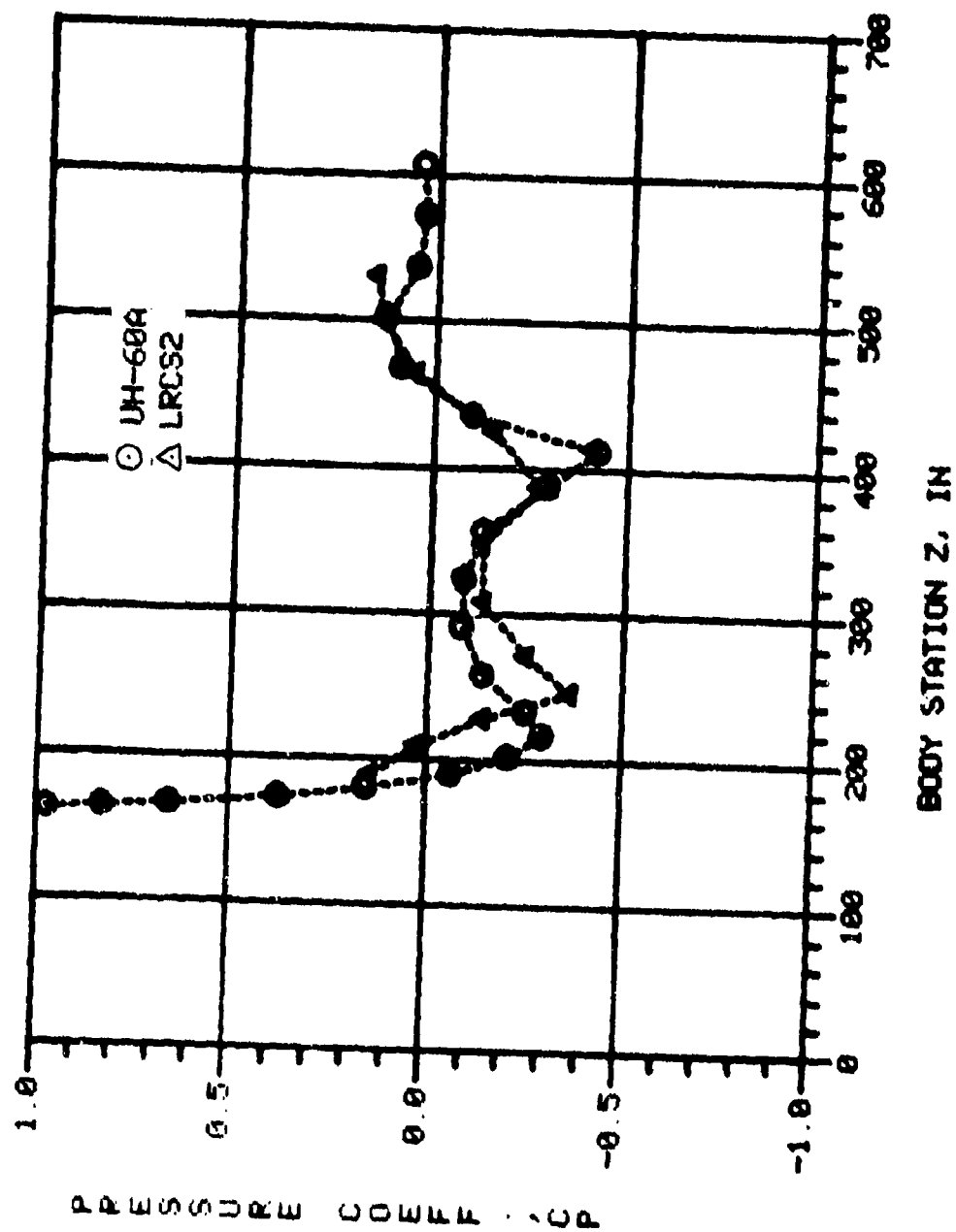


Figure A-29. COMPARISON OF THE UH-60A UTIAS AND LRCS2 CALCULATED SURFACE PRESSURES, LATERAL CENTERLINE, $\alpha = 10^\circ$, $\psi = 0^\circ$

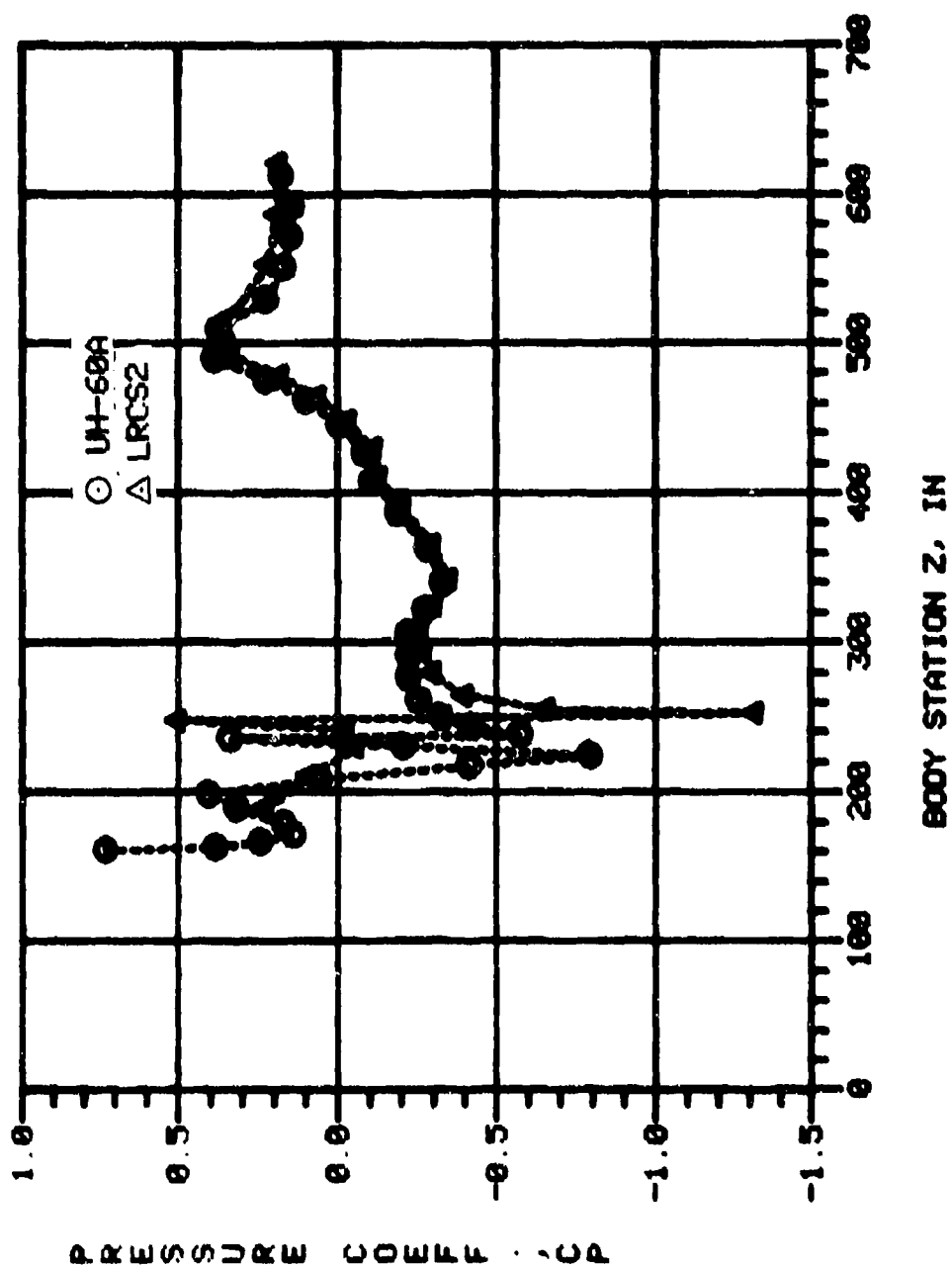


Figure A-30. COMPARISON OF THE UH-60A UTIAS AND LRCS2 CALCULATED SURFACE PRESSURES, TOP CENTERLINE, $\alpha = 8^\circ$, $\psi = 0^\circ$

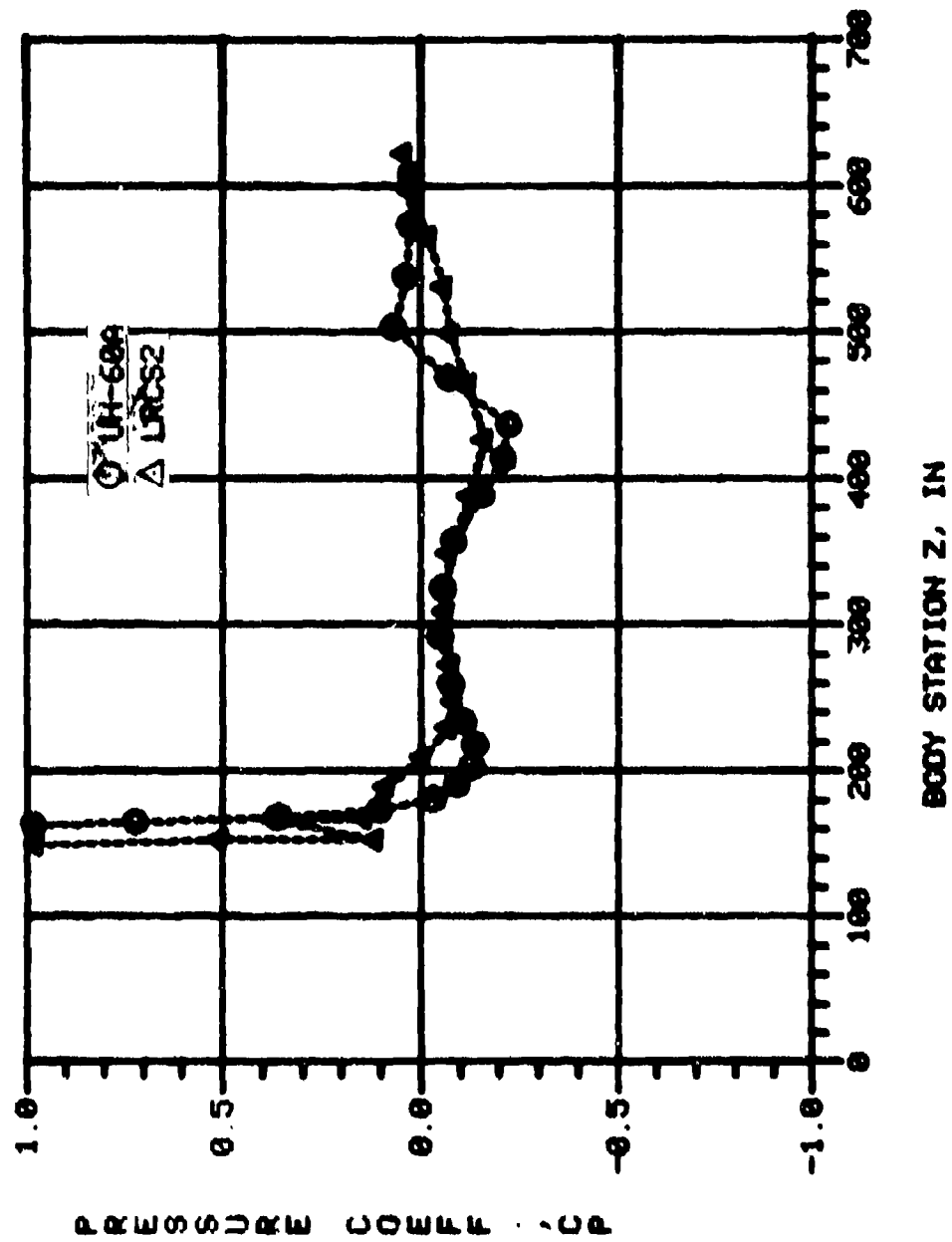


Figure A-31. COMPARISON OF THE UH-60A UFTAS AND LRCS2 CALCULATED SURFACE PRESSURES, BOTTOM CENTERLINE, $\alpha = 3^\circ$, $\psi = 0^\circ$

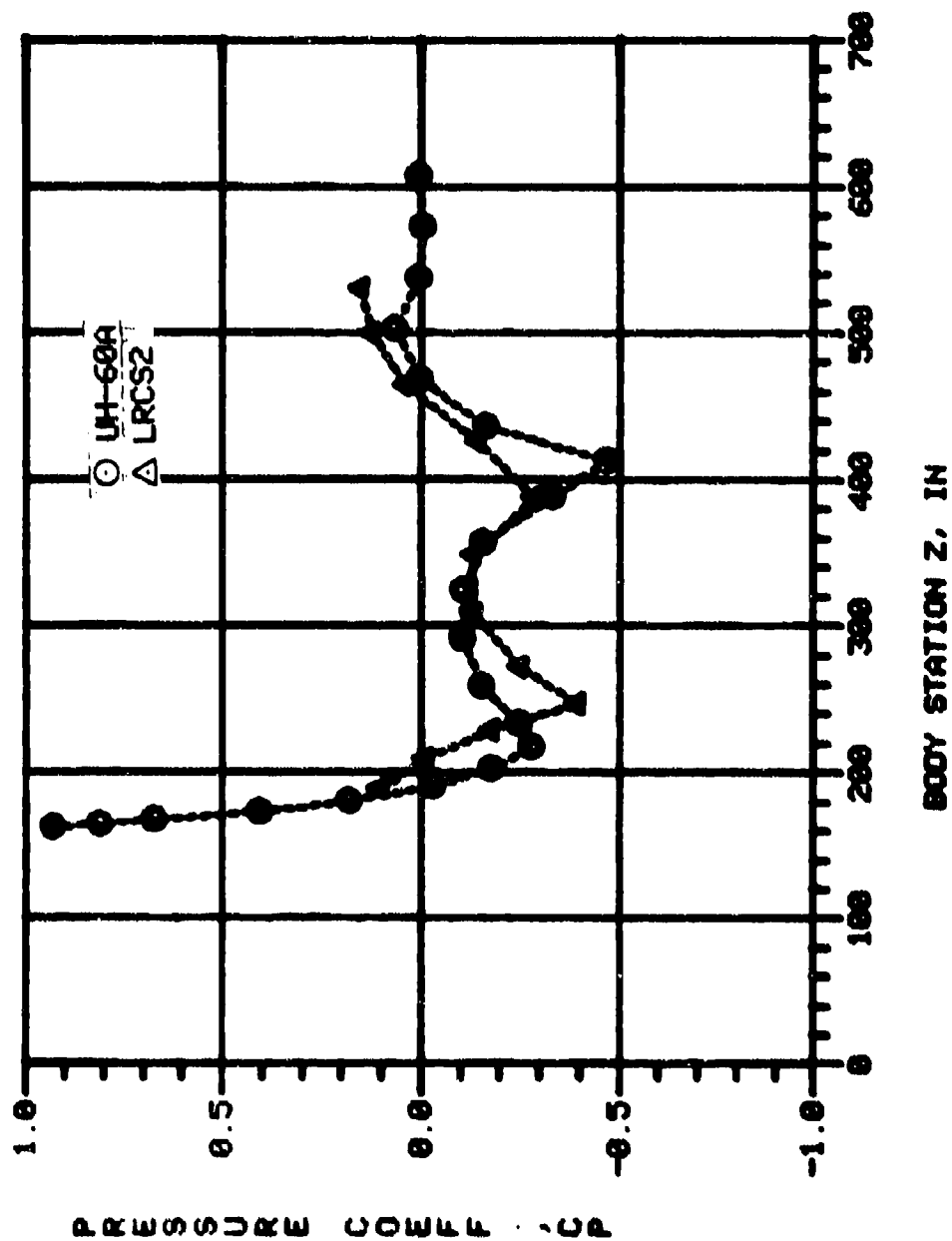


Figure A-32. COMPARISON OF THE UH-60A UTIAS AND LRCS2 CALCULATED SURFACE PRESSURES, LATERAL CENTERLINE, $\alpha = 8^\circ$, $\psi = 0^\circ$

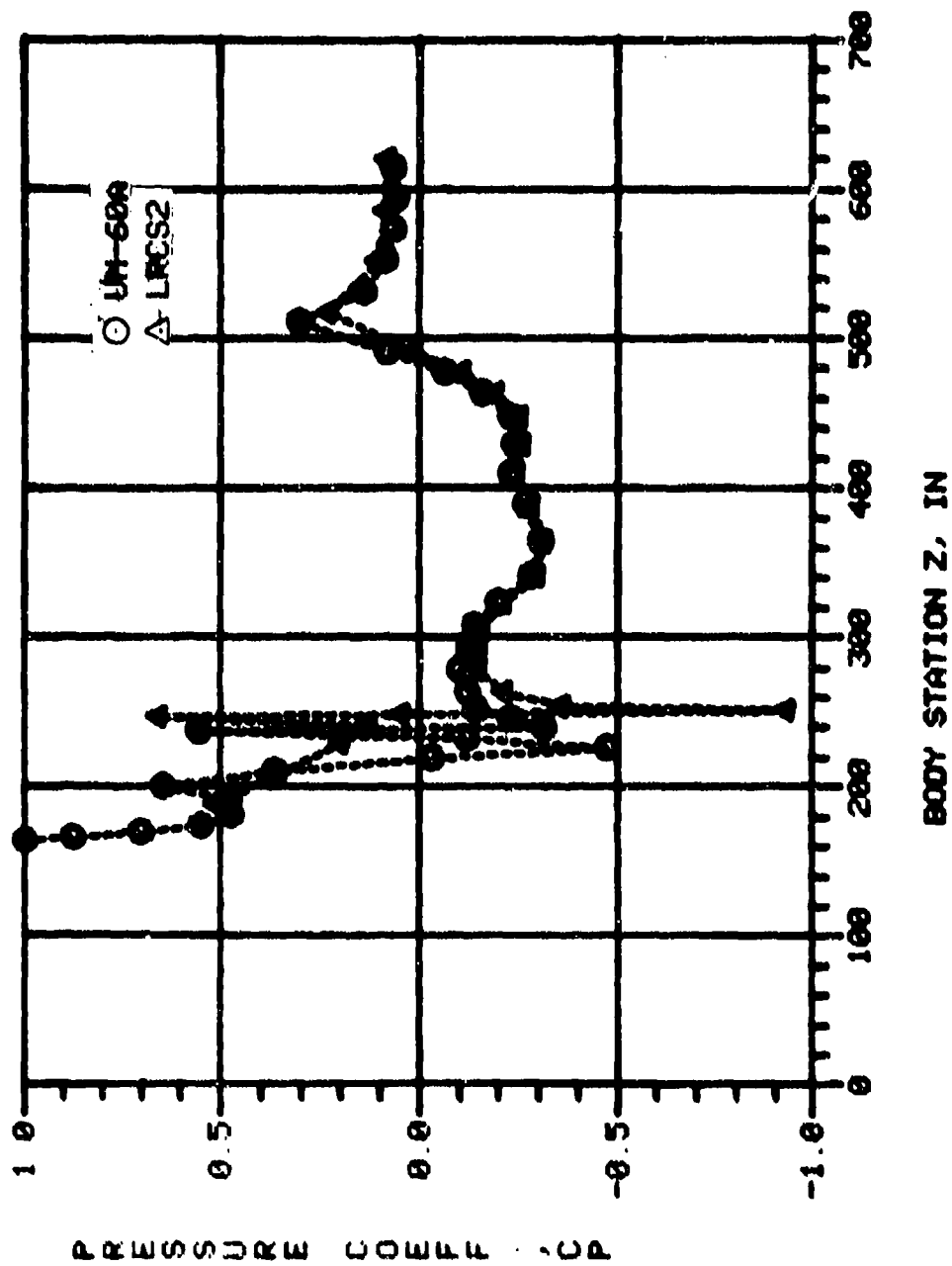


Figure A-33. COMPARISON OF THE UH-60A UFTAS AND LRCS2 CALCULATED SURFACE PRESSURES, TOP CENTERLINE, $\alpha = -4^\circ$, $\psi = 0^\circ$

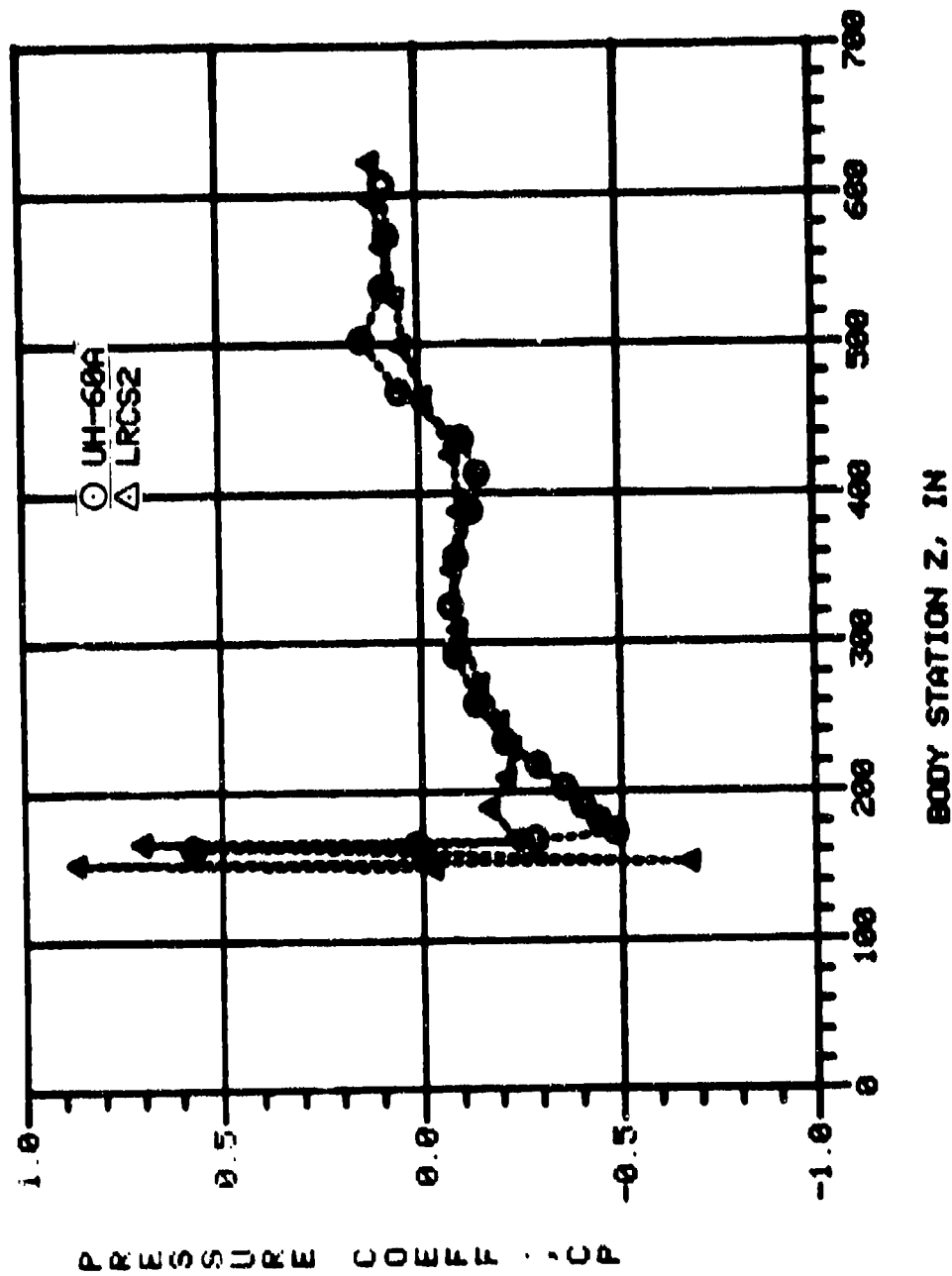


Figure A-34. COMPARISON OF THE UH-60A UTAS AND LRCS2 CALCULATED SURFACE PRESSURES, BOTTOM CENTERLINE, $\alpha = -4^\circ$, $\psi = 0^\circ$

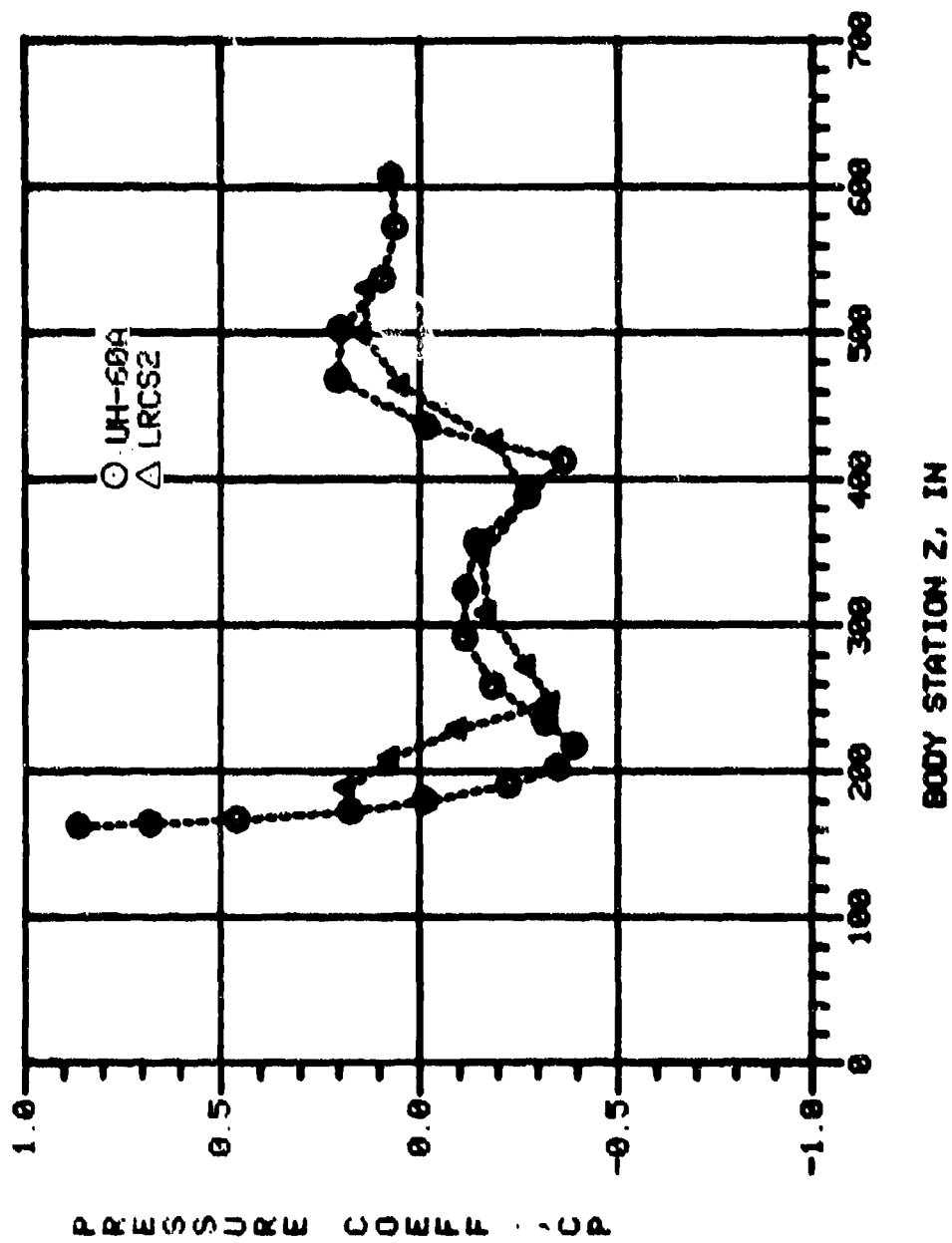


Figure A-35. COMPARISON OF THE UH-60A UTAS AND LRCS2 CALCULATED SURFACE PRESSURES, LATERAL CENTERLINE, $\alpha = -4^\circ$, $\psi = 0^\circ$

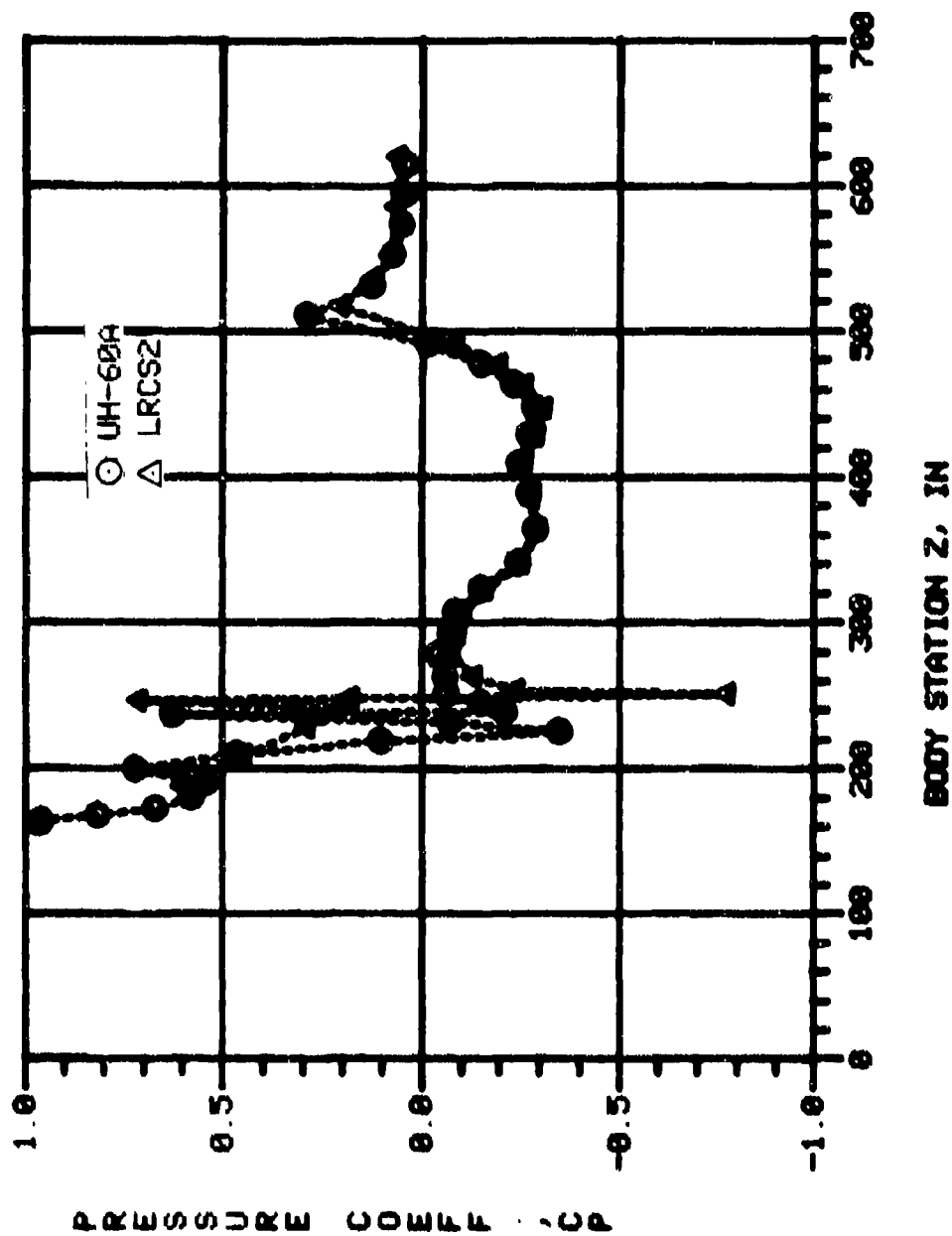


Figure A-36. COMPARISON OF THE UH-60A UTMAS AND LRCS2 CALCULATED SURFACE PRESSURES, TOP CENTERLINE, $\alpha = -8^\circ$, $\psi = 0^\circ$

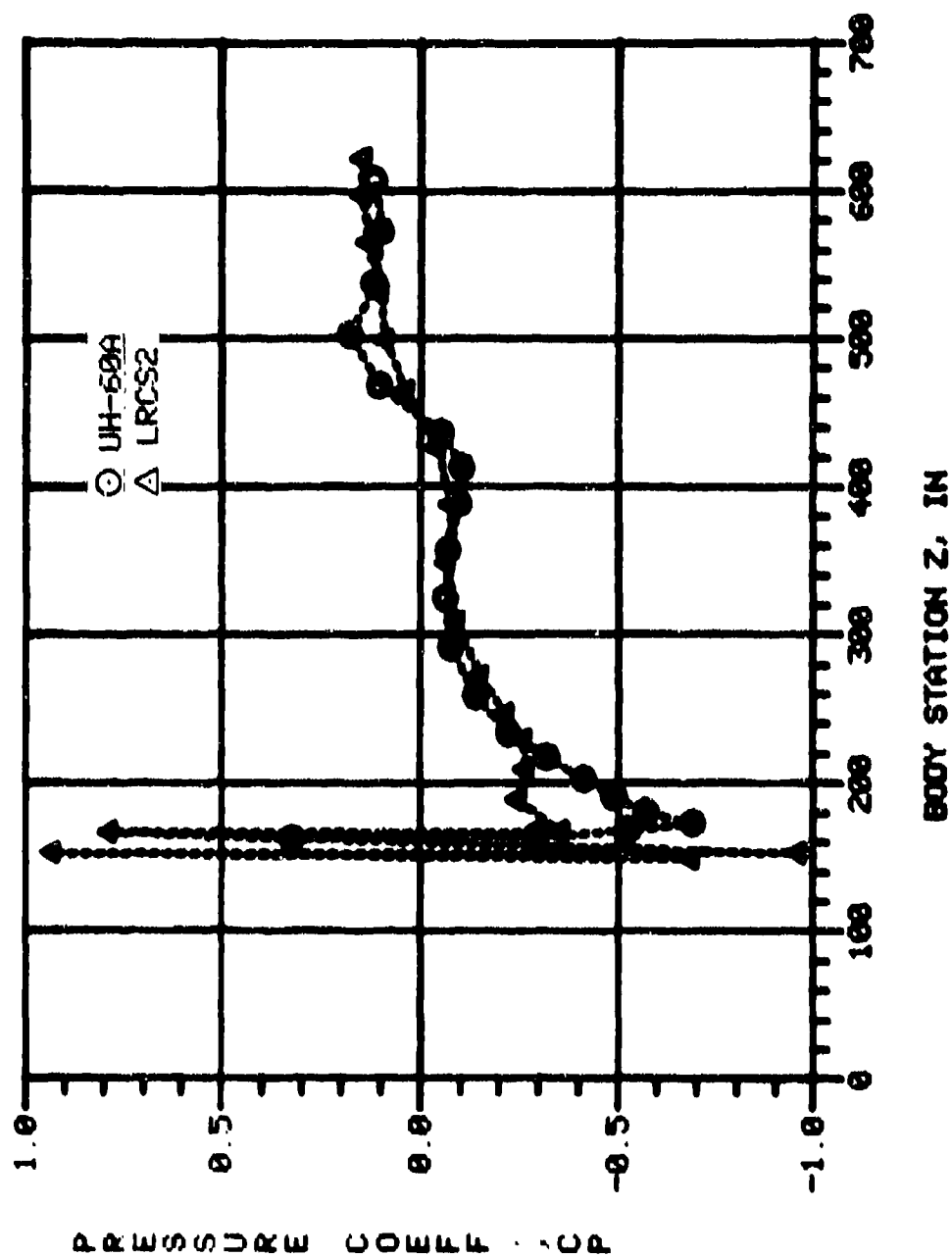


Figure A-37. COMPARISON OF THE UH-60A UTIAS AND LRCS2 CALCULATED SURFACE PRESSURES, BOTTOM CENTERLINE, $\alpha = -80^\circ$, $\psi = 0^\circ$

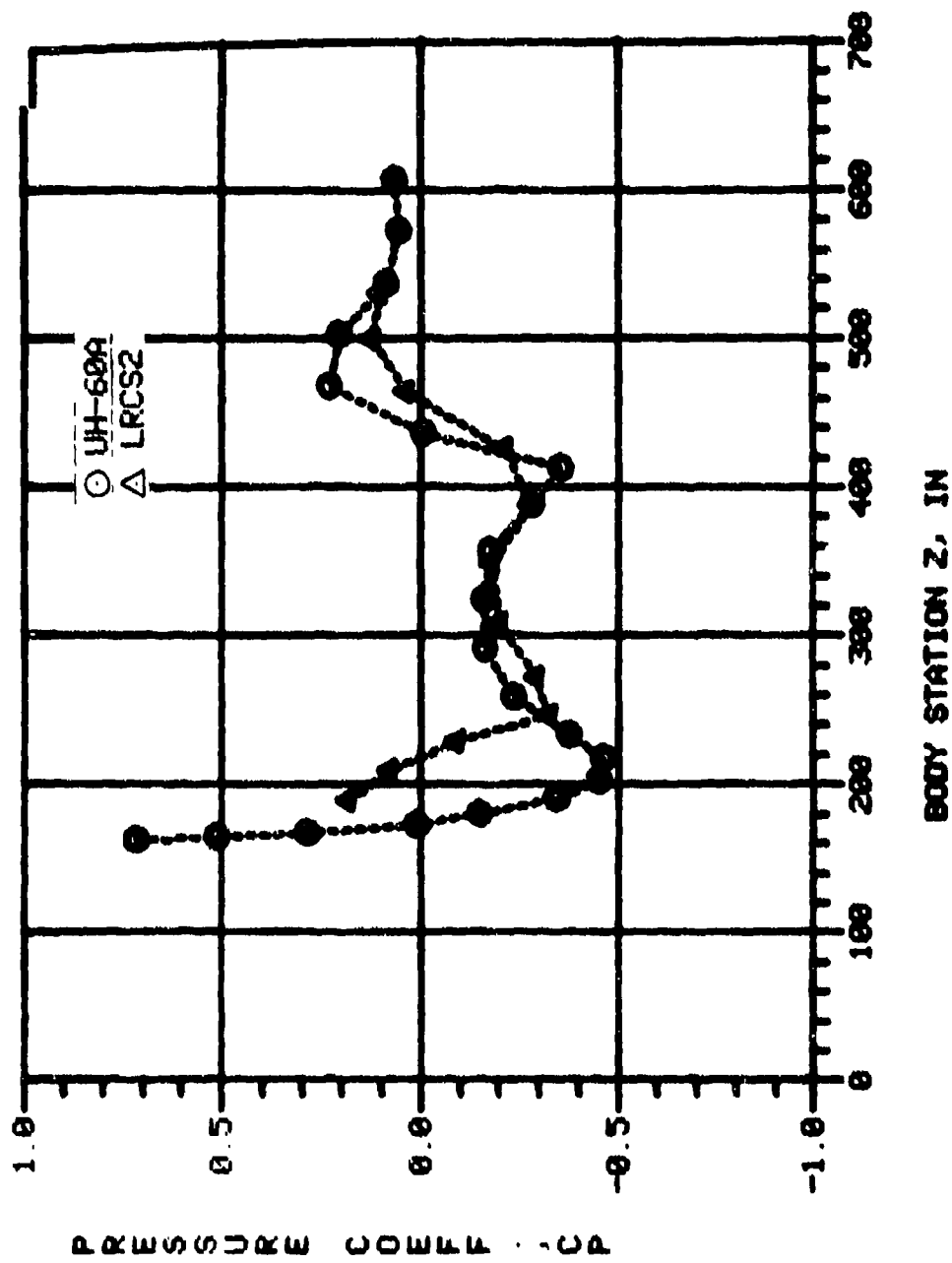


Figure A-38. COMPARISON OF THE UH-60A UTIAS AND LRCS2 CALCULATED SURFACE PRESSURES, LATERAL CENTERLINE, $\alpha = -8^\circ$, $\psi = 0^\circ$

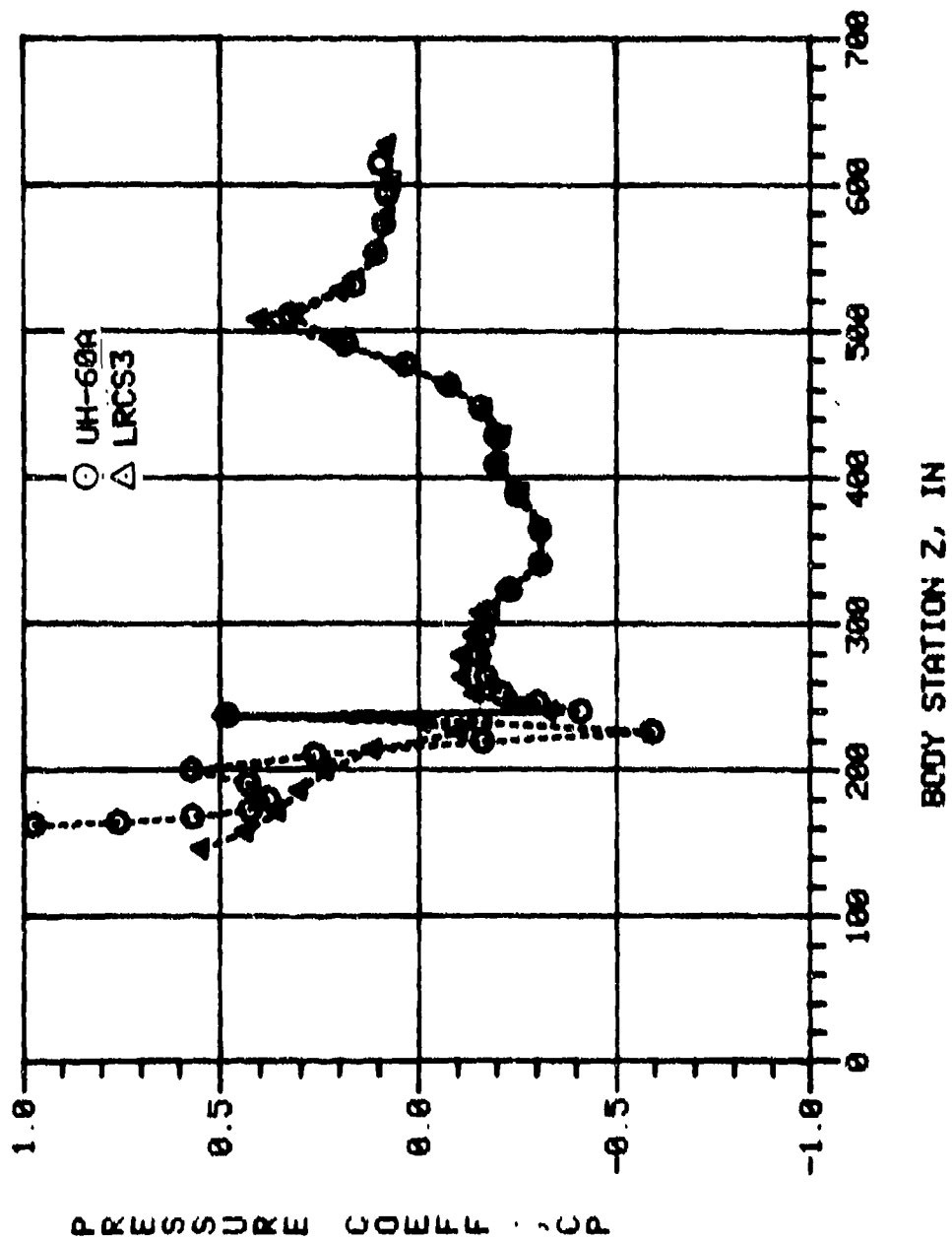


Figure A-39. COMPARISON OF THE UH-60A UTEAS AND LRCS3 CALCULATED SURFACE PRESSURES, TOP CENTERLINE, $\alpha = 0^\circ$, $\psi = 0^\circ$

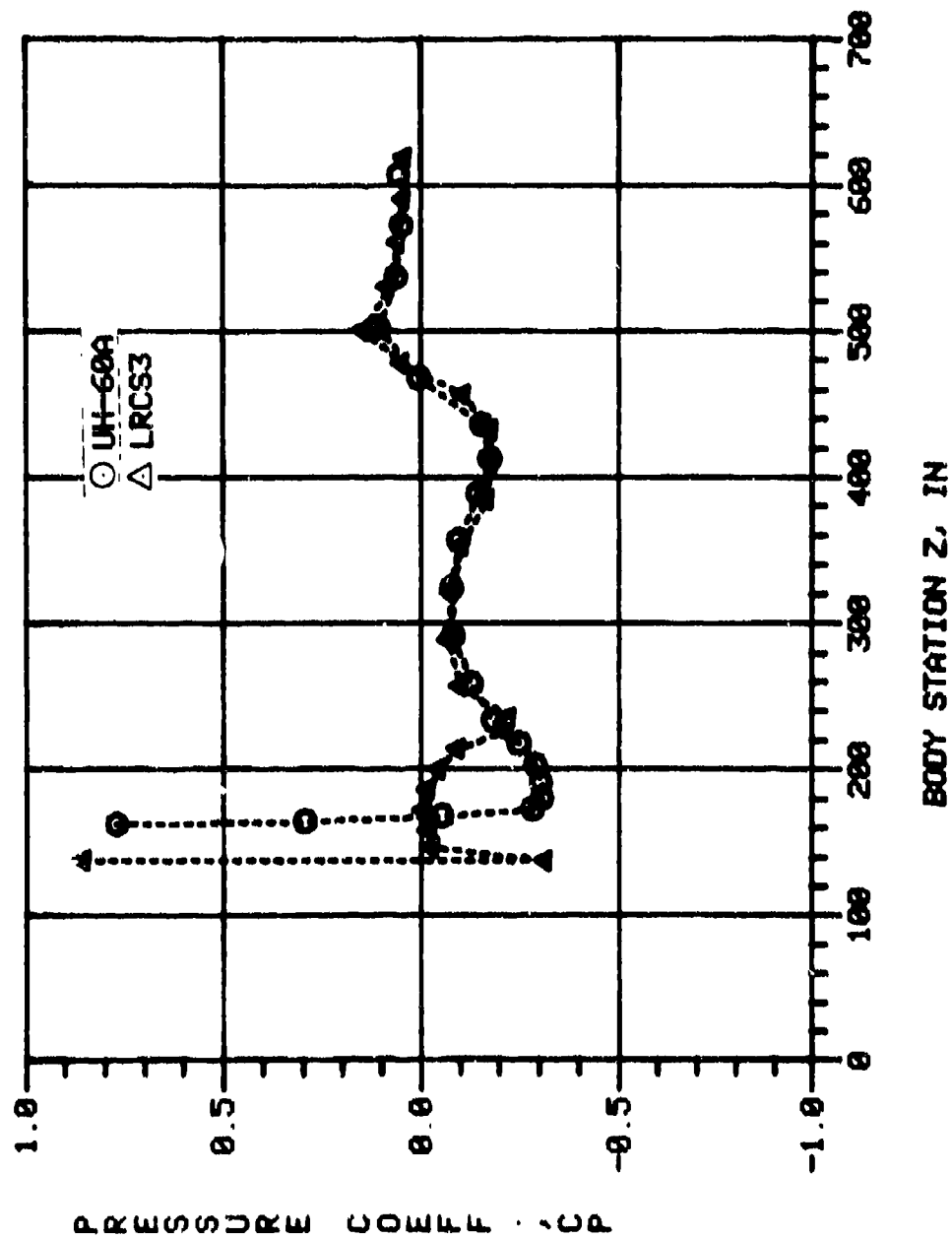


Figure A-40. COMPARISON OF THE UH-60A UTIAS AND LRCS3 CALCULATED SURFACE PRESSURES, BOTTOM CENTERLINE, $\alpha = 0^\circ$, $\psi = 0^\circ$

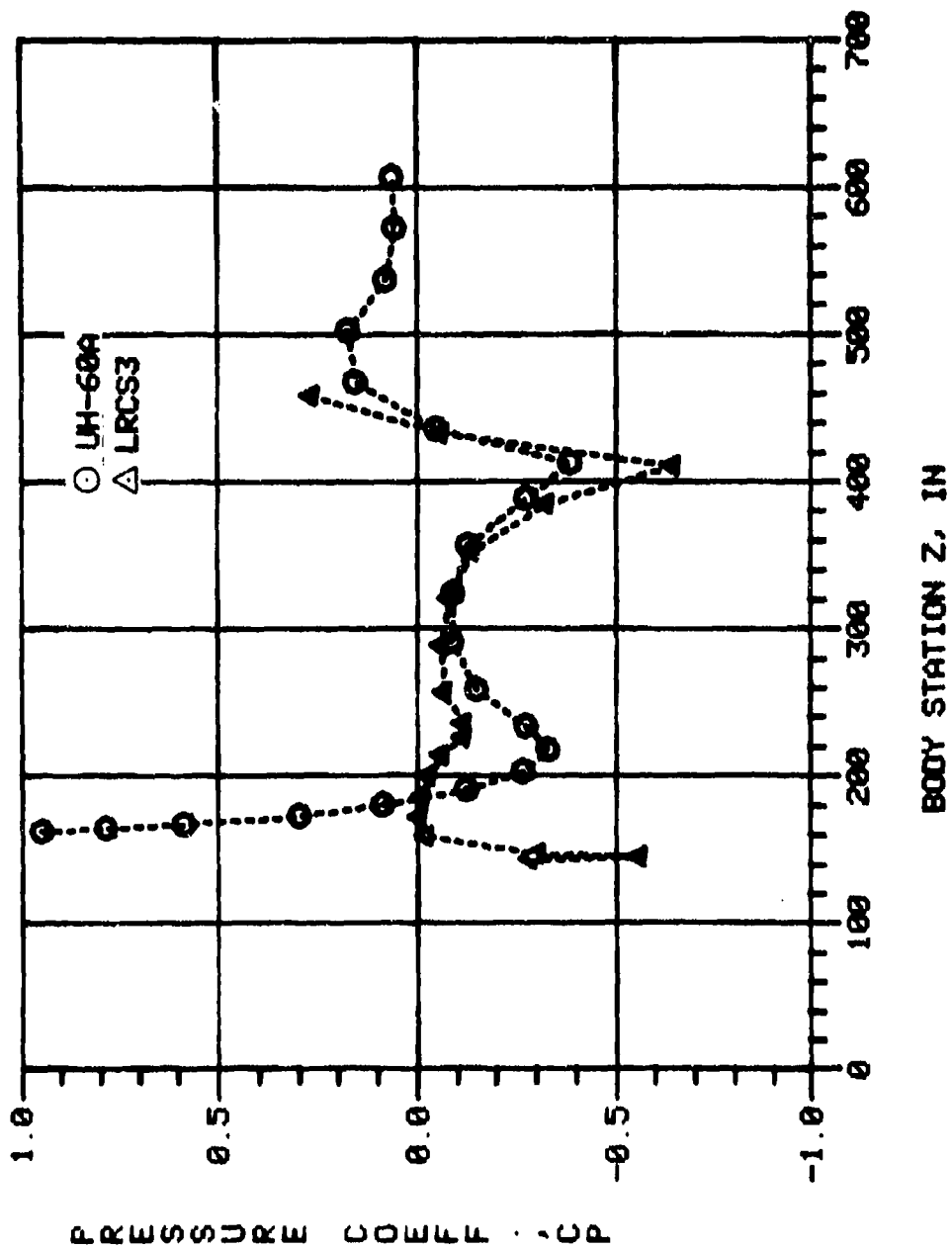


Figure A-41. COMPARISON OF THE UH-60A UTAS AND LRCS3 CALCULATED SURFACE PRESSURES, LATERAL CENTERLINE, $\alpha = 0^\circ$, $\psi = 0^\circ$

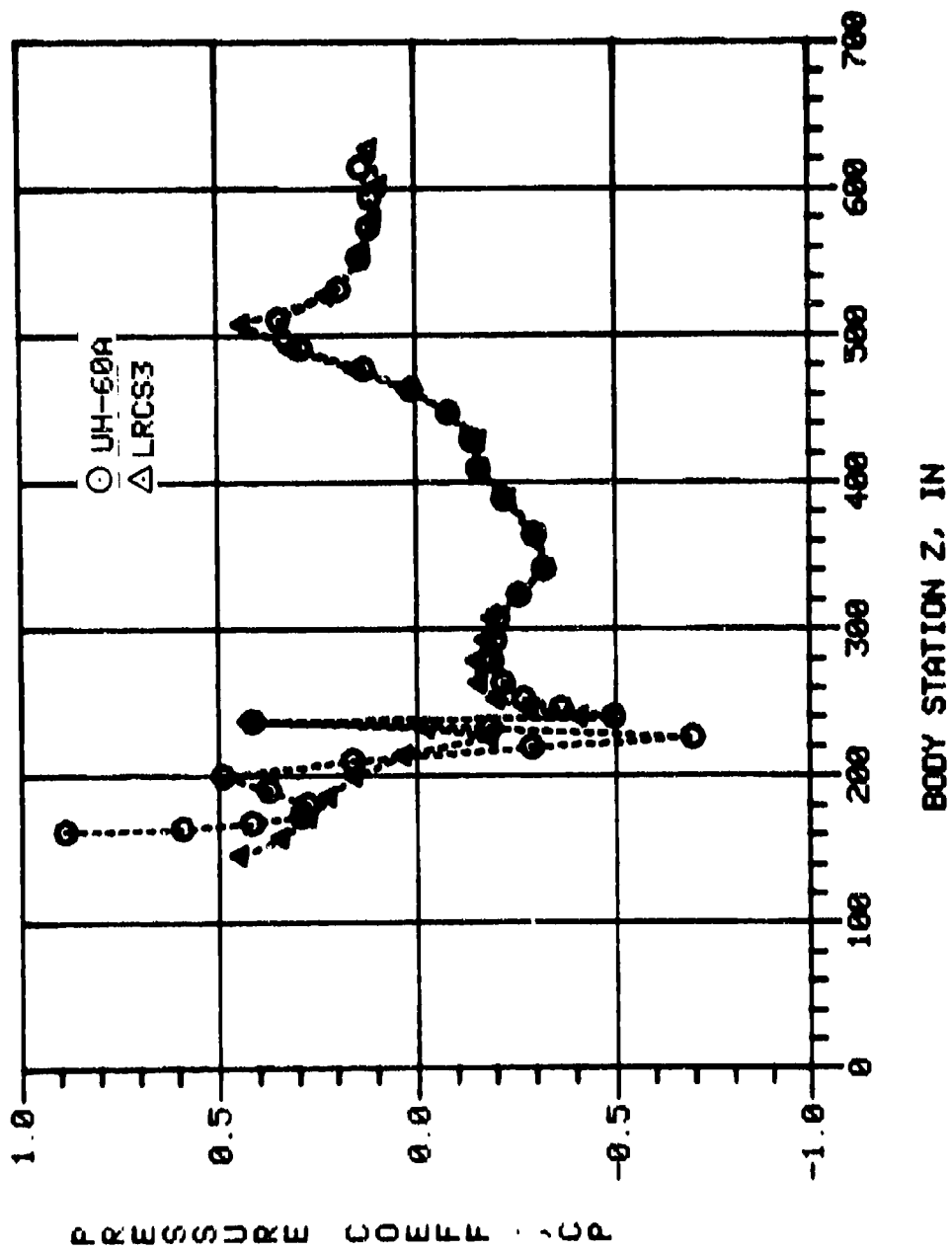


Figure A-42. COMPARISON OF THE UH-60A UTTAS AND LRCS3 CALCULATED SURFACE PRESSURES, TOP CENTERLINE, $\alpha = 4^\circ$, $\psi = 0^\circ$

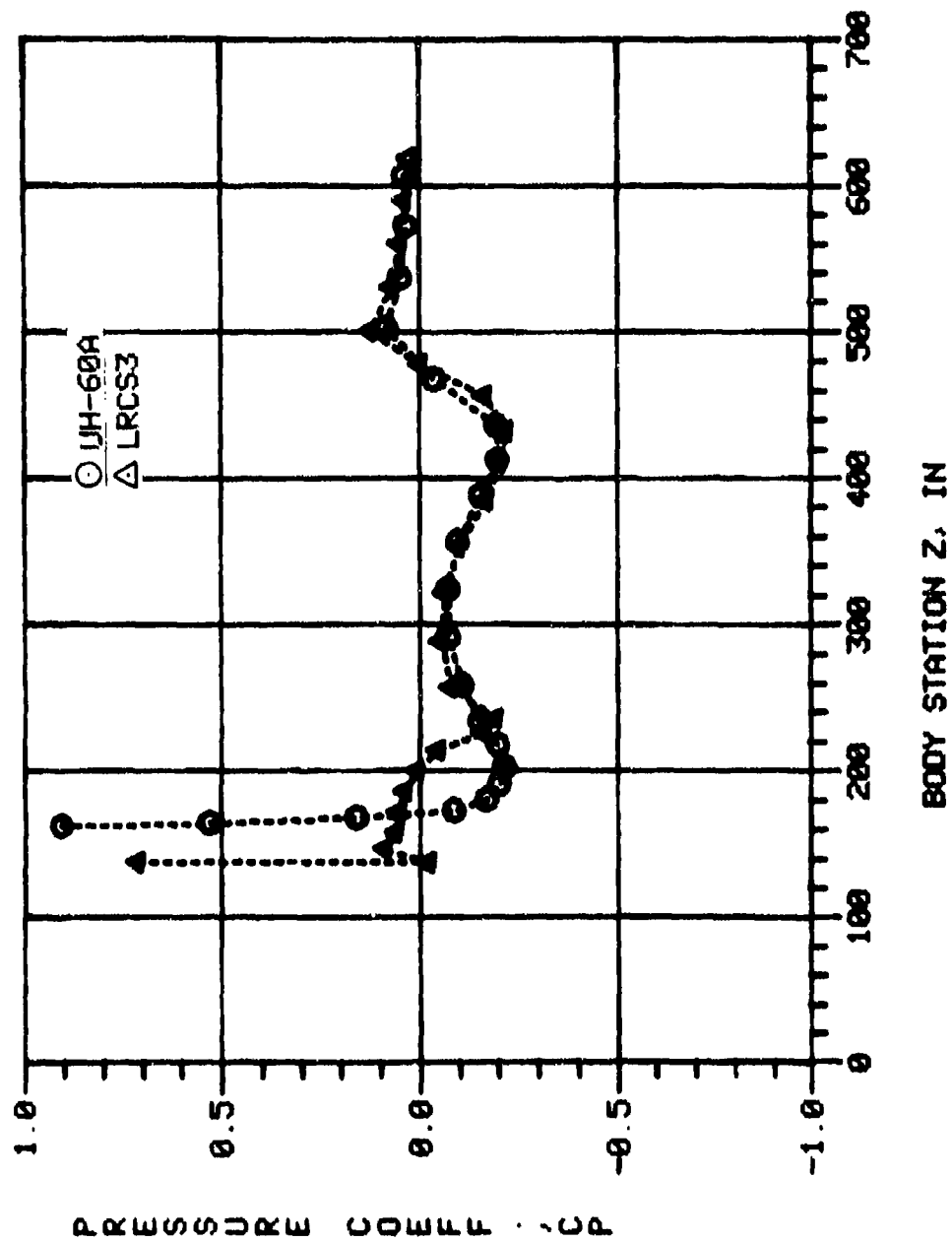


Figure A-43. COMPARISON OF THE UH-60A UTIAS AND LRCS3 CALCULATED SURFACE PRESSURES, BOTTOM CENTERLINE, $\alpha = 4^\circ$, $\psi = 0^\circ$

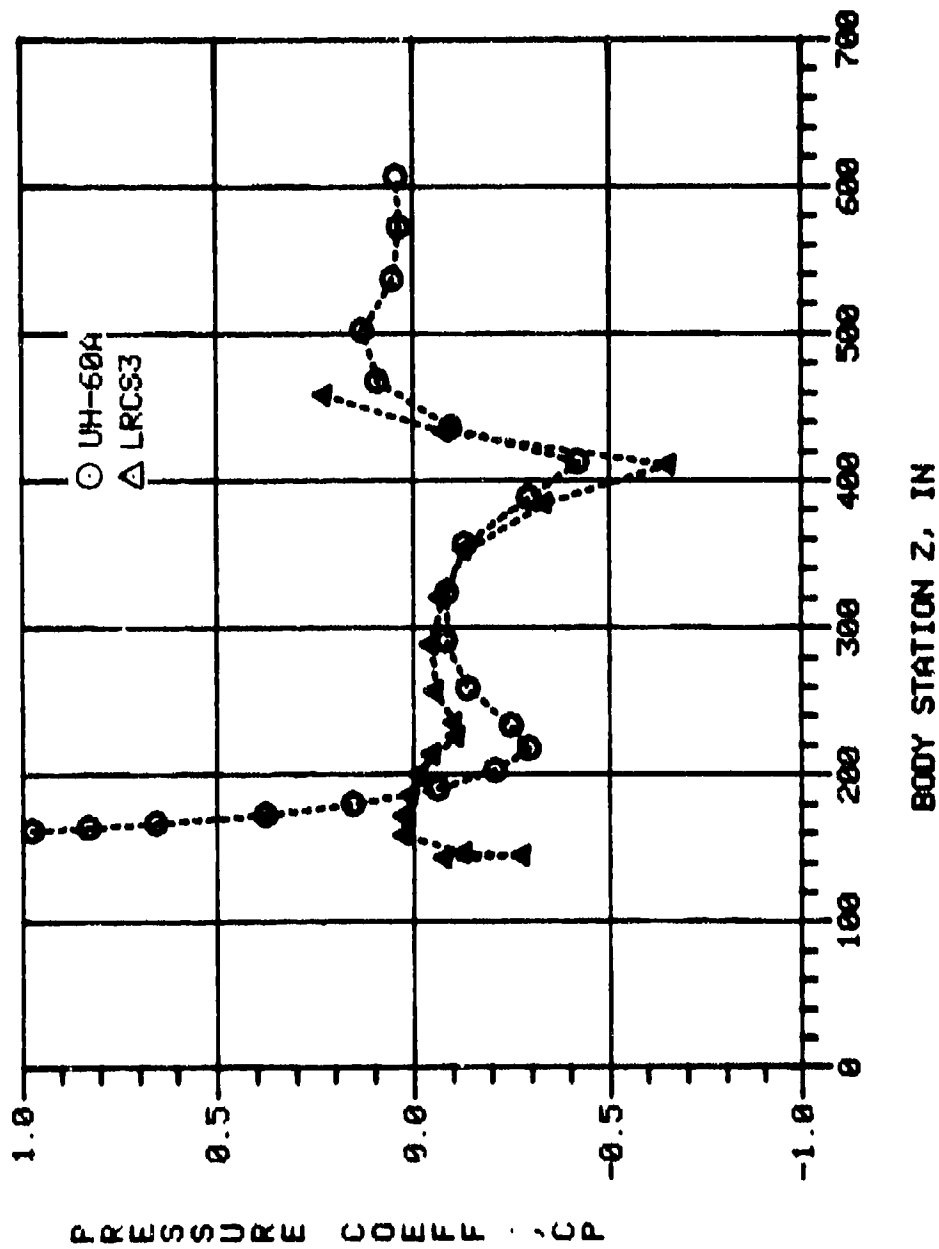


Figure A-44. COMPARISON OF THE UH-60A UFTAS AND LRCS3 CALCULATED SURFACE PRESSURES, LATEAL CENTERLINE, $\alpha = 4.0$, $\psi = 0.0$

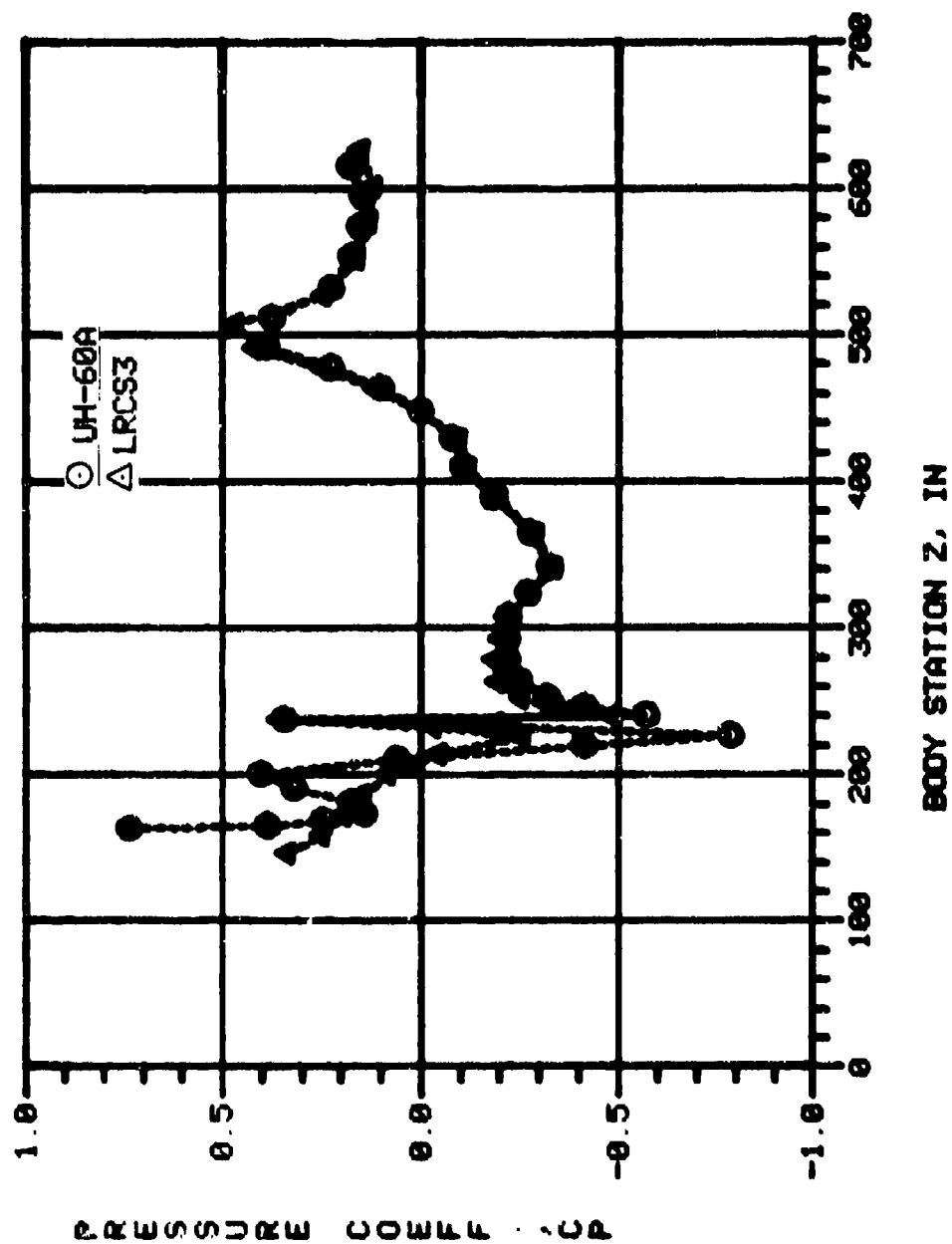


Figure A-45. COMPARISON OF THE UH-60A UTAS AND LRCS3 CALCULATED SURFACE PRESSURES, TOP CENTERLINE, $\alpha = 8^\circ$, $\psi = 0^\circ$

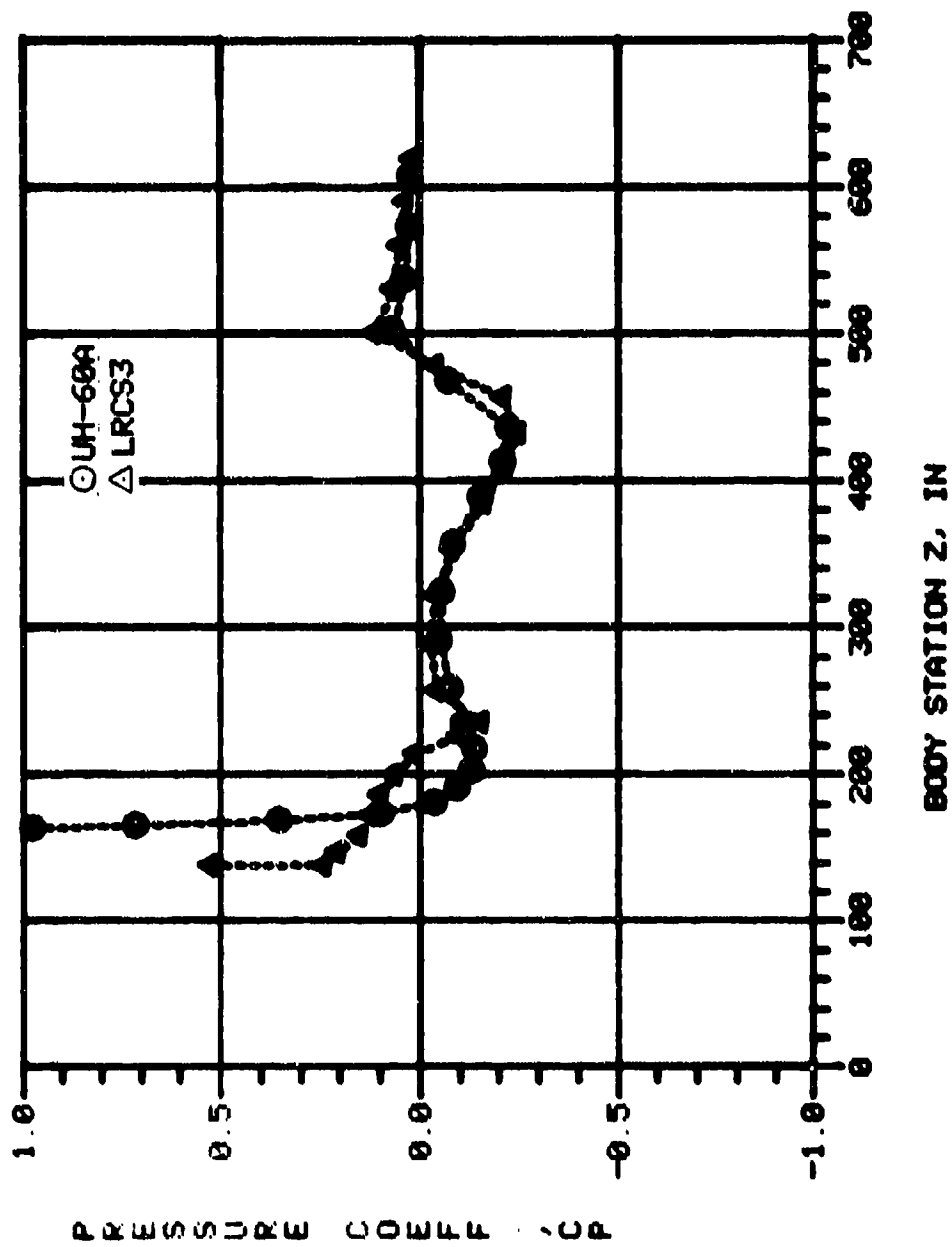


Figure A-46. COMPARISON OF THE UH-60A UTIAS AND LRCS3 CALCULATED SURFACE PRESSURES, BOTTOM CENTERLINE, $\alpha = 8^\circ$, $\psi = 0^\circ$

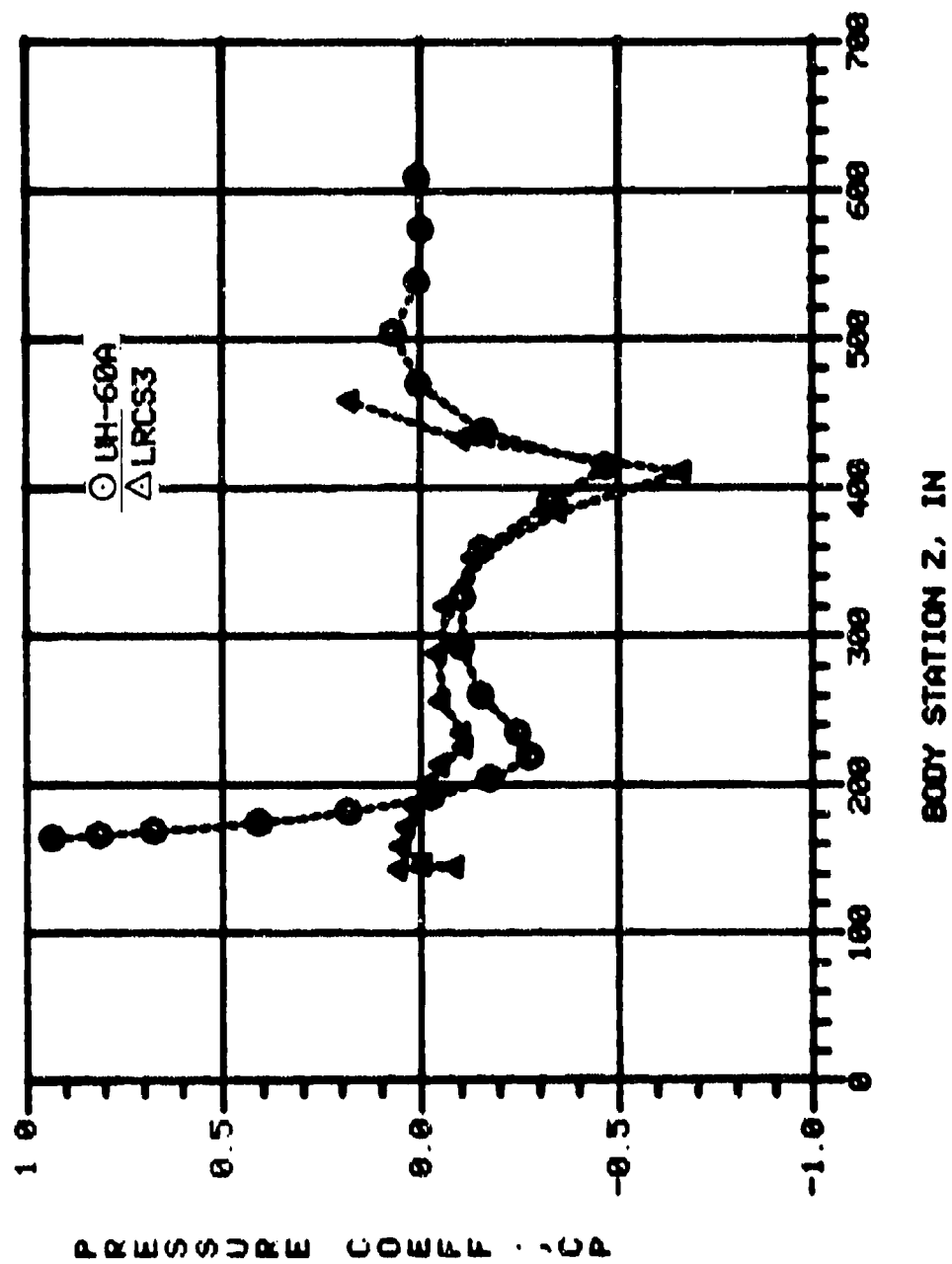


Figure A-47. COMPARISON OF THE UH-60A UFTAS AND LRCS3 CALCULATED SURFACE PRESSURES, LATERAL CENTERLINE, $\alpha = 80^\circ$, $\psi = 0^\circ$

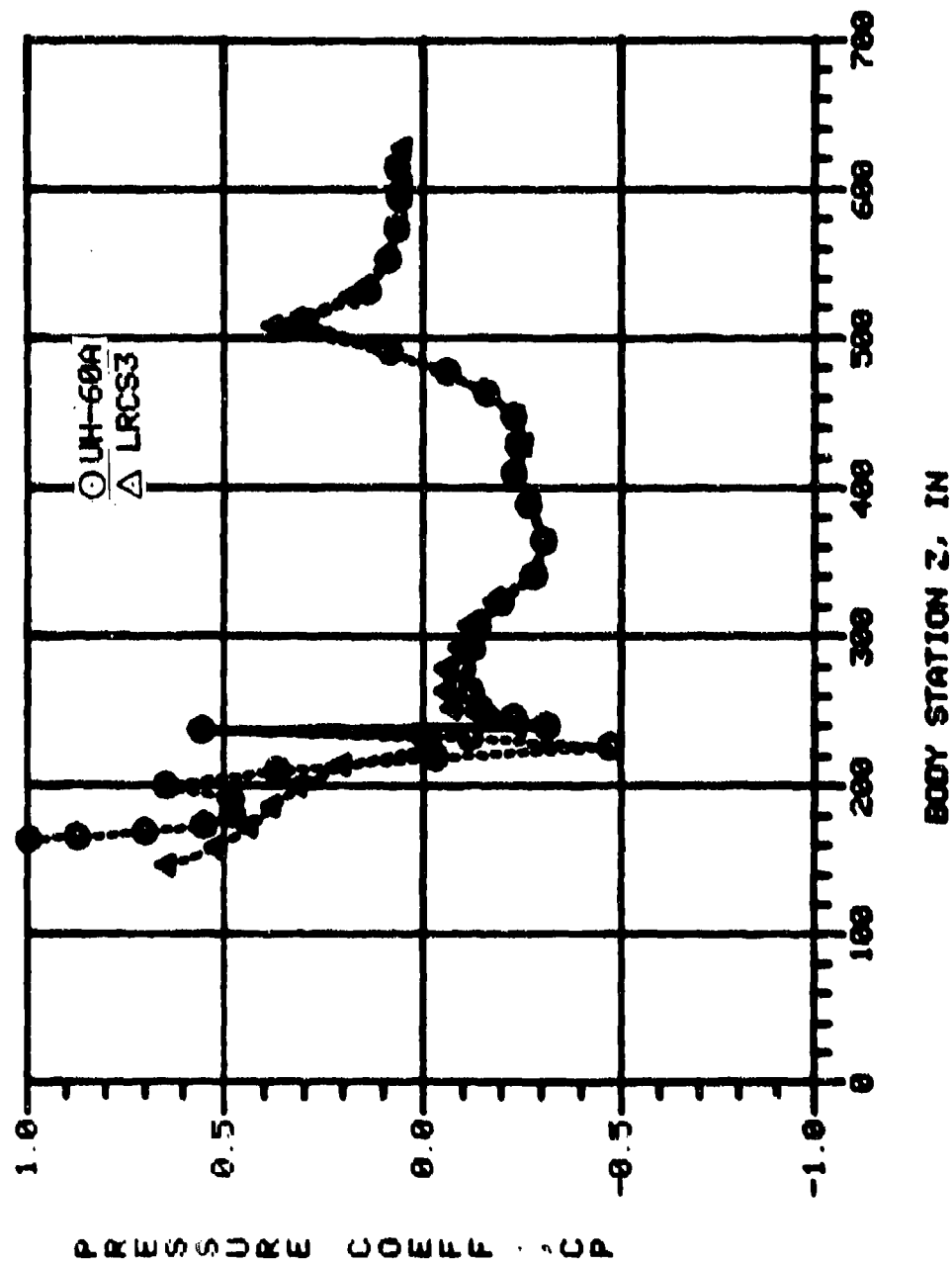


Figure A-48. COMPARISON OF THE UH-60A UFTAS AND LRCS3 CALCULATED SURFACE PRESSURES, TOP CENTERLINE, $\alpha = -4^\circ$, $\psi = 0^\circ$

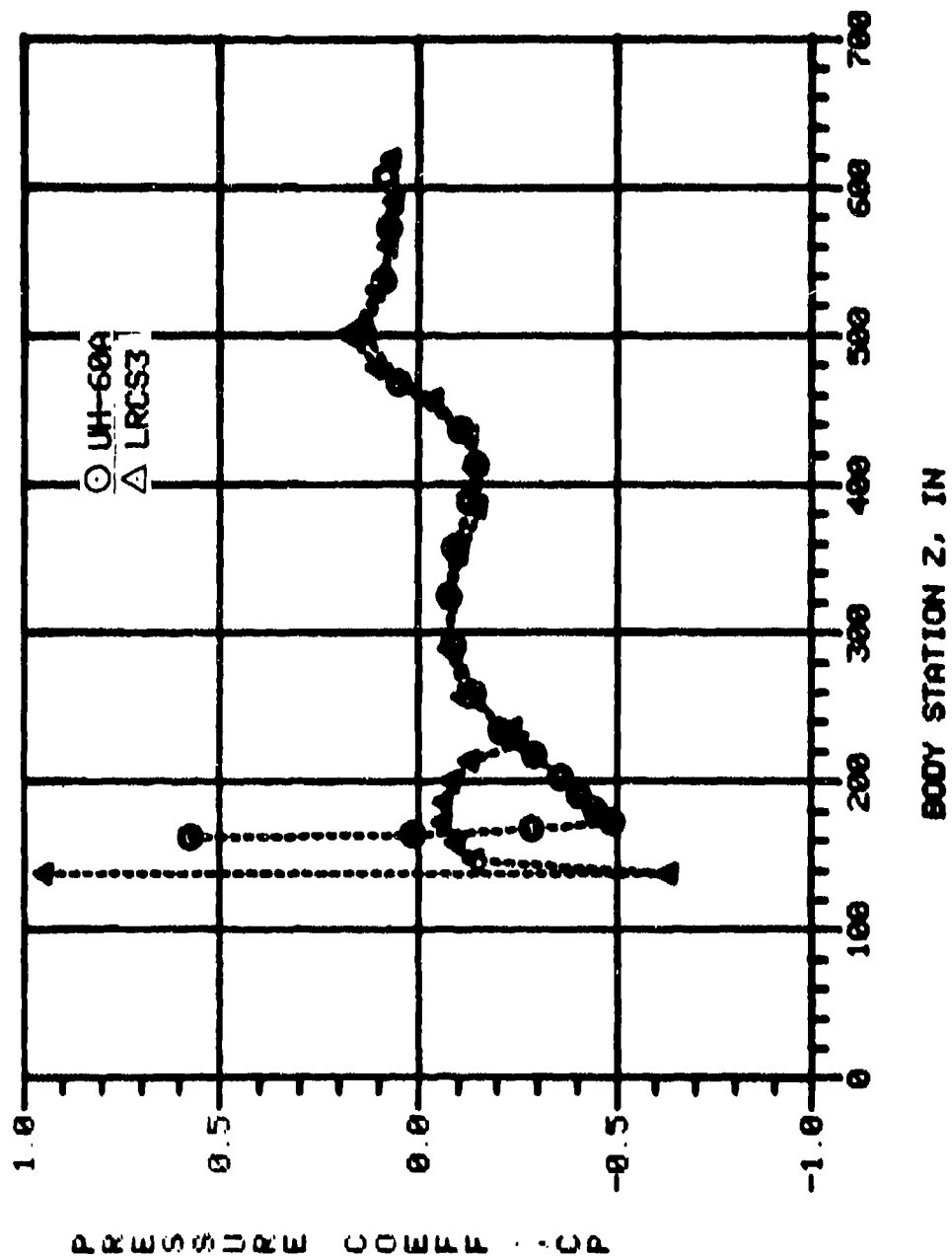


Figure A-49. COMPARISON OF THE UH-60A UTIAS AND LRCS3 CALCULATED SURFACE PRESSURES, BOTTOM CENTERLINE, $\alpha = -4^\circ$, $\psi = 0^\circ$

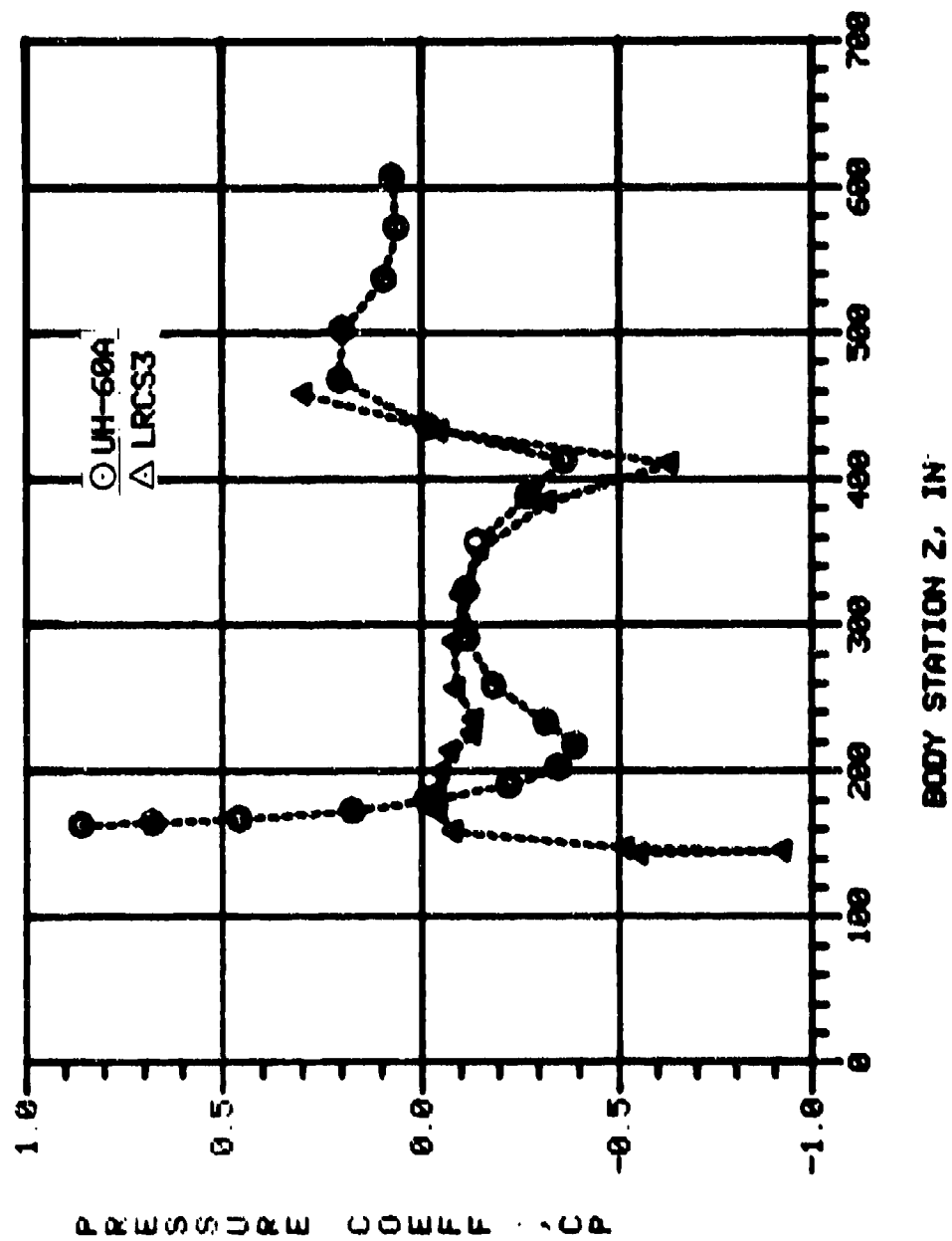


Figure A-50. COMPARISON OF THE UH-60A UTAS AND LRCS3 CALCULATED SURFACE PRESSURES, LATERAL CENTERLINE, $\alpha = -4^\circ$, $\psi = 0^\circ$

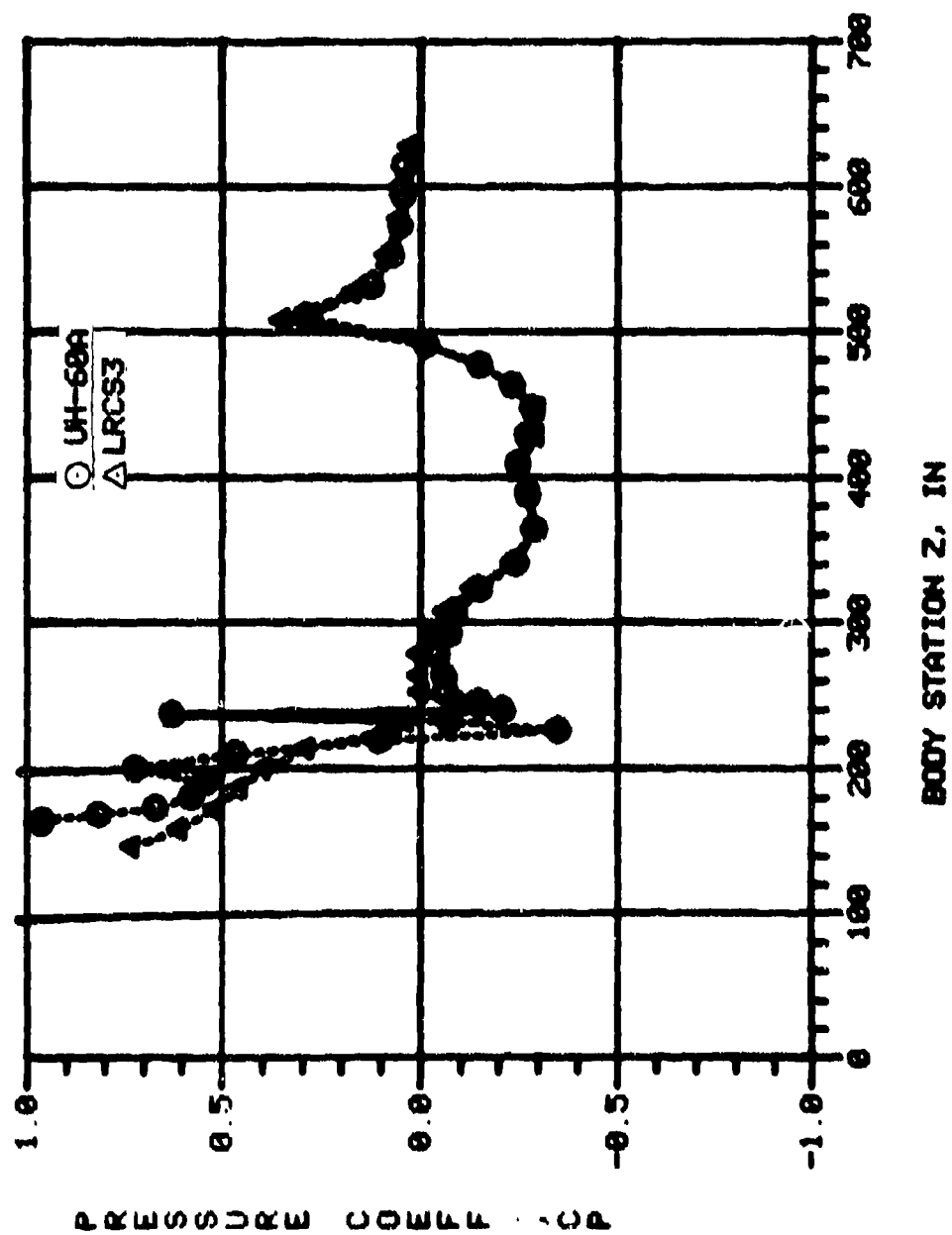


Figure A-51. COMPARISON OF THE UH-60A UTIAS AND LRCS3 CALCULATED SURFACE PRESSURES, TOP CENTERLINE, $\alpha = -8^\circ$, $\psi = 0^\circ$

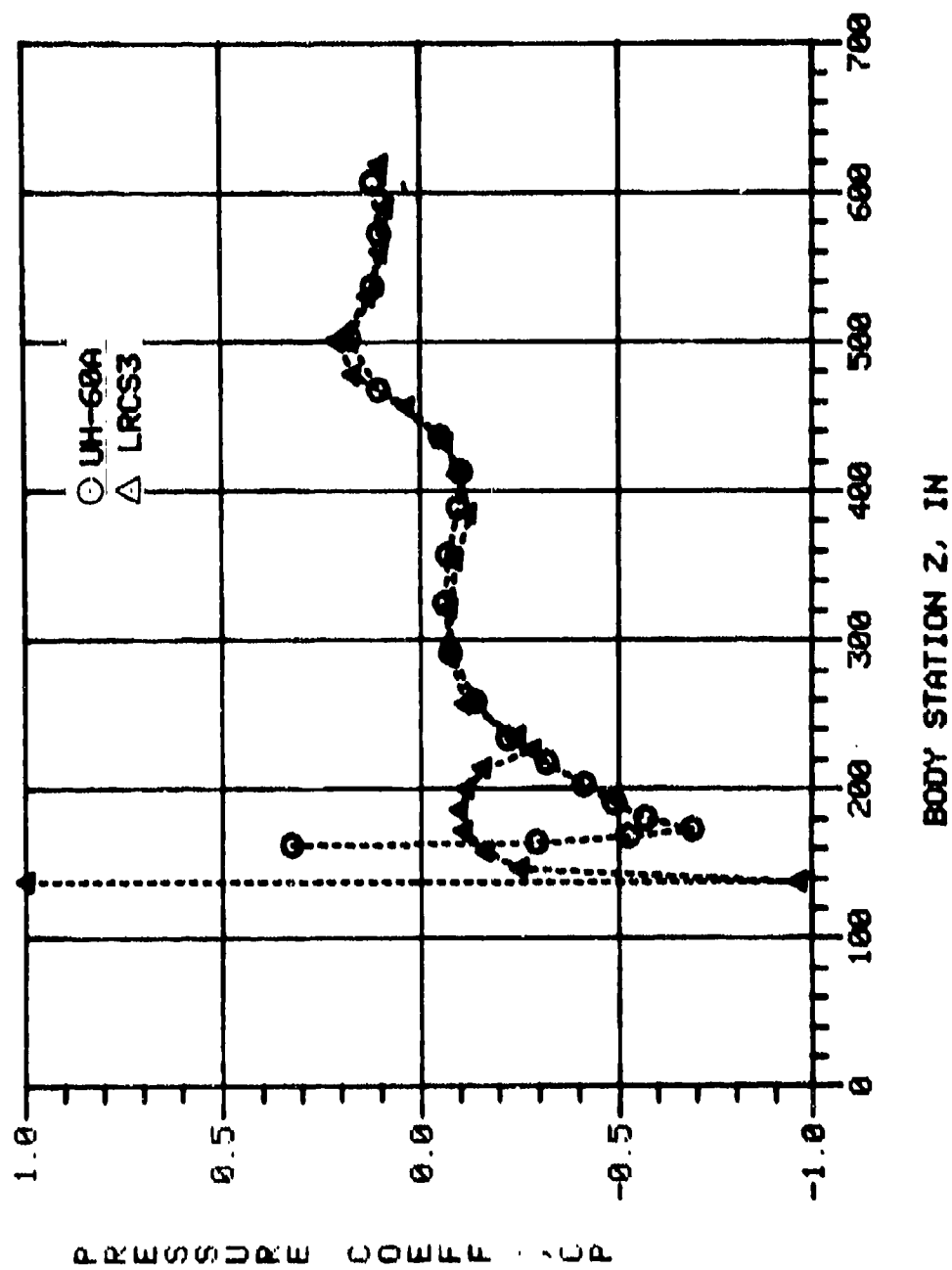


Figure A-52. COMPARISON OF THE UH-60A UPTAS AND LRCS3 CALCULATED SURFACE PRESSURES, BOTTOM CENTERLINE, $\alpha = -8^\circ$, $\psi = 0^\circ$

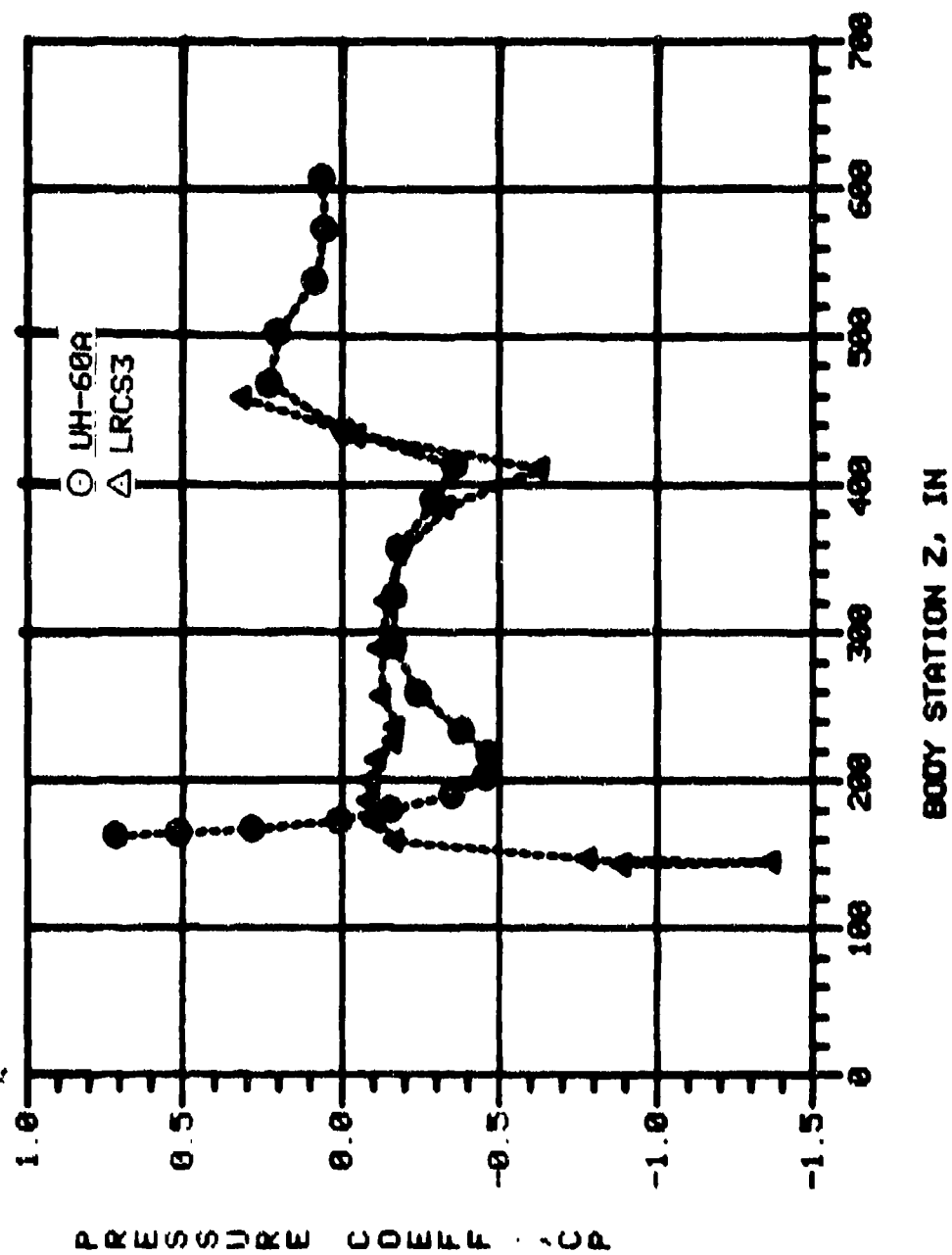


Figure A-53. COMPARISON OF THE UH-60A UTIAS AND LRCS3 CALCULATED SURFACE PRESSURES, LATERAL CENTERLINE, $\alpha = -8^\circ$, $\psi = 0^\circ$

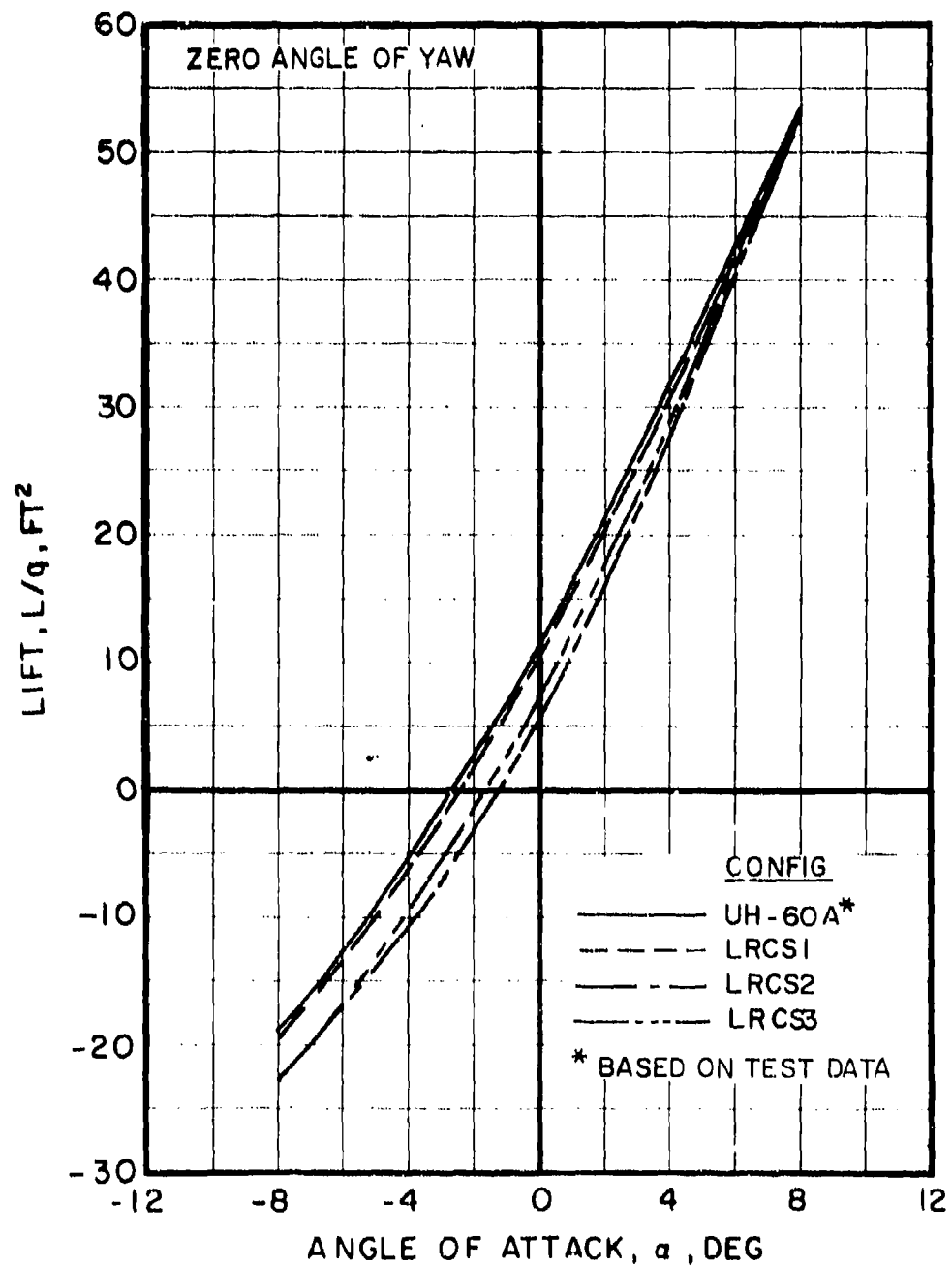


Figure A-54. VARIATION OF LIFT WITH ANGLE OF ATTACK FOR THE UH-60A UTAS, LRCS1, LRCS2, LRCS3 CONFIGURATIONS

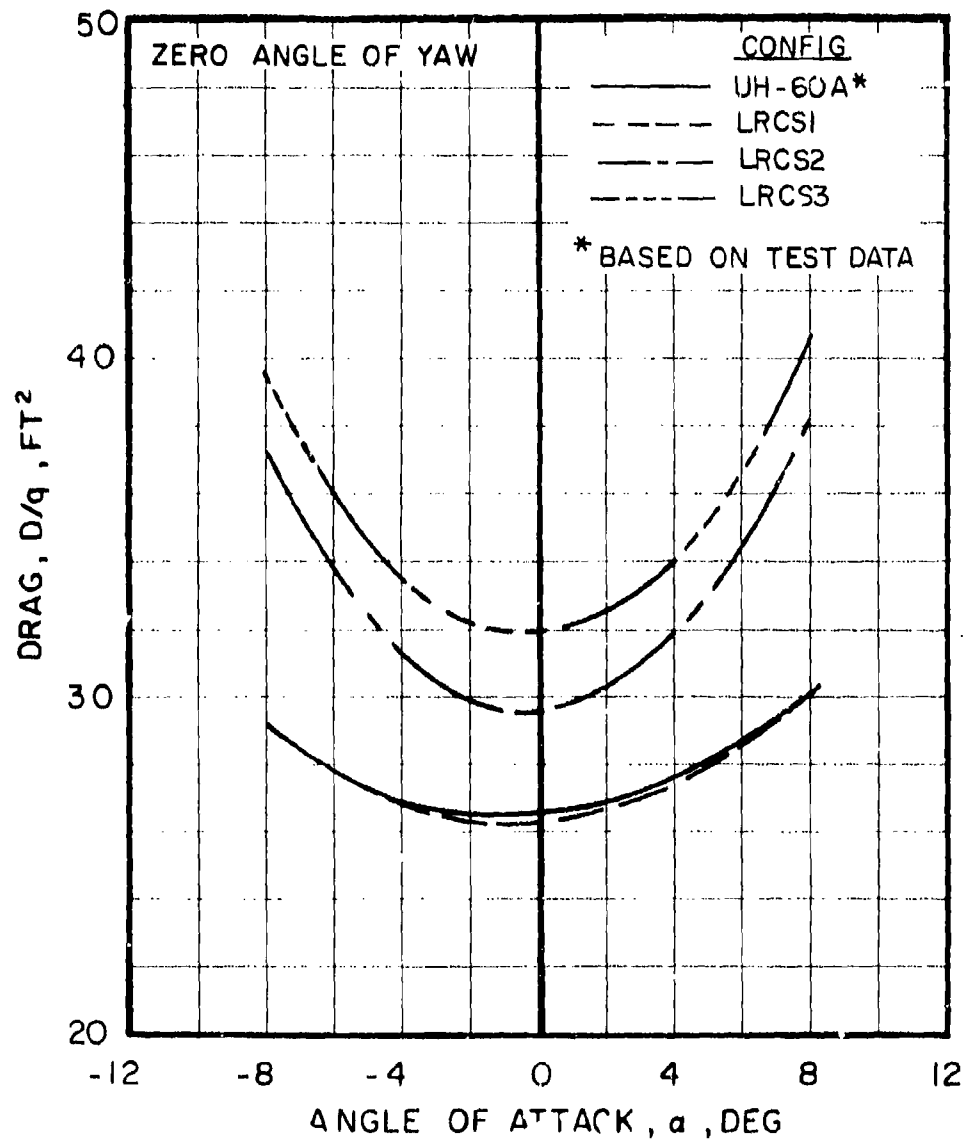


Figure A-55. VARIATION OF DRAG WITH ANGLE OF ATTACK FOR THE UH-60A UTAS, LRCS1, LRCS2, LRCS3 CONFIGURATIONS

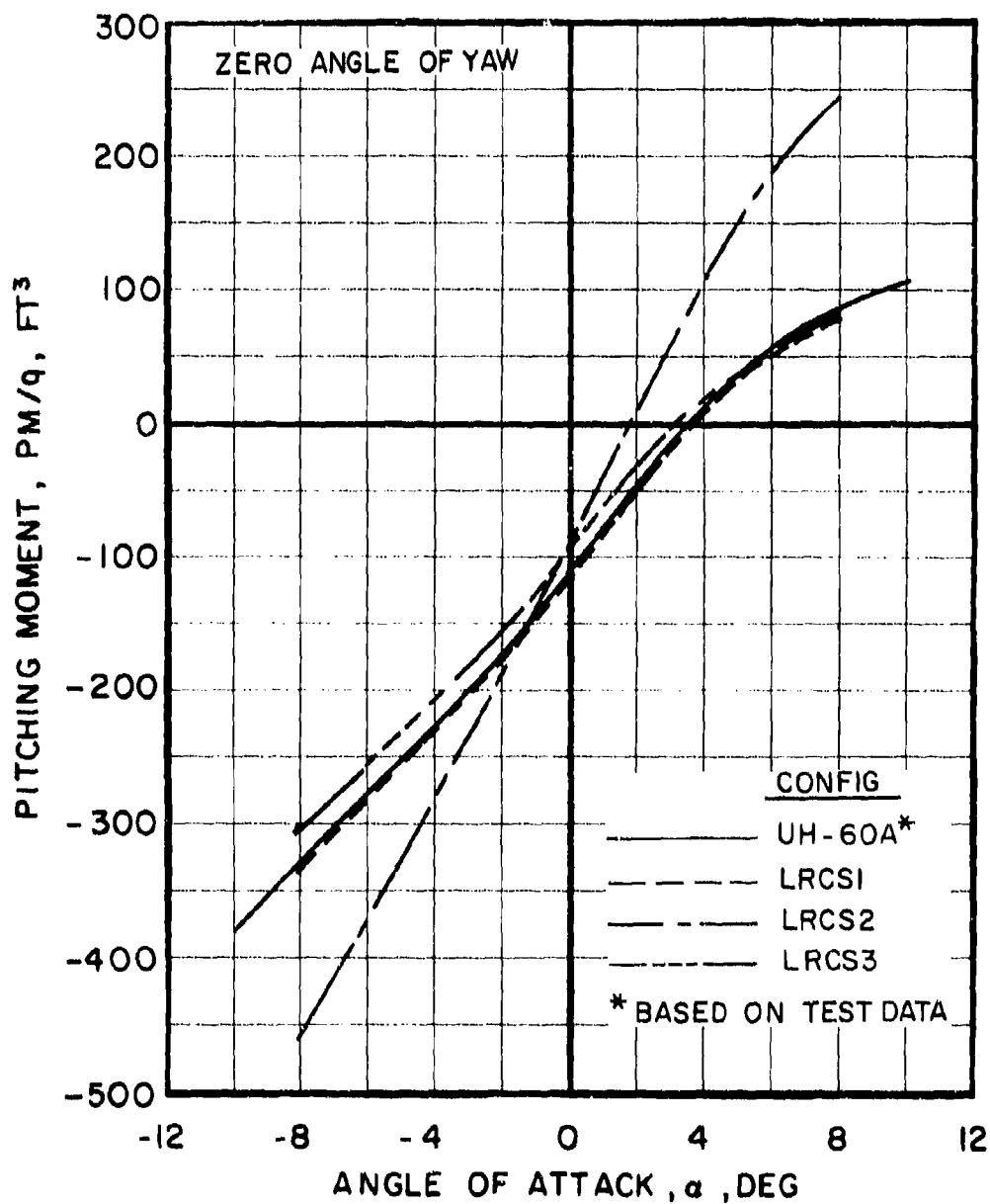


Figure A-56. VARIATION OF PITCHING MOMENT WITH ANGLE OF ATTACK FOR THE UH-60A UTTAS, LRCS1, LRCS2 and LRCS3 CONFIGURATIONS

LIST OF SYMBOLS

A	Elemental area
C _p	Surface pressure coefficient
D/q	Nondimensional airframe drag
F _s	Design shear strength, lb/in. ²
F _{su}	Ultimate shear strength, lb/in. ²
GW	Gross weight, lb
h/R	Nondimensional distance between fuselage surface and rotor plane
l/q	Nondimensional airframe lift
M/q	Nondimensional airframe pitching moment
N _z	Ultimate vertical load factor, specified design limit load factor at design gross weight times 1.5
PL _o	Payload, lb
q	Dynamic impact pressure, lb/ft ²
q _{ult}	Ultimate shear flow allowable, lb/in.
R	Main rotor radius
r/R	Nondimensional blade radial station
S	Wetted surface area, ft ²
t _{req}	Required thickness, in.
TOGW	Takeoff gross weight, lb
WE	Weight empty, lb
X	Fuselage buttline
Y	Fuselage waterline
Z	Fuselage body station
α	Angle of attack

LIST OF SYMBOLS (cont'd.)

$\alpha\beta$	Bodyline angle at $Y=219$ in.
Δp	Pressure change from atmospheric pressure, lb/in.^2
ψ	Angle of yaw